TECHNISCHE UNIVERSITÄT MÜNCHEN

Lehrstuhl für Botanik

Tethering complexes required for plant cytokinesis

Katarzyna Rybak

Vollständiger Abdruck der von der Fakultät Wissenschaftszentrum Weihenstephan für Ernährung, Landnutzung und Umwelt der Technischen Universität München zur Erlangung des akademischen Grades eines

Doktors der Naturwissenschaften

genehmigten Dissertation.

Vorsitzender:	Univ.-Prof. Dr. R. Hückelhoven
Prüfer der Dissertation:	1. Priv.-Doz. Dr. F. Assaad-Gerbert
	2. Univ.-Prof. Dr. J. Durner

Die Dissertation wurde am 04.09.2014 bei der Technischen Universität München eingereicht und durch die Fakultät Wissenschaftszentrum Weihenstephan für Ernährung, Landnutzung und Umwelt am 21.10.2014 angenommen.

Summary

Cytokinesis is the partitioning of the cytoplasm following nuclear division. In plants, cytokinesis starts at the middle of a dividing cell with the formation of a specialized membrane compartment, the cell plate. Tethering factors, which mediate the first specific contact between donor and acceptor membranes, are considered to play a significant role in cell plate formation.

Although many players involved in cytokinesis have been identified over the past few decades, little was known about the role of tethering factors in plant cell division. Moreover, cell plate biogenesis and identity was poorly understood.

In this study, a reverse genetic approach was used to identify tethering factors required for cytokinesis in *Arabidopsis thaliana*. The major focus was on the TRAPPI and TRAPPII tethering complexes, which are thought to mediate flow through the Golgi and at the trans-Golgi network, as well as on the GARP tethering complex, which is thought to tether endocytotic vesicles to the trans-Golgi network. Weak cytokinesis defects were found in TRAPPI mutants and strong cytokinesis defects in TRAPPII mutants. Electron microscopy on TRAPPII mutant seedlings revealed that dividing cells in these mutants are often multinucleate, with gapped or incomplete cross walls. In addition, vesicles accumulating at the equator of dividing cells failed to assemble into a cell plate. Additionally, phenotypic analysis of TRAPPII mutants showed that the TRAPPII complex is implicated in endocytosis. No evidence for cytokinesis defects was found in GARP insertion lines.

Live imaging showed that the TRAPPII complex localizes to the cell plate throughout cytokinesis. A comparison of the localization dynamics of TRAPPII complex and of another tethering complex, the exocyst, in dividing cells was performed. This showed that these two tethering complexes have a sequential appearance, with brief overlap at the onset and end of cytokinesis. Moreover, immunoprecipitation and mass spectrometry provided an evidence that these two complexes interact physically in dividing cells.

Immunostain analysis showed that the TRAPPII is required for cell plate assembly and exocyst for cross wall maturation. Additionally, we demonstrated that the TRAPPII complex is required for protein sorting at the cell plate.

Taken together, we show that TRAPPII plays an important and significant role in plant cytokinesis. We propose that the coordinated action of the TRAPPII and exocyst complexes might orchestrate not only plant but also animal cytokinesis.

Zusammenfassung

Zytokinese beschreibt die Aufteilung des Zytoplasmas nach der Kernteilung. Bei Pflanzen beginnt die Zytokinese durch die Bildung eines spezialisierten Membrankompartiments in der Mitte einer sich teilenden Zelle, der sogenannten Zellplatte. Man nimmt an, dass Annäherungsfaktoren, welche den ersten spezifischen Kontakt zwischen Donor- und Akzeptormembran vermitteln, eine signifikante Rolle in der Zellplattenbildung spielen.

Während der letzten Jahrzehnte konnten zwar viele bedeutende Faktoren für die Zytokinese identifiziert werden, aber dennoch ist noch wenig über die Rolle dieser Annäherungsfaktoren in der Zellteilung von Pflanzen bekannt. Darüber hinaus ist bis heute nur wenig über die Biogenese und die Identität der Zellplatte bekannt.

In dieser Arbeit wurde ein reverser genetischer Ansatz gewählt, um nötige Annäherungsfaktoren für die Zytokinese in *Arabidopsis thaliana* zu identifizieren. Der Schwerpunkt lag auf den Annäherungskomplexen TRAPPI und TRAPPII, von denen man ausgeht, dass sie den Transport durch den Golgi und das trans-Golgi Netzwerk vermitteln. Zudem spielen sie eine wichtige Rolle für den GARP Annäherungskomplex, von welchem angenommen wird, dass er endozytische Vesikel an das trans-Golgi Netzwerk anheftet. Für TRAPPI Mutanten wurden schwache Defekte auf die Zytokinese beobachtet, wohingegen für TRAPPII mutierte Keimlinge ein stark ausgeprägter Zytokinesedefekt beobachtet wurde. Elektronenmikroskopische Aufnahmen von TRAPPII mutierten Keimlingen haben gezeigt, dass die sich teilenden Zellen in diesen Mutanten oft mehrere Zellkerne sowie mit lückenhafte und unvollständige Querwände aufweisen. Zusätzlich werden Vesikel am Äquator der sich teilenden Zellen angereichert, welche nicht zu einer Zellplatte assembliert werden können. Des Weiteren haben phänotypische Analysen von TRAPPII Mutanten ergeben, dass der TRAPPII Komplex an der Endozytose beteiligt ist. In GARP Insertionslinien konnten hingegen keine Hinweise auf Defekte in der Zytokinese beobachtet werden.

Live imaging hat gezeigt, dass der TRAPPII Komplex während der Zytokinese an der Zellplatte lokalisiert ist. Ein Vergleich der Lokalisationsdynamik des TRAPPII Komplexes mit einem anderen Annäherungsfaktor, Exocyst, in sich teilenden Zellen wurde angestellt. Hierbei konnte beobachtet werden, dass die beiden Annäherungskomplexe nacheinander auftreten, wobei sie sich für kurze Zeit zu Beginn und am Ende der Zytokinese überschneiden. Zudem konnte mittels

Immunopräzipitation und Massenspektrometrie die physikalische Interaktion der beiden Komplexe in sich teilenden Zellen nachgewiesen werden.

Untersuchungen mittels Immunfärbung konnten zeigen, dass TRAPPII für die Assemblierung der Zellplatte und Exocyst für die Reifung der Querwand benötigt werden. Zudem konnten wir nachweisen, dass der TRAPPII Komplex für die Sortierung der Proteine an der Zellplatte nötig ist.

Zusammenfassend haben wir in dieser Studie dargelegt, dass TRAPPII eine wichtige und signifikante Rolle in der Zytokinese von Pflanzen spielt. Wir gehen davon aus, dass das Zusammenspiel der TRAPPII und Exocyst Komplexe nicht nur die Zytokinese in Pflanzen, sondern auch in Tieren bestimmt.

Table of contents

Abbreviations

APS	Ammonium persulfate
Arf	ADP-ribosylation factor
At	*Arabidopsis thaliana*
AVFY	Vacuolar targeted fluorophore
BASTA	Glufosinate ammonium
Bet	Blocked early in transport
BiFC	Bimolecular fluorescence complementation
bp	Base pair
BSA	Bovine serum albumin
CCV	Clathrin coated vesicle
CFP	Cyan fluorescent protein
CLSM	Confocal laser scanning microscopy
COG	Conserved oligomeric Golgi
CPAM	Cell plate assembly matrix
Col	Columbia
CTAB	Cetyl-trimethyl-ammonium bromide
DAPI	4',6-diamidino-2-phenylindole
DMSO	Dimethyl sulfoxide
Dsl1	Dependence on Sly1
EDTA	Ethylenediaminetetraacetic acid
EE	Early endosome
ESCRT	Endosomal sorting complex
EtBr	Ethidium bromide
EtOH	Ethanol
FIB/SEM	Focused Ion Beam/Scanning Electron Microscopy
FM4-64	*N*-(3-triethylammoniumpropyl)-4-(6-(4(diethylamino)phenyl)hexatrienyl)pyridinium dibromide
GARP	Golgi-associated retrograde protein
GA-TGN	Golgi-associated trans-Golgi network
GEF	Guanine nucleotide-exchange factor
Gent	Gentamycin
GFP	Green fluorescence protein
GI-TGN	Golgi-released independent trans-Golgi network
GSG1	General sporulation gene 1
HA	Hemagglutinin

HOPS	Homotypic fusion and vacuole protein sorting
HPLC	High-Performance Liquid Chromatography
Hs	*Homo sapiens*
IP	Immunoprecipitation
IPTG	Isopropyl β-D-thiogalactoside
Kan	Kanamycin
kb	Kilobase
kDa	Kilo Dalton
LB	Luria-Bertani medium
mA	Milliampere
MES	2-morpholinoethansulfone acid
MeOH	Methanol
MS	Murashige and Skoog medium
MVB	Multivascular body
NASC	Nottingham Arabidopsis Stock Centre
MTSB	Microtubules stabilizing buffer
OD	Optical density
PBS	Phosphate buffered saline
PCR	Polymerase Chain Reaction
PED	PIN1 expression domain
PEG	Polyethylene
PFA	Paraformaldehyde
PME	Pectin methylesterase
PMSF	Phenylmethylsulfonylfluorid
rER	Rough endoplasmatic reticulum
RFP	Red fluorescent protein
Rif	Rifampicin
Sc	*Saccharomyces cerevisiae*
SCLIM	Super-resolution confocal live imaging microscopy
SDS	Sodium dodecylsulfate
SEM	Scanning Electron Microscopy
SNARE	Soluble N-ethylmaleimide-sensitive factor
SV	Secretory vesicles
TAE	Tris-acetate-EDTA
Tca17	TRAPPII-associated protein 17
TE buffer	Tris-EDTA buffer

TEM	Transmission Electron Micrographs
TEMED	N,N,N,N'-tetramethylethylene diamine
TGN	Trans-Golgi network
TN	Tubular network
TRAPP	Transport protein particle
Trs	TRAPP subunit
TVN	Tubular-vesicular network
V	Voltage
VAMP	Vesicle associated membrane proteins
VHA-a1	Vacuolar H ATPase subunit a1
Vps	Vacuolar sorting
wt	Wild type
Y2H	Yeast two hybrid
YFP	Yellow fluorescent protein

1. Introduction.

1.1. Cytokiensis.

Cytokinesis is a complex multistage process that leads to the precise distribution of cytoplasm and chromosomal components between two daughter cells following nuclear division (Sasebe et al., 2011; Tang, 2012). Due to the presence of the plant cell wall, the process of cytokinesis differs in plants and animals. In animals, cytokinesis starts from the outside of the dividing cell. In telophase, an actinomyosin contractile ring forms a cleavage furrow that bisects the dividing cell (Neto and Gould, 2011). In higher plants, cytokinesis is considered to be a specialized form of polarized secretion, which starts with the delivery of Golgi-derived secretory vesicles to the division plane and their homotypic fusion that gives rise to a plant-specific transient membrane compartment, the cell plate (Samuels et al., 1995; Assaad, 2001; Lucas and Sack, 2012). After centrifugal expansion, the cell plate is attached to the parental cell wall (Schopfer and Helper, 1991).

1.1.1. Origin and cell plate formation.

Cryofixation/freeze-substitution and electron microscopy techniques were used to study cell plate assembly and expansion (Samuels et al., 1995; Segui-Simarro et al., 2004). Its formation starts in late anaphase and is completed by late telophase. The cell plate is formed in ribosome excluding matrix, termed cell plate assembly matrix (CPAM). The assembly and centrifugal development of the cell plate is driven by the centrifugal expansion of plant specific microtubule array, the phragmoplast (Samuels et al., 1995). Cell plate assembly starts with the delivery and homotypic fusion of Golgi-derived vesicles at the equator of the cell, which gives rise to dumbbells localized in phragmoplast initials. Dumbells are next converted into a tubular-vesicular network (TVN). After phragmoplast reorganization, a smooth tubular network (TN) arises from the tubular-vesicular network. At this stage, a new cell wall assembly is initiated and the tubular network is strongly consolidated with callose and very weak cellulose content. After the cell plate fuses to the plasma membrane, the consolidation phase of the cell plate gives rise to a fenestrated cell plate. After callose is exchanged with cellulose, a new cell wall is formed (Fig. 1.2.1; Samuels et al., 1995; Staehelin and Hepler, 1996; Otegui and Staehelin, 2004). At the very end, recycling of the membranes from the cell plate occurs via clathrin coated vesicles (Segui-Simarro et al., 2004). Dynamin-like molecules (mechanoenzymes) are involved in dumbbell formation, which decreases vesicle volume, and in clathrin-coated vesicles formation required for

recycling cell plate membranes from the maturing cell plate (Segui-Simarro et al., 2004). Transition to the tubular network stage is accompanied by loss of phragmoplast microtubules and CPAM at the central region and their movement to the leading edges, leading to ring-shaped phragmoplast (Segui-Simarro et al., 2004).

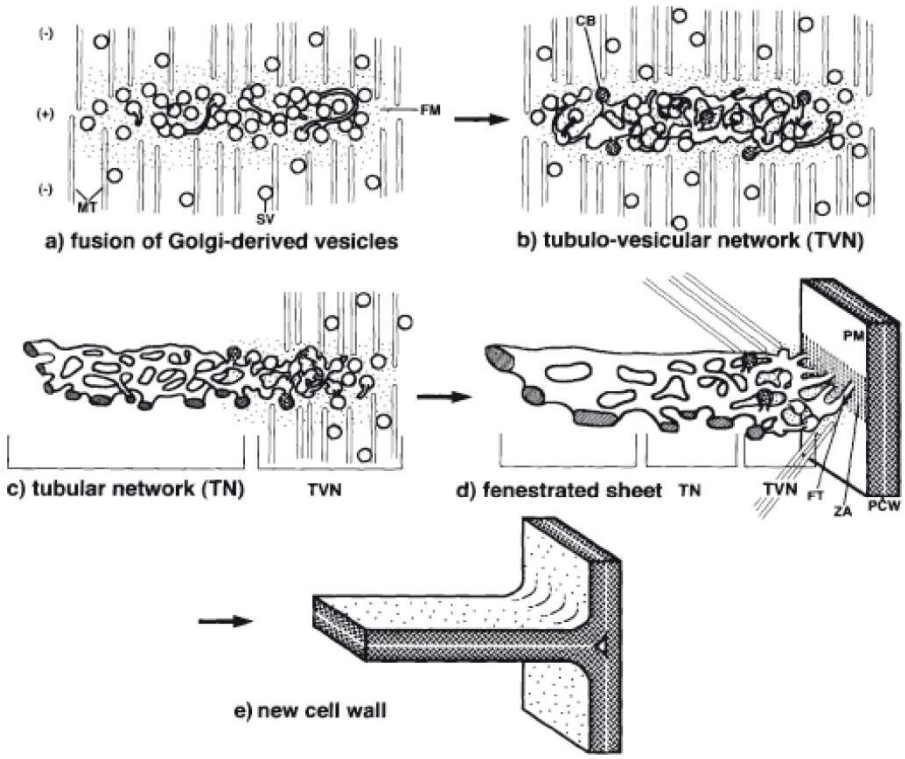

Figure 1.2.1. Model of cell plate formation in a higher plant cells.
Adapted from Samuels et al. (1995). Cell plate formation occurs at the equator of a dividing cell, from anaphase to telophase transiton. (a) transprt of secretory vesicles (SV) to the equator of a dividing cell. (b) vesicle fusions gives rise to a delicate tubular-vesicular network (TVN); phragmoplast is at its solid stage. (c) TVN deposition with callose forms tubular network (TN); phragmoplast reorganizes to the leading edges resulting in ring-shaped phragmoplast. (d) TN becomes a fenestrated sheet membrane compartment, which fuses with lateral walls via finger-like fusion tubes. (e) A new cell wall.

There are many open questions concerning the origin of the cell plate. It was proposed that cell plate formation involves endocytotic vesicles (Dhonukshe et al., 2006). Later studies using drug treatments at different trafficking steps have shown that plant cytokinesis requires exocytosis but not endocytosis; pharmacological inhibition of endocytosis with wortmannin did not affect the growing cell plate (Reichardt et al., 2007). In current models, the cell plate is largely accepted to be a Rab-A, TGN/EE-derived compartment (Dettmer et al., 2006; Chow et al., 2008).

1.2. Cytokinesis-defective mutants.

Due to its short life cycle, small and diploid genome, large seed production and short generation time, *Arabidopsis thaliana* is commonly used as a model organism for studying plant growth and development (Mayer et al., 1991; Liu et al., 1995). Along the apical-basal axis, the *Arabidopsis* seedling consists of four pattern elements, shoot meristem cotyleodons, hypocotyls and root. Along the radial axis, the seedling consists of three pattern elements, the epidermis, cortex and vascular tissues. Cytokinesis-defective mutants of *Arabidopsis* were first accidentally identified in a large-scale screen for mutants affecting seedling body organization (Mayer et al., 1991). The canonical cytokinesis-defective mutant phenotype was described by Söllner et al. (2002), as being characterized by cell wall stubs, incomplete cell walls, multinucleate and enlarged cells.

Genes involved in cytokinesis in somatic tissues can be divided into three classes (Söllner et al., 2002; Thiele et al., 2009). Genes in the first class are required for the correct establishment of the division plane. The second class of genes is responsible for the execution of cytokinesis. Genes in the third class are involved in cell wall establishment and maturation (Söllner et al., 2002; Thiele et al., 2009).

In this study, I focused on the second class of cytokinesis mutants required for the execution of cytokinesis. This group includes CYD (Liu et al., 1995; Yang et al., 1999), KNOLLE (Lukowitz et al., 1996, Lauber et al., 1997; Assaad et al., 1996), KEULE (Waizengger et al., 2000), HINKEL (Strompten et al., 2002), PLEIADE (Müller et al., 2004) and CLUB (Jaber et al., 2010). KNOLLE encodes localized to the cell plate cytokinesis specific syntaxin (Lukowitz et al., 1996, Lauber et al., 1997). KEULE is a member of Sec1/Munc18 and encodes a Sec1 protein (Assaad et al., 2001). Both, together with SNAP25 homolog called SNAP33 form a SNARE complex required for fusion at the cell plate (Heese et al., 2001). *Arabidopsis* HINKEL and PLEIADE/AtMAP65-3 encode a kinesin-like protein and a microtubule-asscociated protein, respectively, and both are required for the proper organization of the phragmoplast microtubules (Strompten et al., 2002; Müller et al., 2004; Takahashi et al., 2010).

1.3. Vesicle trafficking in secretory pathway.

Membrane trafficking is essential for fundamental processes in eukaryotic life, including cell growth and cell division. In the secretory pathway, proteins are synthesized at the rough endoplasmatic reticulm (rER), modified in the Golgi apparatus and sorted at the trans-Golgi network (TGN), from which proteins are transported to their final destination, the plasma membrane or vacuole (Fig. 1.3.1). The transport of newly synthesized molecules occurs via vesicles (Palade, 1975).

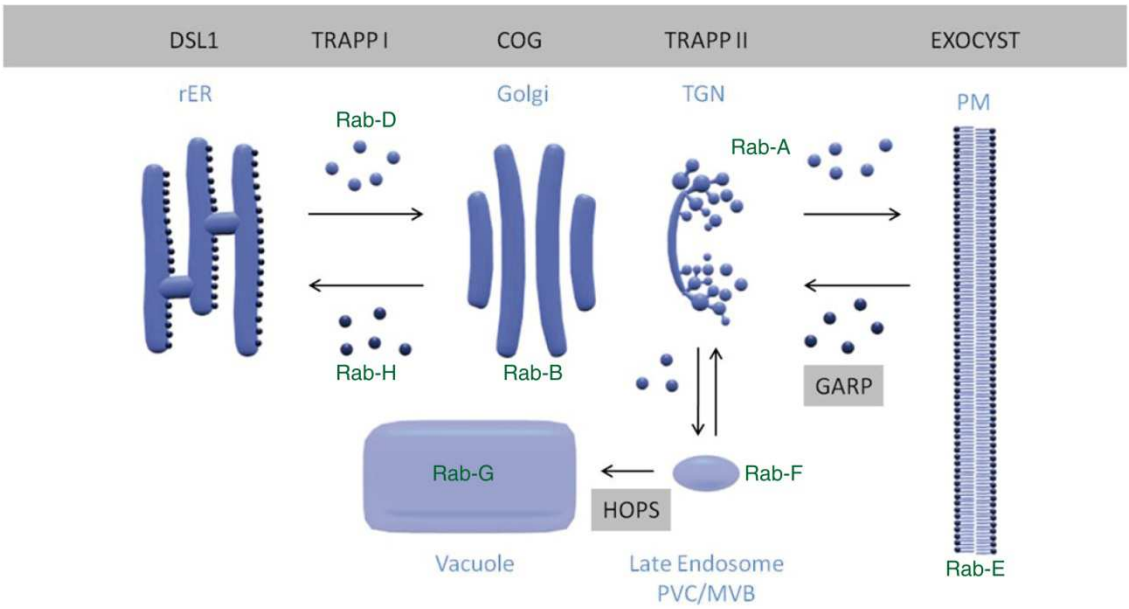

Figure 1.3.1. Conserved tethering complexes and the plant secretory pathway.
As described by Koumandou et al. (2007), the TRAPPI (transport protein particle) complex would mediate ER to Golgi and the COG complex intra Golgi traffic; the TRAPPII complex would mediate exit from the Golgi as well as TGN functions. The GARP complex is also thought to reside on the TGN, where it tethers early and late endocytotic vesicles (Quenneville et al., 2006). From the trans-Golgi, secretion to the plasma membrane would be mediated by the exocyst, whereas vesicles destined for the pre-vacuolar compartment and the vacuole would be tethered by the HOPS (or VPS) complex. Finally, retrograde traffic from the Golgi to the ER would be mediated by the Dsl1 complex on the ER membrane. The TRAPPIII complex is an unknown entity in plants. Rab-GTPases involved in certain trafficking steps (Vernoud et al., 2003) are depicted in green.

The process of vesicle traffic is highly conserved in eukaryotic cells and can be broken down into six steps: budding off the donor membrane and vesicle formation, transport to the target membrane, tethering, docking via SNARE complex formation, fusion and recycling of SNAREs (Fig. 1.3.2). A large number of molecules involved in vesicle trafficking have been intensively studied over past few decades, including coat proteins (clathrin, COPII, COPI), ADP-ribosylation factors (Arfs), tethering factors, soluble N-ethylmaleimide-sensitive factor attachment proteins receptors (SNAREs) and Rab GTPases (Yu and Hughson, 2010).

The Arf GTPases are involved in vesicle formation, as they recruit cytosolic coat proteins to the place of vesicle budding (Vernoud et al., 2003). Vesicle transport occurs via motor proteins and microtubule-associated proteins (Jürgens, 2005). The Rab GTPases are key regulators of membrane traffic at multiple stages of vesicle traffic, including cargo selection, vesicle tethering and membrane fusion. They cycle between inactive, GDP-bound and active GTP-bound form (Sclafani et al., 2010). Rab GTPases constitute the largest family of the small GTP-binding protein superfamily in *Arabidopsis*. Phylogenetic analysis of *Arabidopsis* genome identified 57 AtRab GTPases, which based on sequence similarity were divided into eight subclasses (Rab-A – Rab-H; Vernoud et al., 2003). Distinct subclasses are present in cytosol, as well as associated to the specific membrane compartment, where they play role in vesicle trafficking (Fig. 1.3.1; Stenmark and Olkkonen, 2001; Zerial and McBride, 2001). Rab-A2 and Rab-A3 GTPases were reported to label TGN/EE compartment and the cell plate throughout cytokinesis (Chow et al., 2008).

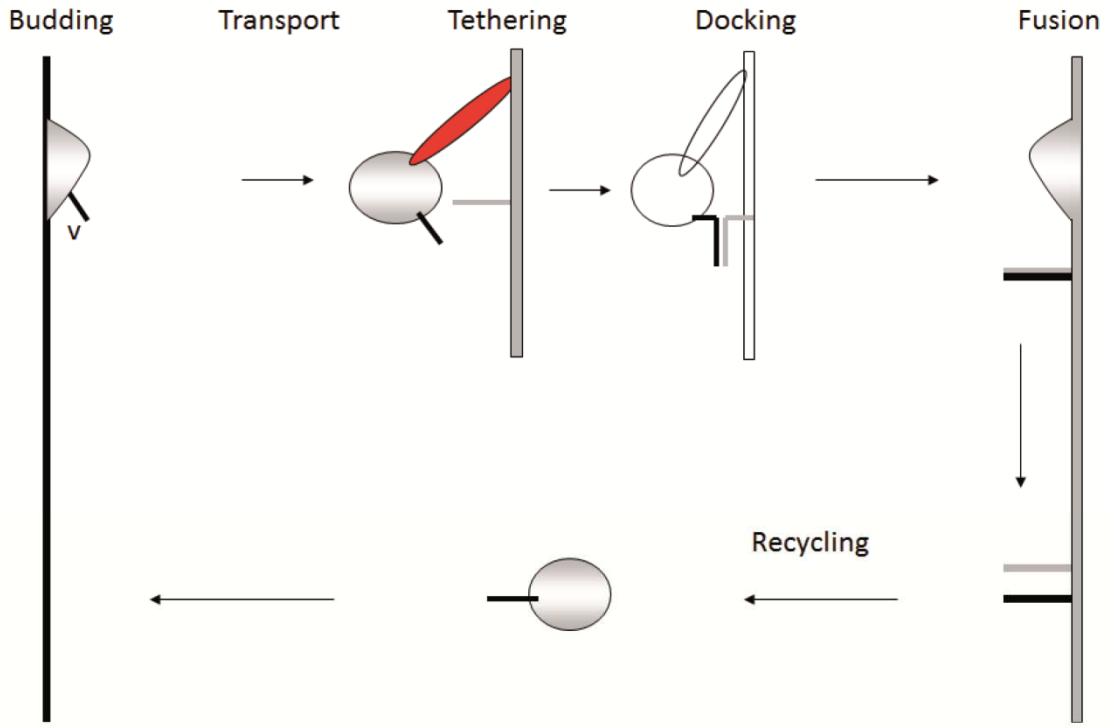

Figure 1.3.2. Six major steps in vesicle traffic.
Adapted from Assaad (2008). A vesicle bud off the donor membrane and subsequently is transported to the target membrane. There a vesicle is tethered by tethering factors and docked via SNARE pin formation to the target membrane. After fusion of vesicle and target membrane, v- and t-SNARE are recycled.

Vesicle fusion is mediated via SNAREs. They are highly conserved coiled-coil membrane-bound proteins, which together with their regulators (Sec1/Munc18) SM proteins are required for membrane fusion in the secretory pathway. *Arabidopsis* genome encodes 54 SNAREs (Uemura et al., 2004), which are divided into t-SNARE (Qa-, Qb-, Qc-SNARE; resides on a target membrane) and v-SNARE (R-SNARE/VAMPs; resides on the transport vesicle). SNARE complex is formed by four-helix bundle that consists of three t- and one v-SNAREs (El Kasmi et al., 2013). After the vesicle is tethered to the target membrane, localized on vesicle v-SNARE interacts with t-SNARE to form a trans-SNARE complex (the SNARE-pin). Subsequently, membrane fusion leads to the cis-SNARE complex formation (Südhof and Rothmann, 2009). After vesicle fuses to the target membrane, the SNARE complex undergoes dissociation by N-ethylmeleimide-sensitive factor (NSF) and recycles (Uemura et al., 2004). SM proteins are accepted to play an important role in trans-SNARE complex formation (Südhof and Rothmann, 2009); they bind to t-SNARE in its closed form and mediate conformational changes leading to an open form of t-SNARE. Cell plate localized t-SNARE/SYP111/KNOLLE is the only specific SNARE involved in cytokinesis so far (Lauber et al., 1997). KNOLLE was shown to interact with SM protein KEULE (Waizenegger et al., 2000; Assaad et al., 2001), t-SNARE AtSNAP33 protein (Heese et al., 2001) and t-SNARE11/NPSN11 (Zheng et al., 2002) and, v-SNARE VAMP721/VAMP722 (Zhang et al., 2011; El Kasimi et al., 2013).

1.3.1. Trans-Golgi network (TGN).

The trans-Golgi network (TGN) is a highly dynamic, tubular-vesicular organelle that develops from the most trans-Golgi cisternae (Kang et al., 2011). It was also reported that the TGN can mature into multivesicular bodies (MVBs; Scheuring et al., 2011). Currently, there are two models for TGN maturation in plants. The first one, proposed by Viotti et al. (2010) suggests that the TGN is a semipernament organelle that cycles onto and off the trans side of the Golgi stack. According to a second model, proposed by Kang et al. (2011), the TGN undergoes a maturation process via cisternal fragmentation. Golgi-associated (GA-) TGN matures into free independent, detached from the Golgi late TGN that produces secretory (SV) and clathrin coated (CCV) vesicles. The differences between these two models might result from the fact that Viotti et al. (2010) used spinning disc confocal microscopy and Kang et al. (2011) more precise electron microscopy and tomography. Recently, Uemura et al. (2014), with the help of the super-resolution confocal live imaging microscopy (SCLIM) technique identified existence of two types of TGN in plants, the Golgi-associated TGN (GA-TGN) located on the trans-side of the Golgi apparatus and the Golgi-released independent

TGN (GI-TGN). The TGN is thought to play role as a major sorting station where endocytic and secretory pathways converge (Dettmer et al., 2006; Chow et al., 2008). Moreover, the TGN was shown to function as an early endosome (Dettmer et al., 2006; Robinson et al., 2008; Viotti et al., 2010).

1.3.2. Tethering and tethering factors

Tethering process refers to an initial specific physical contact between the trafficking vesicle and the target membrane (Cao et al., 1998). Tethering factors were shown to act upstream of SNAREs in order to facilitate recognition before the membrane fusion (Sztul and Lupashin, 2006). Two types of tethering factors have been identified: long coiled-coil proteins and large multi-subunit complexes (Barrowman et al., 2010). Nine tethering factors have been discovered so far. Each of them is localized on a specific membrane compartment and mediates specific membrane fusion events (Fig. 1.3.1; Kim et al., 2005). That includes Dsl1 (dependence on Sly1), COG (conserved oligomeric Golgi), HOPS (homotypic fusion and vacuole protein sorting), TRAPP (transport protein particle, of which there are three forms), CORVET (class C corevacuole/endosome tethering), GARP (Golgi-associated retrograde protein) and exocyst (Whyte and Munro, 2002; Barrowman et al., 2010).

As tethering factors provide an initial contact between donor and acceptor membranes, and the cell plate is formed via vesicle fusion that raises a question, which tethering factors are required for cell plate assembly. That would give us an information about the cell plate origin. If cell plate is formed via fusion of Golgi-derived vesicles then TRAPPI and TRAPPII complexes would be involved in cytokinesis. If endocytosis would play a role in cell plate assembly, mutants in GARP complex would exhibit cytokenesis-defective phenotype. Requirement of TRAPPII or exocyst complex in cell plate assembly would give it TGN or plasma membrane identity, respectively.

1.3.2.1. TRAPPII tethering complex

TRAPP stands for transport protein particle. The multi-subunit TRAPP complex was first identified in yeast, in a genetic screen where the TRAPP blocked early in transport 3 (Bet3p) subunit was found to interact with the ER to Golgi t-SNARE Bet1p. Biochemical approaches using tagged Bet1p led to TRAPP complex isolation (Sacher et al., 1998). Later, gel filtration chromatography of yeast lysates resulted in identification of two forms of TRAPP tethering complex: the TRAPPI and the TRAPPII. Each of them acts at different stage in membrane trafficking (Sacher et al., 2001). Both complexes consist of six-core subunits: Bet3 (two copies), Bet5, TRAPP subunit 20

(Trs20), Trs23, Trs31, Trs33. TRAPPII contains additionally Trs120, Trs130 and Trs65 subunits. An additional subunit, the TRAPPII-associated protein 17 (Tca17), was shown to be a substoichomertic component of TRAPPII, but its role in membrane trafficking is not clear (Montpetitt and Conibear, 2009; Scrivens et al., 2009). Choi et al. (2011) proposed Tca17 to be a stable subunit of the TRAPPII complex in yeast.

Another TRAPP subunit, the Trs85p (also known as GSG1), was initially identified as the subunit of the TRAPPI complex via affinity purification (Sacher et al., 1998), but its function in TRAPPI was not clear. Later studies showed that Trs85p is a component of a third type of TRAPP complexes, the TRAPPIII, which is composed of all seven subunits formally identified as TRAPPI (Sacher et al., 1998), whereas the real TRAPPI complex consists only of six subunits (seven subunits including two copies of Bet3). TRAPPIII tethering complex is required for the macroautophagy and the cytosol to vacuole (CVT) pathway (Lynch-Day et al., 2010). All TRAPP subunits except for Trs33, Trs65, Trs85 and Tca17 have been shown to be essential in yeast (Cox et al., 2007; Choi et al., 2011).

All three TRAPPs complexes contain a guanine nucleotide-exchange factor (GEF) activity that is required for activation of the target Rab (Barrowman et al., 2010). Little is known about the TRAPPII complex in plants. All TRAPPII subunits found in yeasts except for Trs65 are conserved in plants (Table 1.3.1; Cox et al., 2007; Koumandou et al., 2007; Klinger et al., 2013). As TRAPPII resides on TGN and mediates exocytosis and endocytosis in yeast (Cai et al., 2005), it would be interesting to examine these processes in plants.

Yeast subunit	Mammalian subunit	TRAPP complex	*Arabidopsis* homolog
Bet5	C1	I and II	At1g51160
Trs20	C2	I and II	At2g20930
Bet3	C3	I and II	At5g54750
Trs23	C4	I and II	At5g02280
Trs31	C5	I and II	At5g58030
Trs33	C6	I and II	At3g05000
Trs85	KIAA1012	III	At5g16280
Tca17	C2L	II	At1g80500
Trs65	-	II	-
Trs120	C9	II	At5g11040
Trs130	C10	II	At5g54440

Table 1.3.1. TRAPP tethering complex subunits and their *Arabidosis* homologues. Adapted from Thellmann et al. (2010).

1.3.2.2. Exocyst tethering complex.

The exocyst complex was first identified in yeast and was shown to tether vesicles to the bud tip and to the cleavage furrow (TerBush et al., 1996). The exocyst tethering complex consists of eight subunits: Sec3, Sec5, Sec6, Sec8, Sec10, Sec15, Exo70 and Exo84 and plays role in tethering vesicles to the plasma membrane (Boyd et al., 2004; He et al., 2007; Heider and Munson, 2012). The exocyst complex was shown to be required for polarized secretion (Novick et al., 1980, Guo et al., 1999a, Heider and Munson, 2012) and constitutes an effector for several small GTP-binding proteins that directly interact with the exocyst and spatially regulate exocytosis in cells (He and Guo, 2009). The exocyst is one of the most extensively studied tethering complex in plant science. The complex is important for *Arabidopsis* morphogenesis, germination, pollen tube growth and hypocotyl elongation (Synek et al., 2006; Cole et al., 2007; Hala et al., 2008). As cytokinesis is considered to be a specialized form of polarized secretion, it would be interesting to examine the role of the exocyst in cell division. Phylogenetic analyses showed that all of exocyst subunits are conserved among eukaryotic cells and present in land plants (Cvrckova et al., 2001; Elias et al., 2003; Koumandou et al., 2007). Many exocyst subunits in plants are encoded by single or multiple genes, there are for example twenty three EXO70 paralogues in *Arabidopsis* (Synek et al., 2006).

1.3.2.3. GARP tethering complex.

GARP stands for Golgi-associated retrograde protein. The GARP complex was first identified in yeast genetic screens (Conibear and Stevens, 2000; Conibear et al., 2003). It is a tetrameric complex that consists of vacuolar protein sorting 51 (Vps51), Vps52, Vps53 and Vps54. The GARP complex resides on the TGN in yeast and has been implicated in endocytosis via tethering endosome-derieved vesicles at the TGN (Conibear et al., 2003; Cai et al., 2005; Quenneville et al., 2006). The GARP complex was shown to be conserved in higher eukaryotic cells (Koumandou et al., 2007). In *Arabidopsis*, the GARP complex was reported to be required for pollen tip growth (Lobstein et al., 2004; Guermonprez et al., 2008) and resistance to heat and osmotic stress (Lee et al., 2006; Wang et al., 2011). Homozygous mutants in GARP genes are embryo lethal (Lobstein et al., 2004; Guarmonprez et al., 2008). Recently, a fourth subunit, Vps51, has been shown to be required for leaf shape and vein pattern (Pahari et al., 2014).

1.4. Objectives.

The first aim of this study was to search for cytokinesis-defective mutants in tethering factors of *Arabidopsis thaliana* and to use these to define the origin and identity of cell plate membranes. To achieve this, a reverse genetic approach was taken. I focused on the TRAPPI and TRAPPII complexes as they mediate the flow of traffic through the Golgi and at the trans-Golgi network, as well as on the GARP complex, thought to be required for tethering of endocytic vesicles to the trans-Golgi network. Molecular and phenotypic analyses were carried out to characterize the mutants.

The cell plate is formed via vesicle fusion. Tethering is an initial specific physical contact between a vesicle and its target membrane that occurs prior to fusion. Tethering is mediated by tethering factors and different tethering factors could potentially play a role in cytokinesis. I focused on the TRAPPII tethering complex because it mutated to the strongest cytokinesis-defective phenotypes in our screen. In addition, I compared the TRAPPII complex to the exocyst complex, which has also been implicated in cytokinesis. Immunostain analyses were carried out to assess, which of them is involved in cell plate biogenesis. Additionally, the same approach was undertaken to test which tethering factor is involved in cross wall maturation.

The next goal was to determine the intracellular localization of the TRAPPII tethering complex. In order to do so, cell fractionation and live imaging were carried out. Furthermore, as the TRAPPII complex seems to play an important role in cytokinesis, I decided to monitor its localization dynamics throughout cytokinesis and additionally to compare this to the localization dynamics of another tethering complex, the exocyst.

The cell plate is a specialized trans-Golgi compartment and the trans-Golgi network is a major sorting station for membrane proteins. As the endocytosis and exocytosis pathways converge at the trand-Golgi network, both processes were analyzed of in TRAPPII mutants. An additional aim of this study was to test whether or not the TRAPPII complex is required for protein sorting at the cell plate. To this effect, different trans-Golgi network and cell plate markers were monitored in TRAPPII mutant backgrounds.

Finally, immunoprecipitation assays and mass spectrometry analyses were performed in order to identify interactors of the *Arabidopsis* TRAPPII complex.

2. Materials and Methods.

2.1. Materials.

2.1.1. Equipment.

Equipment	Model	Company
Centrifuge	Eppendorf 5415D	Eppendorf AG, Hamburg
	Eppendorf 5424R	Eppendorf AG, Hamburg
	Beckman Avanti J-25	Beckman Coulter Inc., Brea, USA
	Beckman L 7-55 Ultracentrifuge	Beckman Coulter Inc., Brea, USA
Centrifuge rotor	JA-25.50	Beckman Coulter Inc., Brea, USA
	JA-10	Beckman Coulter Inc., Brea, USA
	Type 75Ti	Beckman Coulter Inc., Brea, USA
Chemiluminescence detection system	LAS4000 mini	Fujifilm, FUJIFILM Europe GmbH, Düsseldorf
Confocal laser scanning microscopy	Fluoview FW1000	Olympus
Electroporator	Eppendorf Eporator	Eppendorf AG, Hamburg
Gel documentation		Backofer Laborgeräte, Reutlingen
Saple Mixer	HulaMixer™ Sample Mixer	Invitrogen, USA
Lab balance	Sartorius Analytic A200S	Sartorius AG, Göttingen
	Sartorius BP110S	Sartorius AG, Göttingen
	GT 2100	Ohaus Corporation, Parsippany, USA
Lyophilizer	Lyovac GT2	Amsco Finn-Aqua GmbH, Hürth
Incubator	UF4000	Memmert GmbH & Co. KG, Schwabach
PCR Cycler	Thermocycler ep Gradient	Eppendorf AG, Hamburg
pH-meter	pH 526	WTW GmbH, Weilheim
Photometer	Ultrospec 3000	Pharmacia Biotech., Sweden
Pipette (0.2µl-5ml) pipetman	Gilson	Gilson Inc., Middleton, USA
Power Supply Unit	E844 (400 V- 400 mA)	Consort bvba, Belgium
Pure water system	Milli-Q Academic System	Millipore Corporation, Billerica, USA
SDS-PAGE unit	Mini-PROTEAN Tetra Cell	Bio-Rad Laboratoris Inc., Hercules, USA
Sterile bench	Microflow Laminar Flow Workstation	Nunc HmbH, Wiesbaden-Biebrich
Stereo Microscope	SZX12	Olympus
Thermomixer	Comfort	Eppendorf AG, Hamburg
ThermoShaker	Laboshake	C.Gerhardt GmbH & Co. KG, Königswinter
Vortex	MS-1 MiniShaker	IKA-Werke GmbH, Staufen

2.1.2. Bacterial strains.

Escherichia coli (*E. coli*) strains used in this study:

Strain	Genotype	Obtained from
DH5α	F– Φ80*lac*ZΔM15 Δ(*lac*ZYA-*arg*F) U169 *rec*A1 *end*A1 *hsd*R17 (rK–, mK+) *pho*A *sup*E44 λ– *thi*-1 *gyr*A96 *rel*A1	Invitrogen
DB3.1	F– *gyr*A462 *end*A1 Δ(sr1-*rec*A) *mcr*B *mrr hsd*S20(rB–, mB–) *sup*E44 *ara*-14 *gal*K2 *lac*Y1 *pro*A2 *rps*L20(SmR) *xyl*-5 λ– *leu mtl*1	Invitrogen
TOP10	F– mcrA Δ(mrr-hsdRMS-mcrBC) φ80lacZΔM15 ΔlacX74 recA1 araD139 Δ(ara-leu)7697 galU galK rpsL (Str^R) endA1 nupG	Invitrogen
BL21 (DE3)	F– ompT $hsdS_B$ (r_B-m_B-) gal dcm (DE3)	Invitrogen

Agrobacterium tumefaciens (*A. tumefaciens*) strains used in this study:

Strain	Genotype	Resistance	Obtained from
C58pGV3101:: pPM90	Ti-Plasmid: pPM90 (Koncz and Schell, 1986)	rif^R, $gent^R$	Csaba Koncz (MPI Cologne)
C58pGV3101:: pMP90RK	Ti-Plasmid: pPM90 (Koncz and Schell, 1986)	rif^R, $gent^R$, kan^R	Csaba Koncz (MPI Cologne)

2.1.3. Antibiotics.

Antibiotic	Stock solution	Working solution	Preparation
Carbanicilin	10 mg/ml	20 µg/ml	dissolved in H_2O and sterilized by filtration (0.22 µm)
Chloramphenicol	10 mg/ml	25 µg/ml	dissolved in methanol
Gentamycin	10 mg/ml	20 µg/ml	dissolved in H_2O and sterilized by filtration (0.22 µm)
Kanamycin	10 mg/ml	25 µg/ml (for bacterial culture) 50 µ/ml (for plant cultures)	dissolved in H_2O and sterilized by filtration (0.22 µm)
Rifampicin	10 mg/ml	100 µg/ml	dissolved in methanol

All antibiotic stock solutions were stored at -20˚C.

2.1.4. Chemicals.

All chemicals used in this work were obtained from Sigma-Aldrich (Munich, Germany), Roth (Carl Roth GmbH & Co. KG, Karlsruhe, Germany) or Merck KGaA (Darmstadt, Germany).

2.1.5. Plant material.

The *Arabidopsis thaliana* insertion lines used in this study were in the Columbia ecotype (Col-0) background and this ecotype was used as a wild type control (Table S1). Seeds were obtained from Nottingham Arabidopsis Sock Centre (NASC; http://arabidopsis.info; Scholl et al., 2000); or Arabidopsis Biological Recourse Center (ABRC; https://abrc.osu.edu), as well as from the Institut National de la Recherche Agronomique (http://www-ijpb.versailles.inra.fr; Samson et al., 2002) and GABI (https://www.gabi-kat.de; Rosso et al., 2003).

2.1.6. Primers.

Primers were obtained from MWG Operon (Ebersberg) as lyophilized salt-free or HPLC purified stocks. Primer3 and Oligo Calc: Oligonucleotide Properties Calculator online software's were used to design primers for genotyping and cloning/sequencing, respectively. Cloning primers are listed in chapter 2.2.1.6. Primers used for genotyping

of insertion lines and for complementation analysis are presented in Table S2. Primers used for sequencing are shown in Table S3.

2.1.7. Molecular markers.

2.1.7.1. DNA markers.

GeneRuler™ 100bp DNA Ladder and GeneRuler™ 1kb DNA Ladder (Fermentas, Thermo Scientific) were used as DNA markers.

2.1.7.2. Protein markers.

PageRuler^{TM} Prestained Protein Ladder (Fermentas, Thermo Scientific) was used in this study.

2.2. Methods.

2.2.1. Methods for DNA analysis.

2.2.1.1. Genomic DNA isolation from plants.

Method of genomic DNA isolation from plant tissue was modified after Murray and Thompson (1980). A single leaf or bud was grinded in a eppendorf tube and incubated with 300 µl 2 x CTAB buffer at 65°C for at least twenty minutes. Subsequently, 300 µl of chloroform-isoamyl alcohol was added to the cooled sample. The sample was vortexed and spun down to separate the phases. The upper, aqueous phase was transferred into a fresh reaction tube and well mixed with 300 µl 2-propanol. After ten minutes of centrifugation (18000 x g) the supernatant was removed and the pellet was washed with 500 µl 70% ethanol. The sample was again briefly centrifuged and supernatant was removed. Subsequently, the pellet was left to dry at room temperature. At the end, the pellet was dissolved in 50-100 µl of 1 x TE buffer. 1 µl was used in a PCR reaction.

2 x CTAB buffer	2% Cetyl-Trimethyl-Ammonium Bromide (CTAB) (w/v) 1.4 M NaCl 100 mM Tris-HCl pH 8.0 20 mM EDTA pH 8.0
1 x TE buffer	10 mM Tris-HCl pH 8.0 1 mM EDTA pH 8.0

Chloroform-isoamyl alcohol (24:1)

2-propanol

70% ethanol (v/v)

2.2.1.2. Polymerase Chain Reaction (PCR).

PCR analysis was carried out with GoTag (Promega) for standard purposes or with high fidelity PfuUltra II Fusion HS DNA Polymerase (Agilient Technology inc., Santa Clara, USA) for cloning purposes. Additionally, polymerase KAPA3G (PEQLAB) was used for DNA amplification from crude plant samples. Standard 100 ng of DNA was used per PCR reaction. Components of PCR reaction and PCR conditions are presented below.

PCR mix components	Final concentration
DNA template	10-100 ng
5x Buffer	1x
$MgCl_2$ (7.5 mM)	1.5 mM
dNTPs (10 mM)	0.2 mM
Primer (100 pM/µl)	10 pM
Primer (100 pM/µl)	10 pM
Polymerase (5 U/µl)	0.5 U

Standard PCR conditions used in this study:

Duration	T [°C]	Number of cycles
2 min	95	1
1 min	95	22-40[b]
1.5 min	50-65[a]	
2 min[c]	72	
5 min	72	1

a: Annealing temperature was optimized for each primer pair. b: Number of cycles depends on the template (genomic, cDNA). For genotyping, 38 cycles were used with GoTag and 40 cycles with KAPA3G polymerase. 30-32 cycles were used for colony PCR wirth GoTag polymerase. To amplify inserts, 22-24 cycles were used with PfuUltra II Fusion HS DNA Polymerase. c: Elongation depends on the length of the amplified fragment (0.5-1 kb/min).

2.2.1.2.1. Colony PCR.

Colony PCR was used to determine whether or not a specific colony on plate possesses the plasmid of interest. The pipette tip was used to scratch a part of the bacterial colony off the plate. The tip was dipped into 5 µl sterile water and stirred to release the bacteria, which were then incubated for ten minutes at 95°C. The PCR reaction was performed in 20 µl of final volume as described above using GoTag DNA Polymerase.

2.2.1.3. Electrophoresis of DNA on agarose gels.

DNA was analyzed by agarose gel electrophoresis. Gels (0.8-2.0%) were prepared on the basis of the Ultra-Pure Agarose and TAE buffer. Agarose was dissolved in 1 x TAE by heating to the boil in a microwave and subsequently cooled to about 60°C. Afterwards, ethidium bromide was added (final concentration 1 µg/ml). The solution was poured into a casting tray containing a sample comb. After the gel solidified at room temperature, the comb was removed, and the casting tray containing the gel was inserted into the electrophoresis chamber and covered with 1 x TAE buffer. DNA samples were mixed with 6 x loading dye and then were put on the gel into the sample wells. Gel was run at 200 V and 400 mA.

50 x TAE buffer	242 g/l Tris-Base 57.1 ml/l Acetic Acid 100 ml/l 0.5 M EDTA pH 8.0
6 x Loading dye	50% Glycerol (v/v) 0.25% Orange G (w/v) 1 mM EDTA pH 8.0
Ethidium bromide stock solution	10 mg/ml Ethidium Bromide (w/v)

2.2.1.4. DNA Sequencing.

Sequencing was performed by MWG Operon (Ebersberg). Samples of total volume 15 µl containing purified plasmid DNA (50-100 ng/µl) or purified PCR product (5 ng/µl or 10 ng/µl for 300-1000 bp or 1000-3000 bp length fragments, respectively) were prepared. Primers were provided at a concentration of 10 pmol/µl.

2.2.1.5. Vector design and sequence analysis.

DNA constructs were designed using Vector NTI® Software (Invitrogen). Nucleotide and amino acid sequence analyses were carried out with Basic Local Alignment Search Tool (BLAST; http:// blast.ncbi. nlm.nih.gov/Blast.cgi) and Expert Protein Analysis System (ExPASy; http://www.expasy.org/), respectively.

2.2.1.6. Cloning.

Standard molecular techniques were used for cloning and subcloning (Sambrook et al., 1989). PCR analysis was carried out with high fidelity PfuUltra II fusion HS DNA Polymerase for gene fusions (Agilent Technology inc., Santa Clara, USA). Restriction enzymes were from Promega, NEB or Fermentas. T4 DNA Ligase was from Promega and Antarctic Phosphatase from New England Biolabs (NEB). P_{UBQ}::TRS120-GFP and P_{UBQ}::TRS130/CLUB-GFP gene fusions were constructed by inserting the AtTRS120 and AtTRS130/CLUB genomic sequences in the modified binary vector pCAMBIA2300-GFP. P_{TRS120}::TRS120-GFP was constructed by replacing the UBQ promoter in P_{UBQ}::TRS120-GFP with 1kb of endogenous genomic DNA upstream of the AtTRS120 coding sequence. P_{UBQ}::TRS120-mCherry was constructed by replacing GFP with mCherry in P_{UBQ}::TRS120-GFP. P_{35S}::GFP-TRS120 was cloned into pEGAD vector (Cutler et al., 2000). Y2H and BiFC constructs, as well as C- and N-terminal HA and Myc protein fusion constructs were constructed via the Gateway system (Invitrogen). P_{CLUB}::CLUB-HA and P_{TRS120}::TRS120-HA were constructed in the pEarleyGate 301 vector (ABRC; Earley et a., 2006). P_{35S}::3xHA-CLUB and P_{35S}::3xHA-TRS120 were cloned into pJawohl2B-3HA (Isono et al., 2010). P_{35S}::5xMyc-CLUB and P_{35S}::5xMyc-CLUB were constructed in the pJawohl2C-5xMyc (obtained internally). cDNA sequences of AtTRS130/CLUB and AtTRS120 were cloned into pUBN-nYFP-Dest, pUBN-cYFP-Dest, pUBC-nYFP-Dest, pUBC-cYFP-Dest (Grefen et al., 2010), pDEST-VYNE(R)^{GW} and pDEST-VYCE(R)^{GW} (Gehl et al., 2009) for BiFC purpose and into pDEST-AD and pDEST-DB (Yu et al., 2011) for Y2H experiments. Antigens (CLUB-1 and CLUB-2) for anti-CLUB antibody development were constructed via TOPO® cloning technology (Invitrogen) in pET101/D-TOPO® (Invitrogen). A full length CLUB cDNA was cloned into pET24a(+) (Novagen) and subsequently, a fragment of 1892 bp was subconed due to the 5-bp deletion (1602-1606). Exocyst GFP fusions used in this study were obtained from Viktor Zarsky (IEB, Prague) and have been described elsewhere (Fendrych et al., 2010).

Constructs for cellular localization and co-immunoprecipitation:

Construct	*Arabidopsis thaliana* line	Vector	Template	Primers sequence	
P_{UBQ}:CLUB-GFP	Columbia	pCambia2300-GFP AscI/AatII	F24B18	Forward	5'-ATAGGCGCGCCATGGCGAACT ACT-3'
				Reverse	5'-TATGACGTCCTTGACAGGTAAG CAGT-3'
P_{UBQ}::TRS120-GFP	*trs120-4*/+	pCAMBIA2300-GFP AscI/AatII	pBeloBAC11	Forward	5'-ATAGGCGCGCCATGGAACCTG TCG-3'*
				Reverse	5'-TATGACGTCCAGTGCACCTCCA GCTA-3'
P_{TRS120}::TRS120-GFP	*trs120-4*/+	P_{UBQ}::TRS120-GFP KpnI/AscI	pBeloBAC11	Forward	5'-ATAGGTACCTAGAGAGCCCATG CAATAAAGGAG-3'
				Reverse	5'-TATGGCGCGCCGGCGAGATCA GAGAAGGA-3'
P_{UBQ}::TRS120-mCherry	Columbia, P_{UBQ}::GFP-EXO70A1 (Fendrych et al., 2010)	P_{UBQ}::TRS120-GFP AatII/XbaI	mCherry-mini-SOG C1 (Shu et al., 2011)	Forward	5'-ATATCTAGACTCCGGATTACTT GTACAGCTCGTCCATGCCGCCGG TGGAGTGGCGGCCC-3'
				Reverse	5'-ATAGACGTCGCTGCTGCCGCT GCCGCTGCGGCAGCGGCCATGGT GAGCAAGGGCGAGGAG-3'
P_{35S}::GFP-TRS120	Col-0	pEGAD SmaI/XbaI	pBeloBAC11	Forward	5'-ATACCCGGGGAACCTGACGT CAGTATCGAGACT-3'
				Reverse	5'-ATATCTAGACTCACGTATGTAAG AAAAAGTGGG-3
P_{TRS120}::TRS120-HA	*trs120-3*/+	pEarlyGate301	pBeloBAC11	Forward	5'-GGGGACAAGTTTGTACAAAAAA GCAGGCTCCAGACTTGACAGTAAC AATAGGCA-3'
				Reverse	5'-GGGGACCACTTTGTACAAGAAA GCTGGGTCCTTGACAGGTAAGCA GTAGGAAGAA-3'
P_{CLUB}::CLUB-HA	*club-2*/+	pEarlyGate301	F24B18	Forward	5'-GGGGACAAGTTTGTACAAAAAA GCAGGCTCTGGTACCTTTAGAGAG CCCATGCA-3'
				Reverse	5'-GGGGACCACTTTGTACAAGAA AGCTGGGTCCAGTGCACCTCCAG CTACACAGACA-3'
P_{35S}::3xHA-CLUB	*club-2*/+	pJawohl2B-3HA	F24B18	Forward	5'-GGGGACAAGTTTGTACAAAAA AGCAGGCTTCATGGCGAACTACT TGGCTCAGTTC C-3'
				Reverse	5'-GGGGACCACTTTGTACAAGAAA GCTGGGTCTTACTTGACAGGTAA GCAGTAGGAA-3'
P_{35S}::3xHA-TRS120	*trs120-3*/+	pJawohl2B-3HA	pBeloBAC11	Forward	5'-GGGGACAAGTTTGTACAAAAA AGCAGGCTTCATGGAACCTGACG TCAGTATCGAGA-3'
				Reverse	5'-GGGGACCACTTTGTACAAGAAA GCTGGGTCTCACAGTGCACCTC CAGCTACACAG-3'
P_{35S}::5xMyc-CLUB	*club-2*/+	pJawohl2C-5Myc	F24B18	Forward	5'-GGGGACAAGTTTGTACAAAAA AGCAGGCTTCATGGCGAACTACT TGGCTCAGTTCC-3'
				Reverse	5'-GGGGACCACTTTGTACAAGAA AGCTGGGTCTTACTTGACAGGTA AGCAGTAGGAA-3'
P_{35S}::5xMyc-TRS120	*trs120-3*/+	pJawohl2C-5Myc	pBeloBAC11	Forward	5'-GGGGACAAGTTTGTACAAAAA AGCAGGCTTCATGGAACCTGAC GTCAGTATCGAGA-3'
				Reverse	5'-GGGGACCACTTTGTACAAGAA AGCTGGGTCTCACAGTGCACCTC CAGCTACACAG-3'

* In the forward primer for P_{UBQ}::TRS120-GFP, GAC was replaced by GTC to optimize restriction enzyme sites for subcloning.

Constructs for BiFC:

Construct	Bacterial strain	Vector	Template	Primers sequence	
P_{UBQ10}::nYFP-CLUB	DH5α	pUBN-nYFP-Dest	pET24a(+) CLUB	Forward	5'-GGGGACAAGTTTGTACAAAAAAGCAGGCTTCATGGCGAACTACTTGGCTCAGTTCC-3'
				Reverse	5'-GGGGACCACTTTGTACAAGAAAGCTGGGTCTTACTTGACAGGTAAGCAGTAGAA-3'
P_{UBQ10}::cYFP-CLUB	DH5α	pUBN-cYFP-Dest	pET24a(+) CLUB	Forward	5'-GGGGACAAGTTTGTACAAAAAAGCAGGCTTCATGGCGAACTACTTGGCTCAGTTCC-3'
				Reverse	5'-GGGGACCACTTTGTACAAGAAAGCTGGGTCTTACTTGACAGGTAAGCAGTAGGAA-3'
P_{UBQ10}::CLUB-nYFP	DH5α	pUBC-nYFP-Dest	pET24a(+) CLUB	Forward	5'-GGGGACAAGTTTGTACAAAAAAGCAGGCTTCATGGCGAACTACTTGGCTCAGTTCC-3'
				Reverse	5'-GGGGACCACTTTGTACAAGAAAGCTGGGTCCAGTGCACCTCCAGCTACACAGACA-3'
P_{UBQ10}::CLUB-nYFP	DH5α	pUBC-cYFP-Dest	pET24a(+) CLUB	Forward	5'-GGGGACAAGTTTGTACAAAAAAGCAGGCTTCATGGCGAACTACTTGGCTCAGTTCC-3'
				Reverse	5'-GGGGACCACTTTGTACAAGAAAGCTGGGTCCAGTGCACCTCCAGCTACACAGACA-3'
P_{35S}::nVenus-CLUB	DH5α	pDEST-VYNE(R)^{GW}	pET24a(+) CLUB	Forward	5'-GGGGACAAGTTTGTACAAAAAAGCAGGCTTCATGGCGAACTACTTGGCTCAGTTCC-3'
				Reverse	5'-GGGGACCACTTTGTACAAGAAAGCTGGGTCTTACTTGACAGGTAAGCAGTAGGAA-3'
P_{35S}::cVenus-CLUB	DH5α	pDEST-VYCE(R)^{GW}	pET24a(+) CLUB	Forward	5'-GGGGACAAGTTTGTACAAAAAAGCAGGCTTCATGGCGAACTACTTGGCTCAGTTCC-3'
				Reverse	5'-GGGGACCACTTTGTACAAGAAAGCTGGGTCTTACTTGACAGGTAAGCAGTAGGAA-3'

Constructs for generation of an antibody against CLUB/AtTRS130:

Construct	Bacterial strain	Vector	Template	Primers sequence	
P_{UBQ10}::CLUB CLUB-1-V5/6xHIS	BL21	pET101/D-TOPO®	RAFL09-39-B05	Forward	5'-CACCATGTCAAAAAAGAGAGAAAGGTGCTGTAA-3
				Reverse	5'-TGATCCTTCAGTAAAACTTGGGCG-3'
P_{UBQ10}::CLUB CLUB-2-V5/6xHIS	BL21	pET101/D-TOPO®	RAFL09-39-B05	Forward	5'-CACCATGCTGAATATCAAATATGGAATCCATGG-3'
				Reverse	5'-TTCACTTTCTTTGAGTTCTTTAAGCCTTTC-3'
P_{T7}::CLUB-T7/ HIS	BL21	pET24a(+) BamI/XhoI	RAFL09-39-B05	Forward	5'-ATACTCGAGCTTGACAGGTAAGCAG-3'
				Reverse	5'-ATAGGATCCATGGCGAACTACTTGG-3'
P_{T7}::CLUB-T7/ 6xHIS	BL21	P_{T7}::CLUB-T7/ HIS Bsp119I/Bsp1407I	cDNA from Col-0	Forward	5'-ATATTCGAAAAGCTATGAGACCTGAATC-3'
				Reverse	5'-ATATGTACATGGCCCTGAAGGAAATTTTT-3'

Constructs for yeast two hybrid assay:

Construct	Bacterial strain	Vector	Template	Primers sequence	
P_{ADH1}::CLUB-GAL4 AD	DH5α	pDEST-AD	pET24a(+) CLUB	Forward	5'-GGGGACAAGTTTGTACAAAAAAGCAGGCTTCATGGCGAACTACTTGGCTCAGTTCC-3'
				Reverse	5'-GGGGACCACTTTGTACAAGAAAGCTGGGTCTTACTTGACAGGTAAGCAGTAGAA-3'
P_{ADH1}::CLUB-GAL4 DB	DH5α	pDEST-DB	pET24a(+) CLUB	Forward	5'-GGGGACAAGTTTGTACAAAAAAGCAGGCTTCATGGCGAACTACTTGGCTCAGTTC C-3'
				Reverse	5'-GGGGACCACTTTGTACAAGAAAGCTGGGTCTTACTTGACAGGTAAGCAGTAGGAA-3'

2.2.1.7. Mini-preparation of plasmid DNA.

Isolation of small amount of plasmid DNA (up to 20 µg) was performed using QIAprep® Spin Miniprep Kit (Qiagen). 3 to 5 and 8 to 10 ml of bacterial culture were used for high-copy and low-copy plasmid isolation, respectively.

2.2.1.8. Midi-preparation of plasmid DNA.

Isolation of large amounts of plasmid DNA (up to 100-350 µg) was performed using HiPure Plasmid Filter Midiprep Kit (Invitrogen). 400 and 800 ml of bacterial culture were used for high-copy and low-copy plasmid isolation, respectively.

2.2.1.9. Purification of PCR products.

Purification of PCR products (up to 10 µg PCR products, 100 bp to 10 kb) was performed using QIAquick® PCR Purification Kits (Qiagen).

2.2.1.10. Isolation of DNA fragments from the gel.

Isolation of DNA fragment from the gel (up to 10 µg DNA; 70 bp to 10 kb) was performed using QIAquick® Gel Extraction Kits (Qiagen).

2.2.2. Methods for protein analysis.

2.2.2.1. Total protein extraction and cellular fractionation.

The cell fractionation protocol was according to Isono and Schwechheimer (2010). Briefly, one gram of frozen in liquid nitrogen plant tissue (mix of inflorescences and leaves) was homogenized for one minute (1600U/min) on an ice-filled cooling jacket in 6 ml of ice-cold protein extraction buffer. Samples were allowed to cool for thirty seconds on ice between homogenization cycles (Isono and Schwechheimer, 2010).

The crude lysate (3 x 2 ml) was centrifuged at 4°C for fifteen minutes (8000 x g) to obtain cell associated membrane fraction (P8K). The supernatant (S8K; 2 ml) was subsequently spun down at 4°C for one hour (100000 x g) to obtain P100K containing membrane fraction and S100K containing soluble proteins. P8K and P100K fractions were resuspended in 300 µl and 100 µl of extraction buffer, respectively and supplemented with 1% *n*-Dodecyl β-D-maltoside (DDM). 2 ml of S100K fraction were freeze-dried using lyophilizer Lyovac GT2 (Amsco Finn-Aqua) and dissolved in 500 µl extraction buffer. All fractions were further analyzed via western blot.

Extraction buffer	50 mM Tris-HCl pH 7.5 100 mM NaCl 10% Glycerol (w/v) 50 x Protease Inhibitor Cocktail (S8830, Sigma-Aldrich) (v/v) 100 x Inhibitor of proteasome activity (C2211, Sigma-Aldrich) (v/v) 1000 x PMSF* (v/v)
Wash buffer	50 mM Tris-HCl pH 7.5 100 mM NaCl 10% glycerol (v/v) 0.05% Triton X-100 (v/v) 1000 x PMSF* (v/v)

*PMSF was added every 45 minutes

2.2.2.2. Co-immunoprecipitation.

Co-immunoprecipitation experiments were carried out on three grams of inflorescences, leaves or seedlings using GFP-trap beads (Chromotek) and Anti-HA Affinity Matrix (Roche), as decribed by Park et al. (2012), with the following minor modifications. Plant tissue was grinded in liquid nitrogen, mixed with 3 ml of reaction buffer and incubated for thirty minutes on ice with mild agitation. Subsequently, the sample was centrifuged for fifteen minutes at 4°C (8000 x g). 100 µl of GFP-trap beads (Chromotek) were added to 2 ml of S8K fraction and the sample was incubated with mild agitation for two hours at 4°C. Next, the sample was washed four times with washing buffer. At the end, 70 µl of 1 x Laemmli was added to the beads. The sample was incubated for five minutes at 95°C and then spun down (2700 x g). The

supernatant containing immunoprecipitated proteins was used for mass spectrometry, Comassie Blue Staining and western blot analysis.

Reaction buffer
50 mM Tris-HCl pH 7.5
150 mM NaCl
0.5% Triton (v/v)
100 x Protease Inhibitor Cocktail (P9599, Sigma-Aldrich) (v/v)
100 x inhibitor of proteasome activity (C2211, Sigma-Aldrich) (v/v)
1000 x PMSF* (v/v)

Washing buffer
50 mM Tris-HCl pH 7.5
200 mM NaCl
0.2% Triton (v/v)
100 x Protein Inhibitor cocktail (P9599, Sigma-Aldrich) (v/v)
1000 x PMSF* (v/v)

1 x Laemmli buffer
63 mM Tris-HCl pH 6.8
10% Glycerol
1% SDS
0.0025% Bromophenol Blue
5% β-Mercaptoethanol (v/v)

*PMSF was added every 45 minutes

2.2.2.3 Protein expression.

Antigen1 (CLUB-1) and Antigen2 (CLUB-2) and full-length CLUB cDNA were expressed in BL21 cells via isopropylthio-β-galactoside (IPTG) induction. A time course of expression was determined in order to optimize the best conditions for maximum yield protein (Invitrogen). A final concentration of 0.7 mM IPTG was used. Fractions were collected every hour and analyzed via Coomassie Blue Staining.

2.2.2.4. Generation of CLUB antibody.

The polyclonal CLUB antibody was raised against the CLUB-1 antigen (154-495 amino acids) in rabbit. The CLUB-1 and CLUB-2 antigens were purified on Protino® Ni-TED1000 Packed Columns (Macherey-Nagel) under denaturing conditions (6 M urea)

and freeze-dried using lyophilizer Lyovac GT2 (Amsco Finn-Aqua). 150 µl lyophilized samples were dissolved in 50 µl 1 x Laemmli buffer. As the purification was not complete and as additional unspecific bands were detected, samples of 40 µl were run on 12% polyacrylamide gel and nine bands containing 20 µg of purified CLUB-1 each were cut out of gel, stored in 15% ethanol and 2% acetic acid and sent to Davids Biotechnologie GmbH (Regensburg).

Sera obtained from rabbit 1 and rabbit 2 were tested via western blot analysis. Protein extracts for gel electrophoresis were prepared by homogenizing fresh tissue in an equal volume of 2 x Laemmli buffer. Two concentrations of test sera were tested (1:1000 and 1:5000).

2.2.2.5. Purifying protein from inclusion bodies and protein purification.

Before purification with T7- and His-tag kits, the full length CLUB/AtTRS130 protein was purified from inclusion bodies. A large overnight bacterial culture (600 ml) containing vector of interest was spun down at 6000 x g for twenty minutes. Subsequently, the pellet was resuspended in 3 ml of Buffer A per 1 gram cell pellet. A 16 µl of 50 mg/ml lysosyme per gram of cells pellet was added, mixed and incubated at 37˚C until became viscous. After sonication (10 x 15 seconds bursts with a 15 seconds cooling period in between), the solution was spun at 18000 x g for thirty minutes. P18K supernatant was saved. Pellet was dissolved in Buffer B and 10 µl of Triton X-100 was added per 1 ml solution and subsequently spun down at 20000 x g for twenty minutes. Supernatants S18K, S20K and the final pellet, were proceeded for protein purification using T7-tag Affinity Purification Kit (Immunoaffinity purification: Batch-wise purification; Novagen) and His-tag Purification kit Protino® Ni-TED 2000 packed columns. Purification was done under denaturing conditions. The final pellet was dissolved in T7-tag Bind/Wash buffer supplemented in final urea concentration of 2 M (Novagen) for T7-tag purification and in Denaturing Solubilization buffer (6 M urea, final concentration; Macherey-Nagel) for His-tag purification. 50 µl of T7-tag antibody Agarose (Novagen) was used per 1 ml of each fraction. A PMSF was added every 45 minutes to the final solution of 1 mM. Samples were analyzed via western blot.

Buffer A

50 mM Tris-HCl, pH 8.0
5 mM EDTA
10 mM NaCl

Buffer B

20 mM Na_2HPO_4, pH 7.2
20 mM
5 mM EDTA
25% sucrose (w/v)

2.2.2.6. SDS polyacrylamide gel electrophoresis (SDS-PAGE).

SDS-PAGE was carried out as described by Laemmli et al. (1970). Running gel (8%) and stacking gel (4%) were prepared using Biorad casting system. Samples were mixed with 2 x Laemmli buffer, heated at 95°C for five minutes and loaded onto the gel. The gel was run at constant voltage of 200 V until the blue dye has reached the bottom of the gel.

Gel components	8% Running Gel (for 2 gels)	4% Stacking Gel (for 2 gels)
Acrylamid	4 ml	390 ml
MilliQ H_2O	7 ml	2.3 ml
Tris-HCl pH 8.8	3.8 ml	-
Tris-HCl pH 6.8	-	255 µl
10% SDS	150 µl	30 µl
TEMED	7.5 µl	3 µl
10% APS	75 µl	15 µl

Acrylamid solution 30% Acrylamid (w/v)/ 0.8% Bisacrylamid (w/v)

Running Gel buffer 1.5 M Tris-HCl pH 8.8

Stacking Gel buffer 0.5 M Tris-HCl pH 6.8

SDS solution 10% SDS (w/v)

APS solution 10% Ammonium persulfate (w/v)

1 x SDS Running buffer

25 mM Tris-Base
192 mM Glycine
0.1% SDS (w/v)

2 x Laemmli buffer

90 mM Tris-HCl pH 6.8
2% SDS (w/v)
20% Glcerol (v/v)
0.01% Bromophenol Blue (w/v)
5% β-Mercaptoethanol (v/v)

2.2.2.7. Coomassie Blue Staining.

In order to visualize proteins on a SDS-PAGE gel, a rapid Coomassie Blue Staining was done as described by Wong et al. (2000). First, SDS-PAGE gel was fixed in fixation solution for ten minutes. Subsequently, gel was stained in staining solution for one hour with gentle agitation. Afterwards, gel was destained with several changes of destainig solution I and then destainig solution II until background of the gel was fully destained. A band of 5 ng or more can be observed. All steps were carried out at room temperature.

Fixation solution

50% Methanol (v/v)
10% Acetic Acid (v/v)

Staining solution

0.25% Coomassie Blue R-250 (w/v)
50% Methanol (v/v)
10% Acetic Acid (v/v)

Destaining solution I

30% Methanol (v/v)
10% Acetic Acid (v/v)

Destaining solution II

50% Methanol (v/v)
7% Acetic Acid (v/v)

2.2.2.8. Western blot analysis.

Western blot analysis was performed as described by Sambrook et al. (1989). 8% SDS-PAGE gel was blotted onto PVDF Immobilon-P membranes (Millipore). The blotting “sandwich” was assembled as shown below and placed in a holding cassette that was finally inserted into a blotting chamber. Everything was covered with 1 x transfer buffer and run for one hour at 100 V. Subsequently, the membrane was incubated in blocking buffer for an hour at room temperature on an orbital shaker. That reduces non-specific antibody binding during subsequent incubation steps. The primary

antibody was diluted 5% milk in TBST and applied to the membrane overnight at 4°C. Next, the membrane was washed with TBST (4 x 10 minutes) and incubated with secondary peroxidase-conjugated antibody for one hour with mild agitation at room temperature. Afterwards, the membrane was washed as described above, incubated for five minutes with peroxidase substrate (SuperSignal West Femto Maxiumum Sensitivity Substrate, Pierce, Thermo Scientific) and monitored with chemiluminescence detection system (LAS4000 mini). Primary and secondary antibodies used in this study for western blot analysis are listed in the table below.

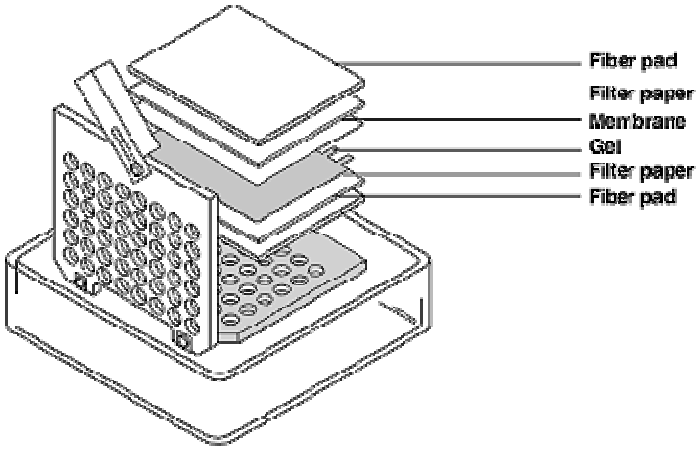

Transfer buffer	48 mM Tris, pH 9.2 39 mM Glycine
TBS (Tris-buffered saline)	20 mM Tris-HCl, pH 7.4 13 mM NaCl
TBST	1 x TBS 0.05% Tween 20 (v/v)
Blocking buffer	5% nonfat dried milk in 1 x TBST (w/v)

Antibodies used in this study for western blot analysis:

Primary antibody	Obtained from	Concentration
Polyclonal Rabbit-Anti-GFP	Invitrogen	1:2000
Polyclonal mouse Anti-SEC6	Hala et al., 2008	1:1000
Polyclonal mouse Anti-EXO84b	Victor Zarsky (Prague)	1:2000
Polyclonal rabbit Anti-EXO70A1	Victor Zarsky (Prague)	1:4000
Anti-HA Peroxidase-conjugated (3F10)	Roche Diagnostics	1:1000
Anti-T7 HRP Conjugate	Novagen	1:10000

Secondary antibody	Obtained from	Concentration
Goat-Anti-Rabbit	Pierce, Thermo Scientific	1:6000
Goat-Anti-Mouse	Pierce, Thermo Scientific	1:6000

2.2.2.9. LC-MS/MS analysis and Peptide and Protein Identification/ Data analysis.

Immunoprecipitated samples of CLUB-GFP and TRS120-GFP were analyzed via mass spectrometry in cooperation with Prof. Dr. Bernhard Küster and Susan Kläger (Chair of Proteomics and Bioanalytics, Technische Universität München, Freising) as described by Rybak et al. (2014).

2.2.3. Methods for microbiological analysis.

2.2.3.1. Generation of Electrocompetent *E. coli* and *A. tumefaciens* cells.

The bacterial cells of interest were streaked on a fresh LB-agar plate (supplemented with rifampicin for *A. tumefaciens*). A pre-culture was made by inoculation of 5 ml LB with a single bacterial colony and grown overnight (250 rpm.; 37°C and 30°C for *E. coli* and *A. tumefaciens*, respectively). Subsequently, 1 ml of pre-culture was used to inoculate 400 ml of LB medium and grown until the culture had reached an OD_{600} of 0.4 and 0.6 for *E. coli* and *A. tumefaciens*, respectively. Then, the culture was transferred on ice and incubated for thirty minutes. Subsequently, cells were collected by centrifugation at 4°C for twenty minutes (1000 x g). The supernatant was discarded and the pellet was resuspended in 500 ml of ice-cold MilliQ water. The cells were harvested again at 4°C for twenty minutes (1000 x g), and then resuspended in 250 ml

of ice-cold 10% glycerol (v/v). Centrifugation was repeated again and the pellet was resuspended in 10 ml of ice-cold 10% glycerol (v/v). Finally, cells were spun down and resuspended in ice-cold 10% glycerol to a concentration of 2 x 10^{10} to 3 x 10^{10} cells/ml. At the end, the cells were aliquoted in 40 µl portions, frozen in liquid nitrogen and stored at -80°C.

2.2.3.2. Electroporation.

Electrocompetent cells were thawed on ice, mixed with plasmid DNA (100 ng) and incubated for one minute on ice. Subsequently, the transformation culture was pipetted into an electroporation cuvette, which was then placed into an electroporator set to deliver an electrical pulse of 2.5 µF, 2.5 kV and 200 Ω. After a short electric pulse, about 2400 V/cm, 1 ml of SOC medium was immediately added to the cells and culture was transferred into a clean eppendorf tube and incubated wit shaking for one hour at 37°C and 30°C for *E. coli* or *A. tumefaciens*, respectively. After incubation, bacteria were streaked on LB-agar plates containing the selective antibiotic and grown overnight at 37°C or 30°C for *E. coli* and *A. tumefaciens,* respectively.

LB (Luria-Bertani) medium	10 g/l Peptone/Tryptone 5 g/l Yeast Extract 10 g/l NaCl pH 7.0
SOB (Super Optimal Broth) medium	20 g/l Peptone/Tryptone 5 g/l Yeast Extract 10 mM NaCl 10 mM $MgCl_2$ 2.5 mM KCl pH 7.0
SOC medium	SOB medium 20 mM Glucose pH 7.0

All media were sterilized by autoclaving.

2.2.4 Methods for plant analysis.

2.2.4.1 *Arabidopsis thaliana* seed sterilization.

Arabidopsis thaliana seeds were sterilized by rinsing with 80% (v/v) ethanol and incubated for fifteen minutes in sterilization buffer. Afterwards, seeds were washed five times with ddH_2O and stratified for two days at 4°C in 0.15% sterile agar (v/v), and plated on MS (Murashige-Skoog)-medium agar plates (pH 5.7 with KOH; Murashige and Skoog, 1962) supplemented with B5 vitamins and 1% sucrose. Five-day-old plate-grown seedlings were used for light, confocal and electron microscopy.

Sterilization buffer

10% SDS (w/v)
12% NaClO (v/v)

80% ethanol (v/v)

10 x MS-macrosalts

16.5 g/l NH_4NO_3
19 g/l KNO_3
1.7 g/l KH_2PO_4
3.32 g/l $CaCl_2$ x 2 H_20
3.7 g/l $MgSO_4$ x 7H_20

1000 x MS-microsalts

27.2 g/l $FeSO_4$ x 7 H_20
36.5 g/l Na_2EDTA
0.83 g/l KI
10 g/l $MnSO_4$ x 4 H_20
6.2 g/l H_3BO_3
2 g/l $ZnSO_4$ x 4 H_20
0.25 g/l Na_2MoO_4 x 2 H_20
0.025 g/l $CuCl_2$ x 5 H_20
0.025 g/l $CoCl_2$ x 6 H_20

B5 vitamins

1 mg/l Nicotinic acid
10 mg/l Thiamine hydrochloride
1 g/l Pyridoxine hydrochloride
100 mg/l Myo-inosytol

2.2.4.2. Growing conditions for *Arabidopsis thaliana*.

Sterilized seeds were plated on MS-agar plates and grown at 23°C in a cell culture room under constant light conditions (50 µE m^{-2} s^{-1}). Plants were grown in the greenhouse, under controlled temperature conditions and with supplemental light, or under controlled growth chamber conditions (16/8 hour photoperiod at 250 µM $m^{-2}s^{-1}$).

2.2.4.3. Genotyping and complementation analysis.

Due to their seedling lethality, mutant lines (listed in Table S1) were propagated as hetero or hemizygous. Insertion lines were selected via the TAIR and NASC web sites (Swarbreck et al., 2008). For complementation analysis hemizygous lines were transformed and transgenic lines were selfed over three generations. Mutants rescued progeny 50% cytokinesis-defective mutant seedlings and 100% of their progeny carried both the T-DNA insertion and the gene fusion construct. Genotyping was carried out with the primers described in Table S2.

2.2.4.4. Agrobacterium-mediated transformation of *Arabidopsis thaliana.*

All constructs were introduced into *Agrobacterium tumefaciens* strain GV3101::pMP90. A simplified floral dip method of *Agrobacterium*-mediated transformation was carried out according to Clough and Bent (1998). *A. tumefaciens* strain carrying gene of interest on a binary vector was cultivated in 400 ml of LB medium containing a selective antibiotic. *A. tumefaciens* culture was centrifuged (6000 x g) for fifteen minutes at 4°C. The pellet was resuspended in 5% sucrose (w/v). Silvet L-77 was added to a concentration of 0.05% (v/v). Above-ground parts of plant were dipped in *Agrobacterium* solution for 2-3 seconds, with gentle agitation. Afterwards, plants were covered with a dome for twenty four hours to keep high humidity. The procedure was repeated after five days. T1 plants were selected for transformants on MS-medium agar plates containing 50 µg/ml kanamycin or on soil supplemented with 50 mg/ml glufosinte ammonium (BASTA).

2.2.4.5. Antibody staining.

Antibody stains were carried out as described by Völker et al. (2001). The five-day-old *A. thaliana* root tips were fixed in 4% paraformaldehyde in MTSB and vacuum infiltrated for one hour. Subsequently, they were washed five times with sterile water and left overnight to dry at room temperature on SuperFrost® Plus slides (Menzel-

Gläser, Thermo Scientific). Next day, root tips were encircled with a water repellent PAP pen (Sigma-Aldrich) and rehydrated with MTSB for ten minutes. Driselase cocktail was made and spun down for two minutes (10000 x g). The supernatant was spread over the slides and the slides were incubated at 37°C for fifty minutes in order to permeabilize the cell wall. Afterwards, root tips were rinsed four times for five minutes with PBS. To permeabilize the membranes, permeabilization solution was spread over the slides and incubated at room temperature for one hour. After incubation, the root tips were washed six times for five minutes with PBS and then blocking solution was applied to slides and left for one hour incubation at 37°C. Subsequently, primary antibody was diluted in blocking solution), spread over the slides and left to incubate for four hours at 37°C or overnight at 4°C. Next, slides were washed three times for ten minutes with 0.01% Triton in PBS and afterwards three times for ten minutes with PBS. Quick wash with blocking solution was done to prepare the root tips for application of secondary antibody. Secondary antibodies, dilutes in 4% BSA in PBS were applied to the slides and incubated for three and a half hours at 37°C. Subsequently, slides were washed four times with PBS and two times with H_2O for ten minutes each followed. Afterwards, DAPI was diluted in H_2O to concentration of 1 µg/ml and spread over the slides and left for incubation for twenty minutes at 37°C. After washing six times with water for five minutes, 2-3 drops of Citifluor were applied to the slide, covered with a cover glass and stored at 4°C. All antibodies used in this study in immunostaining are presented in table below.

Microtubule Stabilisation Buffer (MTSB)	50 mM Pipes 5 mM EGTA 5 mM $MgSO_4$ x $7H_2O$ pH 6.9-7.0
Fixation buffer	4% paraformaldehyde (PFA) in MTSB PFA was dissolved in MTSB pH 11 (KOH) by heating at 60°C, afterwards solution was cooled down to room temperature and pH was adjusted to pH 7.0 (H_2SO_4).

PBS (Phosphate buffered saline)

137 mM NaCl
2.7 mM KCl
10 mM Na_2HPO_4
2 mM KH_2PO_4
pH 7.4

Driselese cocktail

2% Driselese (SIGMA-Aldrich) in MTSB

Permeabilization solution

10% DMSO (v/v)
3% Nonidet P40 (v/v)
MTSB

Blocking solution

4% BSA (v/v) in PBS

Pap pen (Sigma-Aldrich)

Anti bleaching solution Citifluor

Antibodies used in this study for immunostain:

Primary Antibody	Company; References	Labeling	Concentration
anti-KNOLLE (rabbit monoclonal)	Lauber et al., 1997	Cell plate	1:2000
anti-RAB-A2a (rabbit monoclonal)	Chow et al., 2008	Cell plate	1:3000
anti-tubulin (mouse monoclonal)	Sigma-Aldrich	Microtubule	1:2500
anti-tubulin (sheep polyclonal)	Cytoskeleton	Microtubule	1:200
CCRC-M1 (mouse monoclonal)	Carbon Source; Puhlmann et al., 1994	Xyloglucan	1:10
CCRC-M2 (mouse monoclonal)	Carbon Source; Puhlmann et al., 1994	Pectin (RGI)	1:10

Primary Antibody	Company; References	Labeling	Concentration
CCRC-M7 (mouse monoclonal)	Carbon Source; Puhlmann et al., 1994	Pectin (RGI)	1:10
CCRCM38 (mouse monoclonal)	Carbon Source; Pattathil et al., 2010	Pectin (HG)	1:10
JIM5 (rat monoclonal)	Carbon Source; Knox et al., 1990	Pectin (HG)	1:10
JIM7 (rat monoclonal)	Carbosource; Clausen et al., 2003	Pectin (HG)	1:10
LM5 (rat monoclonal)	Plant Probes; Jones et al., 1997	Pectin (RGI)	1:10
LM6 (rat monoclonal)	Plant Probes; Willats et al., 1998	Pectin (RGI)	1:10
LM14 (rat monoclonal)	Plant Probes; Moller et al., 2008	AGP- glycan	1:10
LM15 (rat monoclonal)	Plant Probes; Marcus et al., 2008	Xyloglucan	1:10
LM25 (rat monoclonal)	Plant Probes; Pedersen et al., 2012	Xyloglucan	1:5
CBM3a	Plant Probes; Blake et al., 2006	Cellulose	1:100

Secondary antibody	Company	Concentration
Cy3-conjugated goat anti-mouse	Jackson ImmunoResearch	1:400
Alexa Fluor® 488-conjugated goat anti-rat	Molecular Probes	1:100
Alexa Fluor® 488-conjugated goat anti-rabbit	Molecular Probes	1:600
Alexa Fluor® 488 conjugated goat anti-sheep	Jackson ImmunoResearch	1:100

2.2.5. Methods for microscopy.

2.2.5.1. Confocal laser scanning microscopy (CLSM) and image analysis.

Confocal laser scanning microscopy was carried out with an Olympus FV1000 setup using an inverted IX81 stand and FluoView software (FV10-ASW version 01.04.00.09; Olympus Europa GmbH, Hamburg, Germany). GFP and FM4-64 were excited at 488 nm and detected from 502-536 nm and 610-672 nm, respectively. CFP and mCherry were excited using 405 nm and 561 nm laser line, respectively. A 60X water immersion 0.9 numerical aperture objective (Olympus) was used. Due to weak fluorescence and extensive photobleaching of the samples, time lapses were taken at four minute intervals. For the time lapse movies, however, we used an Olympus Fluorview 1000 equipped with a high sensitivity detector unit with two gallium arsenide phosphide photomultipliers. This enabled us to carry out extended time lapses at one minute intervals. A quantitative analysis of confocal scans was carried out in ImageJ. Line graphs of mean signal were corrected for photobleaching during the course of a time lapse.

2.2.5.2. Analysis of secretion.

Ruthenium red staining of the extruded mucilage was carried out as described by Arsovski et al. (2009). Wild-type and mutant seed were placed directly in 0.01% (w/v) ruthenium red (Sigma-Aldrich). Pictures were taken at five minute intervals for thirty minutes with Digital Colour Camera XC10 connected to Olympus SZX12 stereo microscope using cellSens Dimention Software (Olympus).

2.2.5.3. Analysis of endocytosis.

Endocytosis studies were performed with FM4-64 as described by Dettmer et al. (2006). For time lapses experiments, five-day-old wild-type and mutant seedlings were placed in 4 µM FM4-64 (Invitrogen) on microscope slide and imaged via CLSM. Time lapses were measured as a percent of cell in which FM4-64 positive endocytotic residues were observed at two minute intervals.

2.2.5.4. Focused Ion Beam/Scanning Electron Microscopy (FIB/SEM).

Five-day-old *Arabidopsis* seedlings were infiltrated as described by Assaad et al. (1996). Infiltrated samples were embedded in Spurr. High-pressure freezing and freeze substitution as well as electron microscopy was done in cooperation with Prof. Dr.

Gerhardt Wanner and SEM images with Dr. Eva Facher (Faculty of Biology, Ludwig-Maximilians-Universität, München) as described by Rybak et al. (2014).

2.2.6. Statistics and image analysis.

P values were determined with the standard Student's two-tailed t-test and set at a cutoff of 2%. Images were processed with Adobe Photoshop, analyzed with ImageQuant LAS 4000 (Fujifilm) or ImageJ and assembled with Adobe Illustrator.

3. Results.

3.1. A screen of insertion mutants in tethering factors of *Arabidopsis thaliana* leads to the identification of new players involved in cytokinesis.

The aim of this study was to search for tethering factor mutants showing cytokinesis defects. In this study, out of eight tethering complexes, I focused on three of them: TRAPPI, TRAPPII and GARP. The GARP and the TRAPPII tethering complexes were reported to reside on TGN in yeast and both were shown to be involved in endocytosis, while TRAPPII complex additionally was shown to be implicated in exocytosis (Conibear et al., 2003; Cai et al., 2005; Quenneville et al., 2006). TRAPPI resides on cis-Golgi and is required for vesicles tethering coming from rER to the cis-Golgi (Wang et al., 2000). The yeast TRAPPII complex consists of six-core TRAPPI complex (Bet3, Bet5, Trs20. Trs23, Trs31, Trs33) and three TRAPPII specific subunits (Trs120, Trs130, Trs65; Yu and Liang, 2012). All subunits except for Trs65 are conserved in plants (Thellmann et al., 2010). Recently, a new nonessential TRAPPII specific subunit was identified, Tca17 (Monpetit and Conibear, 2009; Scrivens et al., 2009; Choi et al., 2011). A comparative genomic analysis showed that Tca17 is a conserved protein in twenty two species including *Arabidopsis thaliana* (Klinger et al., 2013).

3.1.1. Mutations in the TRAPPI and the TRAPPII but not in the GARP tethering complexes lead to a cytokinesis-defective seedling phenotype.

In search of cytokinesis-defective mutants in tethering complexes in *Arabidopsis thaliana*, a reverse genetic approach was performed. The nine TRAPPII subunits are encoded in *Arabidopsis* by ten genes. Out of six subunits in TRAPPI complex, insertion lines for four of them (Bet3, Bet5, Trs31 and Trs33) were obtained. The two TRAPPII specific subunits Trs120 and Trs130 are encoded by single genes in *Arabidopsis*. *club-2/trs130-2* was identified in a forward genetic screen and described by Jaber et al. (2010) as a strong cytokinesis-defective mutant with reduced T-DNA transmission (51%; Fig.3.1.1C). Four insertion lines were obtained and surveyed for Trs120. The GARP tethering complex consists of four subunits. Three of them (Vps52, Vps53, Vps54) are encoded by unique genes in *Arabidopsis* and insertion lines were available for all these three loci. All insertion lines characterized in this study are shown in Table S1. An assessment of T-DNA transmission was carried out for all insertions lines. Genomic DNA was isolated from selfed hemizygous individual plants grown on soil and the presence or the absence of the T-DNA was checked by PCR. For seedling lethal mutations, we would expect 67% of hemizygous and 33% of wild type plants in the

progeny of selfed hemizygous line. A reduced transmission rate was observed for all TRAPPII (7.7% to 23.8%) insertion lines (Table. 3.1.1). Out of 324 plants screened, not a single one was homozygous for T-DNA insertion. Based on that, we conclude that the null mutations in AtTRS120 are lethal. A transmission rate was also reduced for almost all TRAPPI and GARP insertion lines (Table 3.1.1).

Locus	Allele	Polymorphism	Accesion No.	Cytokinesis defective[a]	Transmission[b]
TRAPPI					
Bet3	*bet3-1*[e]	GABI_318C08	N430464	0% (n = 200)	7.6% (n = 66)
Bet5	*bet5-1*	SALK_099482	N599482	1% (n = 192)	15.2% (n = 79)
	bet5-2	SAIL_634_G07	N827313	1% (n = 98)	67.2% (n = 64)
Trs31	*trs31-1*[e]	FLAG_488E06	EWSTV26T3	1% (n = 211)	13.6% (n = 59)
Trs33	*trs33-1*	SALK_109244	N609244	5.7% (n = 614)	55.6% (n = 36)
	trs33-2	SALK_109724	N609924	2.9% (n = 104)	15.9% (n = 69)
TRAPPII					
Trs120	*trs120-1*	SALK_125246	N625246	6.3% (n = 221)	11.8% (n = 34)
	trs120-2	SALK_021904	N521904	8.4% (n = 455)	7.7% (n = 78)
	trs120-3[e]	SALK_111574	N611574	11% (n = 349)	13.1% (n = 107)
	trs120-4[e]	SAIL_1285_D07	N879232	11% (n = 617)	23.8% (n = 105)
GARP					
Vps52	*vps52-2*[d]	SAlK_055433	N555433	0% (n = 169)	50% (n = 56)
vps53	*vps53-2*	SAIL_87_D06	N870946	0% (n = 540)	2.5% (n = 69)
	vps53-3	GABI_400C01	N344145	0% (n = 620)	82% (n = 62)
	vps53-4	SAIL_117_D11	N871277	0% (n = 221)	50.8% (n = 59)
	vps53-5	GABI_463D10	N344181	0% (n = 600)	87.8% (n = 49)
vps54	*vps54-1*[d]	SALK_036485	N536485	0% (n = 196)	25.5% (n = 55)
	vps54-2[d]	SALK_062261	N562261	0% (n = 340)	39.1% (n = 69)

Table 3.1.1. Cytokinesis-defective phenotype and transmission in insertion lines used in this study.

n: Total number of analyzed individuals in this study. *homozygous mutant. **embryo lethality. a: Cytokinesis-defective mutant seedlings on the plate in the progeny of a self hemizygous line (%). b: Hemizygous or homozygous segregants in the progeny of a hemizygous line grown on soil (%). c: For *trs120-1*, cytokiensis-defective mutants scored in the progeny of individual lines. d: These alleles were described by Guermonprez et al. (2008). e: These alleles were screened by Martha Thellmann.

Subsequently, we looked at the phenotype segregation of all surveyed insertion lines. The typical canonical cytokinesis-defective phenotype is seedling lethal, was described by Söllner et al. (2002) and is characterized by reduced growth of shoot and root meristems, bloated, enlarged cells, gapped and incomplete cell wall. A weak cytokinesis-defective phenotype was observed for TRAPPI lines (Fig. 3.1.1B) but no evidence of cytokinesis defects was found in seven GARP insertion lines used in this study, although in five out of seven insertion lines the transmission rates were reduced (Table 3.1.1; shown also by Guermonprez et al. 2008). A canonical cytokinesis-

defective phenotype was observed in Trs120 insertion lines (Fig. 3.1.1D; Thellmann et al., 2010). The Trs120 lines segregated 6% to 11% of cytokinesis-defective seedlings phenotype (Table 3.1.1). Additionally, histological sections and electron micrographs of *trs120* and *trs33* insertion lines showed cell wall stubs and incomplete cell plates (Thellmann et al., 2010).

Two alleles, *club-2* and *trs120-4* show the strongest cytokinesis-defective phenotype, therefore they were used in subsequent study for further analyses.

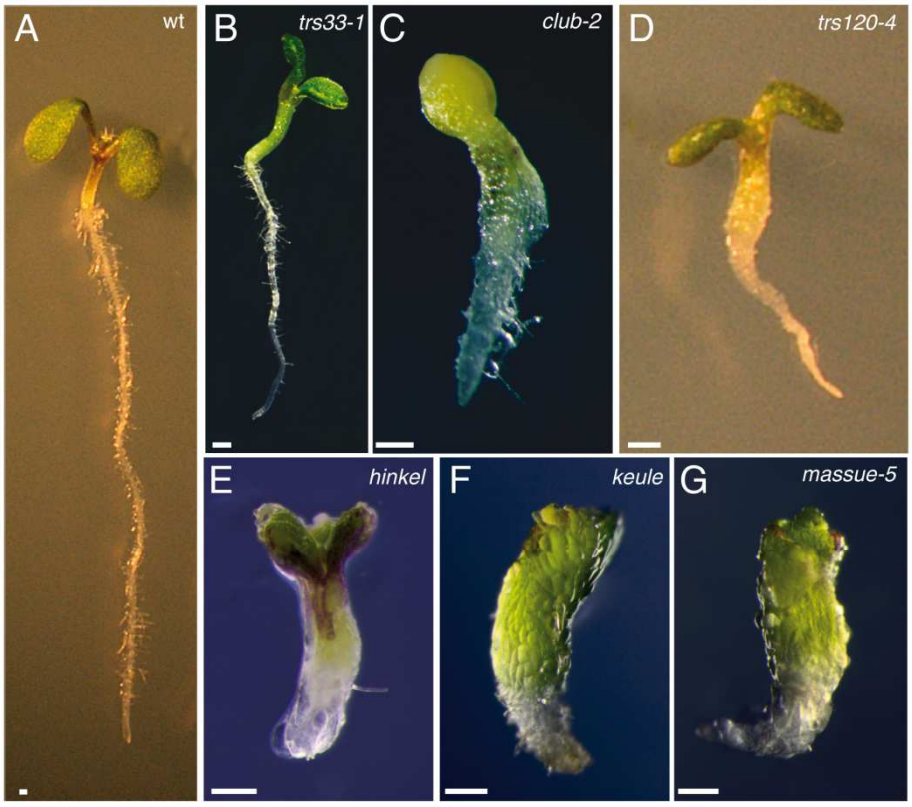

Figure 3.1.1. Phenotypes of TRAPPI and TRAPPII mutants and their comparison to canonical cytokinesis-defective mutants.
(A) Wild type.
(B) *trs33-1*.
(C) *club-2*.
(D) *trs120-4*.
(E) *hinkel*.
(F) *keule*.
(G) *massue-5*.
Bars = 500 µm.

3.1.2. The TRAPPII complex is required for endocytosis.

The trans-Golgi network (TGN) works as a hub for the secretory, vacuolar and endocytic trafficking. Secretory, plasma membrane and cell wall cargoes, like secreted form of green fluorescent protein (secGFP), the receptor kinase BRASSINOSTEROID INSENSITIVE1 (BRI1) and xyloglucans, were reported to pass through the TGN (Viotti et al., 2010). Endocytosed material from plasma membrane is targeted to TGN prior other destinations (Dettmer et al., 2006; Viotti et al., 2010). Rab-A2a was shown to be localized to TGN/EE (Chow et al., 2008) and co-localized with Rab-A1c (Qi et al., 2011). Rab-A1c was co-localized to TRS130-YFP, a TRAPPII specific subunit (Qi et al., 2011), indicating its localization and possible function at the TGN. If TRAPPII specific subunits CLUB/AtTRS130 and AtTRS120 act at the TGN we would expect impaired secretion and endocytosis in those mutants. In order to check requirement of TRAPPII complex in exocytosis and endocytosis, both processes were monitored in TRAPPII mutants.

3.1.2.1. The TRAPPII complex does not appear to be required for the secretion of seed mucilage.

Analysis of secretion was done via mucilage secretion. Mucilage consists mainly of pectin rhamnogalacturonan and is produced by the seed coat after seed exposure to water. Extruded mucilage can be stained by ruthenium red and is observed as two layers: inner adherent and outer loosely attached (Young et al., 2008, Haughn and Western, 2012). We found no difference in mucilage secretion between wild type and two TRAPPII mutants, *club-2* and *trs120-4,* but no extruded mucilage was seen in the TRAPPI mutant *bet5-2,* most likely due to impaired traffic between the ER and Golgi. (Fig. 3.1.2). Based on our data, we conclude that TRAPPII is not required for secretion at the seed development stage.

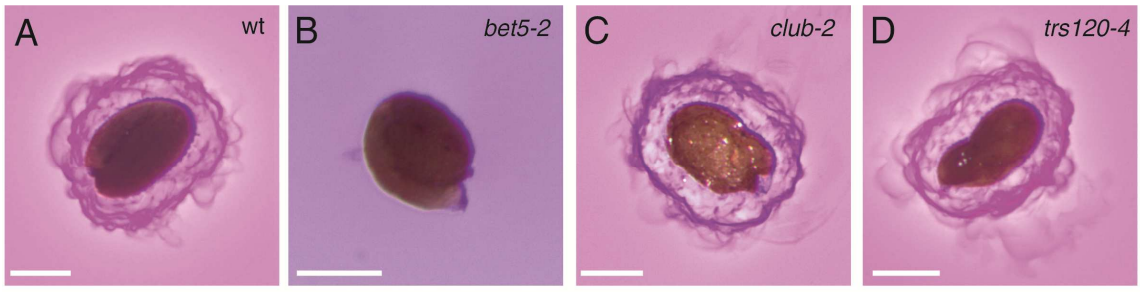

Figure 3.1.2. Analysis of secretion in TRAPPI and TRAPPII mutants.
Mucilage (pink halo) stained with ruthenium red extruded from wild type (A), *bet5-2* (B), *club-2* (C) and *trs120-4* (D) seed (n = 11, n = 11, n = 5, n = 2, respectively; n: numer of seed analyzed). No mucilage secretion was observed in *bet5-2* mutant (B). Pictures were taken at 5 minute intervals for 30 minutes. Seed pictures shown in the figure were taken at 0 minute time point.
Bars = 200 µm.

3.1.2.2. The TRAPPII complex is required for endocytosis.

Analysis of endocytosis was done via FM4-64 dye internalization (Bolte et al., 2004; Jelínková et al., 2010). FM4-64 dye is an endocytic tracer that internalizes via endocytosis from the plasma membrane to the tonoplast. It was shown that about six minutes after FM4-64 dye application to the wild-type root tip, TGN/EE is stained (Dettmer at al., 2006). We monitored co-localization of FM4-64 dye with the TGN marker VHA-a1-GFP (Dettmer et al., 2006) in *club-2* and *trs120-4* mutant root tips. We compared in quantitative analysis different time lapses in the wild type and mutants. In both mutants internalization of the dye was delayed. The delay was more severe in the *trs120-4* mutants (Fig. 3.1.3A). FM4-64 uptake for *club-2* was observed fourteen minutes after dye application and about thirty minutes in *trs120-4* mutants. Additionally, we observed less TGN compartments labeled by VHA-a1-GFP in *club-2* mutant compared to the wild type (Fig. 3.1.3B-D). The difference was two-fold (an average, 32.5 vesicles per cell in wild-type root tip and 13.8 in *club-2* were detected). Taken together, we found that both TRAPPII specific subunits are required for endocytosis in *Arabidopsis* root tips.

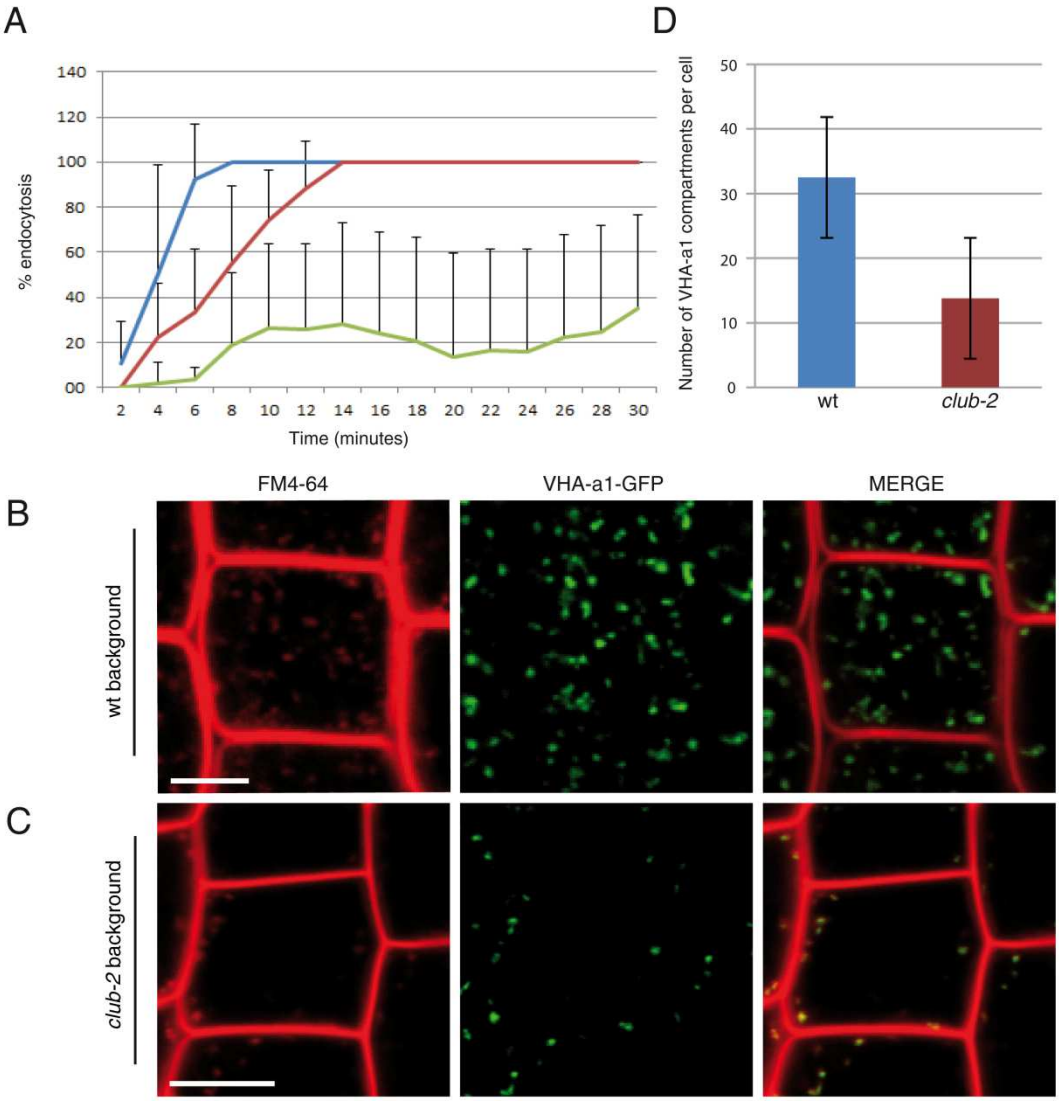

Figure 3.1.3. Analysis of endocytosis in TRAPPII mutants.
(A) Time lapses of endocytosis were measured as the percentage of cells in which endocytotic vesicles (FM4-64 positive compartments) were observed; wild type (blue; n = 16), *club-2* (red; n = 10), *trs120-4* (green; n = 8); n: number of time lapses. Note the severe impairment in *trs120-4* mutants.
(B-D) The number of VHA-a1 compartments in the wild type (B) and *club-2* mutant (C). The number of VHA-a1 labeled compartments per cell is clearly reduced in *club-2* mutants in comparison to the wild type (n = 39 for wild type, n = 22 for *club-2*; n: numer of cells analyzed) (D).
Bars = 5 µm.

3.2. Characterization of the TRAPPII specific subunits in vivo *in planta.*

TRAPPII complex was reported to be implicated in cytokinesis in plants (Jaber et al., 2010; Thellmann et al., 2010; Qi et al., 2011). Both TRAPPII specific subunits CLUB/AtTRS130 and AtTRS120 were shown to be required for cell plate assembly (Jaber et al., 2009; Thellmann et al., 2010, respectively). CLUB/AtTRS130 subunit was co-localized with TGN/EE in non-dividing cells (Qi et al., 2011). The cell plate is accepted to be a TGN compartment, a major sorting station of secretory and endocytic cargoes (Dettmer et al., 2006; Chow et al., 2008). So far, CLUB/AtTRS130 and AtTRS120 subunits were not localized in dividing cells over time *in planta*. The objective of this study was to determine intracellular localization of the TRAPPII specific subunits in dividing cells in *Arabidopsis* root tips.

3.2.1. Generating an antibody against CLUB/AtTRS130.

CLUB/AtTRS130 is encoded by a single gene in *Arabidopsis* genome. The full length CLUB/AtTRS130 cDNA encodes a polypeptide of 1259 amino acids, corresponding to a molecular mass of 140.3 kDa (TAIR). In order to generate an antibody against CLUB, two antigens with the most conserved antigenic regions were cloned into pET101/D-TOPO vector (Invitrogen). Overexpressed antigens yielded a maximum amount of protein six hours after induction with IPTG (final concentration 0.7 mM; Fig. 3.2.1A). Antigen 1, referred to as CLUB-1, is 40.9 kDa (43.1 kDa, including C-terminal V5 and His-tags; Table 3.2.1) and antigen 2, referred to as CLUB-2, is 9.6 kDa (13.0 kDa, including C-terminal V5 and His-tags; Table 3.2.1). Antigens were purified with the His-tag (Macherey-Nagel). CLUB-1 was sent to Davids Biotechnology GmBH (Regensburg) for the immunization of two rabbits. CLUB-2 was not taken into account as unspecific bands were detected in its fraction.

A test serum against CLUB-1 from rabbit 1 and rabbit 2 were tested via western blot analysis. Samples containing Col-0, *hinkel* (*hik*^{G235}) and *massue-5/massue-5* seedlings were used as a positive control and *club-2/club-2* seedlings as a negative control. A western blot with test serum from rabbit 2 gave a faint specific band at the right size of 140.3 kDa, at the antibody concentration of 1:1000. We also observed a lot of background bands (Fig. 3.2.1B). No signal was detected with rabbit 1. Affinity purification of the antibody will be carried out by Davids Biotechnology GmBH.

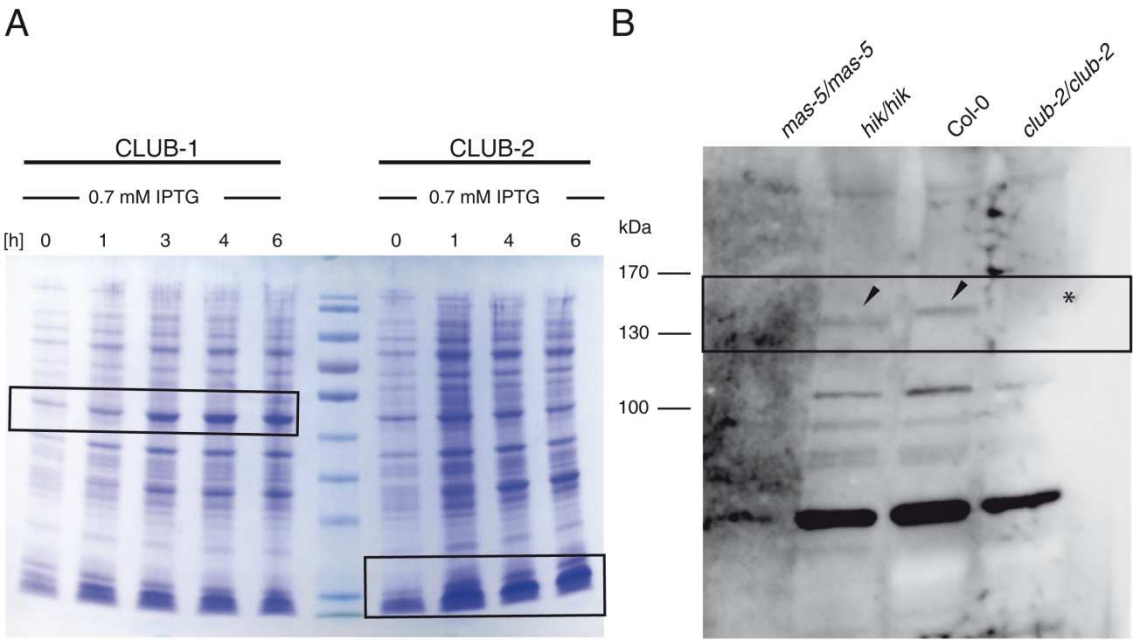

Figure 3.2.1. Generation of an antibody against CLUB/AtTRS130.
(A) Optimization of expression of target protein. Antigen CLUB-1 (43.15 kDa) and CLUB-2 (13.0 kDa) were overexpressed in BL21 (DE3) cells. Polyacrylamide gel stained with Coomassie Brilliant Blue shows fractions at different time points in hours after induction with IPTG (final concentration 0.7 mM). The maximum level of overexpressed protein was detected 6 hours after IPTG induction. As a protein marker, a PageRuler Prestained Protein Ladder (Invitrogen; sixth lane) was used (from the top 170, 130, 100, 70, 55, 40, 35, 25, 15 kDa).
(B) A western blot of *massue-5*, *hinkel,* Col-0 (positive control) and *club-2* (club knock-out, homozygous mutant, negative control) probed with test serum from rabbit 1 against CLUB-1 at concentration of 1:1000. Weak specific bands were detected in two out of three positive controls at the right size of 140 kDa (arrowheads). No signal was detected in *club-2* knock-out negative control (asterisk).

Antigen	Position in gene	Number of CLUB amino acids	Total number of amino acids*	Size of the overexpressed protein [kDa]*
CLUB-1	1023 (460-1485 bp)	341 (154-495)	375	43.1
CLUB-2	251 (3241-3492 bp)	83 (1081-1164)	117	13.0

Table 3.2.1. CLUB-1 and CLUB-2 antigens.
*total number of amino acids and protein size [kDa] includes linker, C-terminal V5 domain and 6xHIS-tag.

Additionally, we attempted to generate an antibody against the CLUB full length coding region. For this purpose, CLUB/AtTRS130 cDNA was cloned into the pET24a(+) vector (Novagen). The CLUB/AtTRS130 cDNA clone, RAFL09-39-B05 (RIKEN), possesses a substitution (G/A, 204 bp) and a 5 bp deletion (1602-1606 bp). A fragment of 1892 bp was subcloned. The final construct contains 3 substitutions (listed in Table 3.2.2), which do not change the amino acid coding sequence.

	DNA sequence change	Predicted change in CLUB protein (Total lenght: 1259 aa)
1	CTG-CTA, 84 bp	L28-L28
2	GGA-GGT, 510 bp	G170-G170
3	GGC-GGT, 2166 bp	G722-G722

Table 3.2.2. Substitutions in CLUB/AtTRS130 cDNA sequence in pET24a (+) vector. Note that substitutions do not change the amino acid coding sequence.

Full length CLUB/AtTRS130 cDNA was overexpressed in BL21 (DE3) cells via IPTG induction. Purification with T7-tag (Novagen) and with His-tag affinity purification kit (Macheray-Nagel) were performed. A very faint band was detected after purification with T7-tag from P18K and the final pellet (data not shown; see Materials and Methods). Lack of non-specific bands on the gel indicated complete purification. However, because of the very low efficiency of the isolated and purified protein, at this point, the method of CLUB isolation and purification must be optimized to proceed further.

Taking into account the time needed for generation of an antibody, we decided to use small epitope tags instead. To this end, CLUB/AtTRS130 and other TRAPPII specific subunit AtTRS120 were fused with a C-terminal HA-tag under control of their endogenous promoters. HA (hemagglutinin) is a small epitope (nine amino acids: YPYDVPDYA) that does not appear to disturb the activity and localization of recombinant proteins and facilitated us for their immunodetection *in planta*.

3.2.2. TRAPPII specific subunits localize to the cell plate and cytosol.

Two TRAPPII specific subunits CLUB/AtTRS130 and AtTRS120 were fused with C-termal GFP under both the endogenous promoter (for AtTRS120) and the strong ubiquitin promoter (for CLUB and AtTRS120) and they were shown to be functional (Fig. 3.2.2). The rescued mutant (Fig. 3.2.2A-C, right on each panel) did not differ from the wild type Columbia control (Fig. 3.2.2A-C, left on each panel). PCR analysis was used to detect the GFP fusions and to assess the genotype of the plant (presence or absence of the T-DNA isertion). Because the gene fusion constructs contained full-length genomic sequence, genotyping was done by segregation analysis over three generations. The rescued mutants segregated roughly 50% cytokinesis-defective mutant seedlings and 100% of their progeny carried the gene fusion construct.

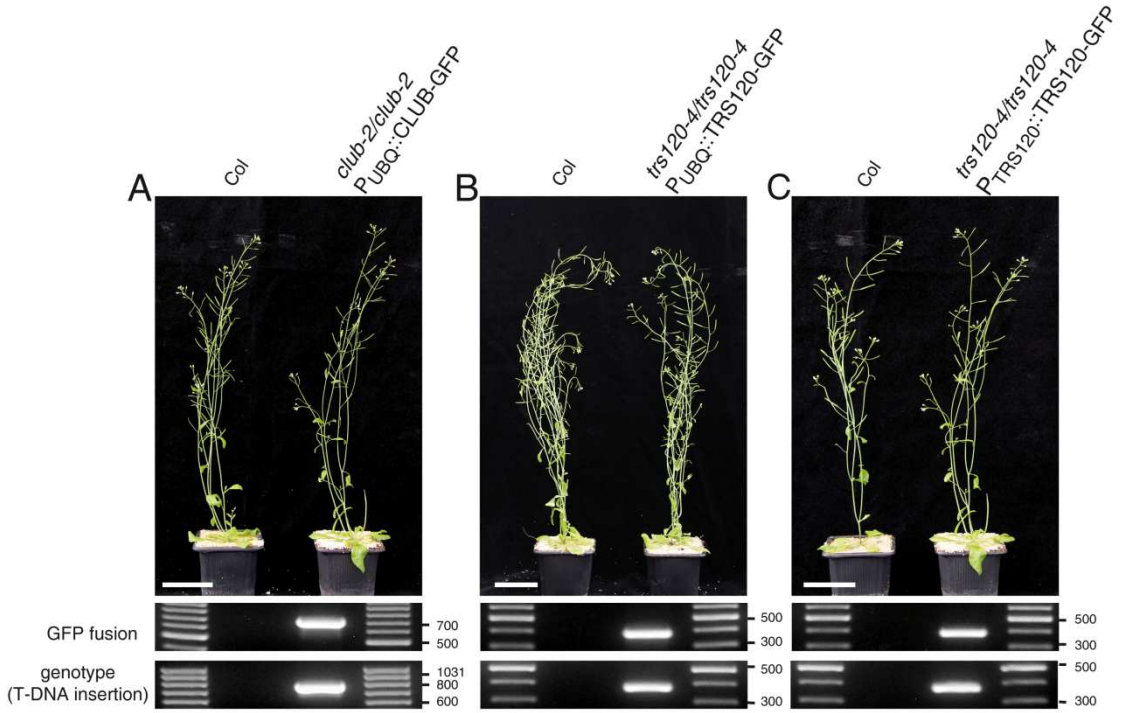

Figure 3.2.2. Complementation analysis.
(A) *club-2*/*club-2* hemizygous for P_{UBQ}::CLUB-GFP.
(B) *trs120-4*/*trs120-4* hemizygous for P_{UBQ}::TRS120-GFP.
(C) *trs120-4*/*trs120-4* hemizygous for P_{TRS120}::TRS120-GFP.
See text for a detailed description.
Bars = 5 cm.

Confocal images showed that both CLUB-GFP and TRS120-GFP localized to the cell plate in dividing cells as well as in the cytosol and in unidentified endo-membrane compartments (Fig. 3.2.3A). These results were confirmed by cell fractionation and western blot analysis where, as we can see, CLUB-GFP and - HA and TRS120-HA gene fusions were detected in the microsomal (P100K) and soluble (P100K) fractions (Fig. 3.2.3B).

Fractionation experiments were carried out with two biological replicates for CLUB and TRS120 HA C-terminal fusions and with one replicate for CLUB GFP C-terminal fusions. Ultracentrifugation in first experiment with CLUB-HA and TRS120-HA was carried out for thirty minutes, in the second experiment with additional CLUB-GFP, for one hour. A clear difference was observed, as after one hour of ultracentrifugation 6 - and 24 - fold higher amount of proteins (TRS120-HA and CLUB-HA, respectively) were found in P100K fraction. 97.5% of TRS120 protein was found in the soluble fraction after thirty minutes of ultracentrifugation, while the amount of protein decreased to 86% after one hour. A similar effect was observed for the CLUB protein where, after one hour of ultracentrifugation, the amount of protein in the S100K fraction was reduced from 99.6% to 90.6%. What's more, an increased expression level in the P_{UBQ}::CLUB-

GFP fraction in comparison to P_{CLUB}::CLUB-HA was observed (Table 3.2.3). However, quantification is difficult due to different tags, antibodies and detection exposure times. Time permitting, it would in retrospect have been better to carry fractionation out using stable transgenic plants expressing 3HA-CLUB and 3HA-TRS120 under the strong 35S promoter, to do western blot using anti-HA and then to compare this to C-terminal fusion proteins under the endogenous promoter.

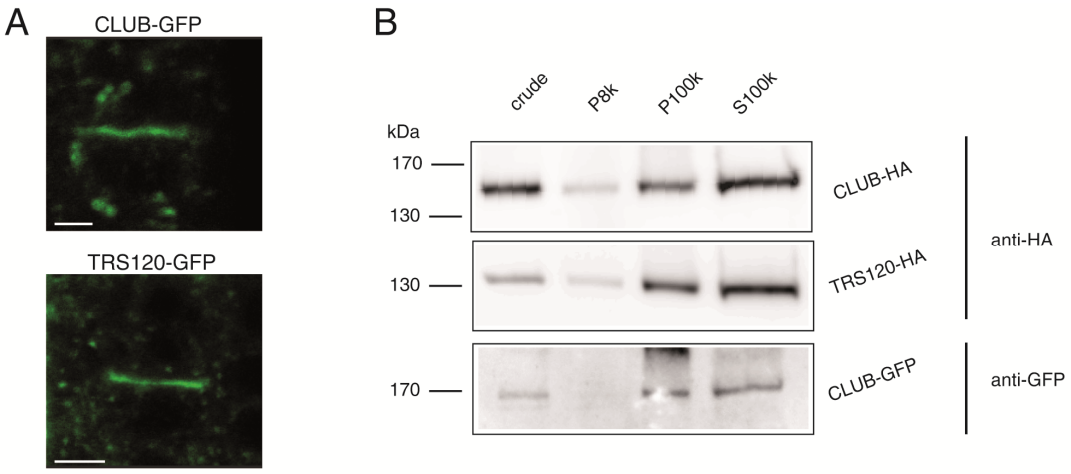

Figure 3.2.3. Intracellular localization of TRAPPII gene fusions.
(A) Cell plate localization of P_{UBQ}::CLUB-GFP (top panel) and P_{TRS120}::TRS120-GFP (lower panel).
(B) Cell fractionation showing that CLUB-GFP, CLUB-HA and TRS120-GFP can be detected in both the membrane (P100K) and soluble (100K) fractions. Samples of 10 µl were loaded on 7.5% polyacrylamide gel. See text and Table 3.2.3 for a detailed description.
Bars = 5 µm.

Protein fusion	Fractions	Replicate 1 (30 min ultracentrifugation)		Replicate 2 (60 min ultracentrifugation)			
		HA C-terminal signal [%]	fold enrichment in soluble fraction	GFP C-terminal signal [%]	fold enrichment in soluble fraction	HA C-terminal signal [%]	fold enrichment in soluble fraction
TRS120	P100K	2.5		-		14.0	
	S100K	97.5		-		86.0	
	S100K/P100K		39				6
CLUB	P100K	0.4		7.7		11.1	
	S100K	99.6		92.3		88.9	
	S100K/P100K		248		12		8

Table 3.2.3. A quantitative analysis of fractionation.
A quantitative analysis of fractionation was carried out with ImageQuant (Fujifilm, FUJIFILM Europe GmbH, Düsseldorf). The relative percentage of protein fusions in P100K and S100K fractions is shown. Ultracentrifigation was carried out for 30 and 60 minutes for replicate 1 and replicate 2, respectively. 10 µl samples were loaded on 7.5% polyacrylamide gel. One gram of plant tissue was homogenized in 6 ml of extraction buffer. P8K (obtained from 2 ml of crude) and P100K (obtained from 2 ml of S8K) fractions were resuspended in 300 µl and 100 µl of extraction buffer, respectively. The S100K fraction was concentrated by a factor of four via lyophilization.

Also, N-terminal GFP CLUB/AtTRS130 and AtTRS120 fusions under 35S promoter were analyzed via CLSM. Several *Arabidopsis* transgenic lines were screened. No signal at the cell plate was detected. Therefore, C-terminal GFP fusions with TRAPPII specific subunits were used for further analyses.

Subsequently, we looked at CLUB-GFP and TRS120-GFP localization over time in dividing cells. Time lapses of CLUB-GFP and TRS120-GFP with mCherry-TUA5, a microtubule marker (Guttierez et al., 2009), were carried out (Fig. 3.2.4A and 3.2.4B, respectively). Both subunits appeared at the cell equator at the onset of cytokinesis labeling the cell plate throughtout cytokinesis, subsequently reorganised to the leading edges (Fig. 3.2.4, white arrowhead) and disappeared after cell plate insertion to the lateral walls (Fig. 3.2.4). Both TRAPPII specific subunits show the same localization dynamics at the cell plate (Fig. 3.2.4; Rybak et al., 2014). As AtTRS120 gene fusions give us brighter signal, we used TRS120 for subsequent analyses.

Additionally, the subcellular localization of CLUB and TRS120 at the electron microscopy level was initiated. Stable transgenic plants expressing both genes, CLUB and TRS120 fused with N-terminal c-Myc under endogenous promoter were generated to carry out an immunogold labeling of the Transmission Electron Micrographs (TEM) with the anti-c-Myc antibody. Cryofixation/freeze-substitution, ultrasectioning, immunolabelenig and electron microscopy remain to be done (Hung et al., 2004; Wilson and Bacic, 2012).

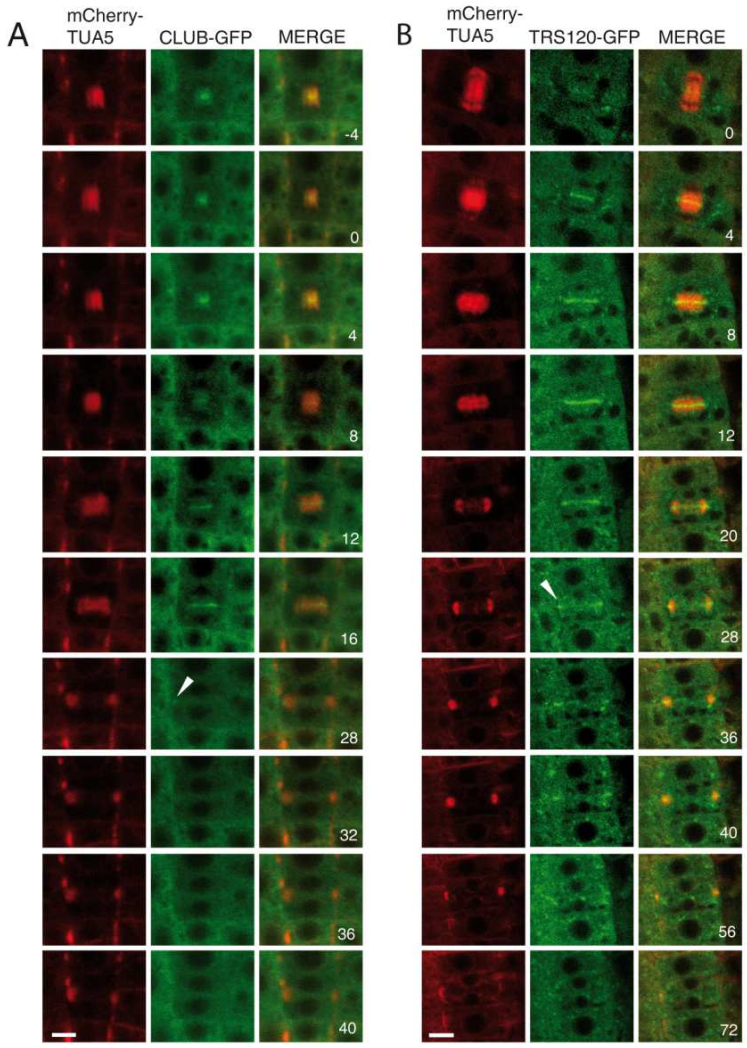

Figure 3.2.4. CLUB-GFP and TRS120-GFP localization and phragmoplast microtubule dynamics.
(A) P_{UBQ}::CLUB-GFP with mCherry-TUA5.
(B) P_{UBQ}::TRS120-GFP with mCherry-TUA5.
Time lapses are shown, with minutes indicated in the right panel. The 0 minute time point corresponds to cell plate initiation. Arrowheads point to the leading edge of the cell plate, where CLUB-GFP and TRS120-GFP have relocated at the ring-shaped phragmoplast stage.
Bars = 5 µm.

3.2.3. Different expression levels of TRS120 do not influence localization dynamics throughout cytokinesis.

In order to assess the localization dynamics of AtTRS120 fusion protein under strong the ubuiqitin promoter as opposed to the native promoter, we looked at GFP expression levels of multiple independent samples under fixed conditions and carried out time lapses throughout cytokinesis. A mean GFP fluorescence intensity through the confocal scans was measured and showed that TRS120 expression levels under ubiquitin promoter were about three-fold higher than under endogenous promoter (Fig. 3.2.5A). Time lapses of P_{TRS120}::TRS120-GFP and P_{UBQ}::TRS120-GFP showed that

overexpression had no influence on localization dynamics throughout cytokinesis (compare Fig. 3.2.4B with Fig. 3.2.5B). Because of lack of antibodies against native TRAPPII subunits, we were unable to compare endogenous protein expression level of AtTRS120 with TRS120 protein fusion. We conclude that the three-fold difference in TRS120 fusion protein expression levels had no effect on localization dynamics throughout cytokinesis.

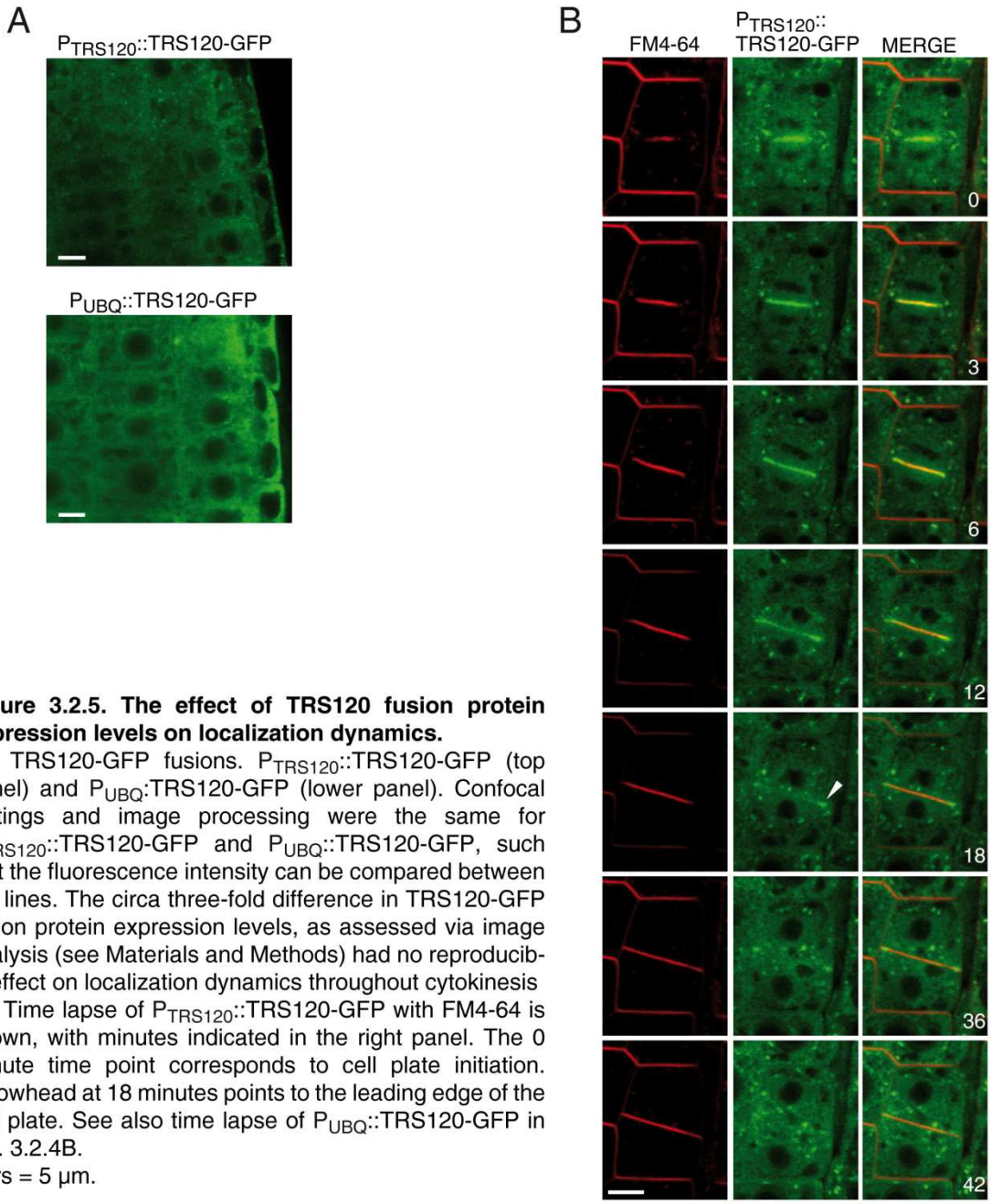

Figure 3.2.5. The effect of TRS120 fusion protein expression levels on localization dynamics.
(A) TRS120-GFP fusions. P_{TRS120}::TRS120-GFP (top panel) and P_{UBQ}:TRS120-GFP (lower panel). Confocal settings and image processing were the same for P_{TRS120}::TRS120-GFP and P_{UBQ}::TRS120-GFP, such that the fluorescence intensity can be compared between the lines. The circa three-fold difference in TRS120-GFP fusion protein expression levels, as assessed via image analysis (see Materials and Methods) had no reproducible effect on localization dynamics throughout cytokinesis
(B) Time lapse of P_{TRS120}::TRS120-GFP with FM4-64 is shown, with minutes indicated in the right panel. The 0 minute time point corresponds to cell plate initiation. Arrowhead at 18 minutes points to the leading edge of the cell plate. See also time lapse of P_{UBQ}::TRS120-GFP in Fig. 3.2.4B.
Bars = 5 µm.

3.2.4. CLUB/AtTRS130 appears to be required for protein sorting at the cell plate.

To ask whether TRAPPII complex is required for protein sorting at the cell plate, different plasma membrane, TGN markers and polysaccharide stains were monitored in the wild-type and *club-2* mutant backgrounds. Four plasma membrane markers: closely related KNOLLE/SYP1 family members, SYP121 and SYP122, the auxin efflux carriers PIN1 and PIN2 were used in this study (Benková et al., 2003; Collins et al., 2003; Assaad et al., 2004; Abas et al., 2006). GFP-SYP121 signal localized to the plasma membrane and cell plate in the wild type but labeled neither the cell plate nor plasma membrane in *club-2* (Fig 3.2.6A; n = 14 for wild type, n = 7 for *club-2*, where n stands for number of cell plates found). By contrast, CFP-SYP122 was absent from cell plates in the wild type, but clearly labeled the cell plate in *club-2* (Fig. 3.2.6B; n = 13 for wild type, n = 5 for *club-2*). In wild type, PIN1-GFP and PIN2-GFP labeled weakly cell plates, and labeled cell plates in *club-2* mutant background with equal relative intensity as FM4-64 (Fig. 3.2.6C and 3.2.6D, respectively; n = 10 and 8 for wild type, n = 10 and 16 for *club-2* for PIN1 and PIN2, respectively). A TGN marker VHA-a1-GFP (Dettmer et al., 2006) was excluded from the cell plate in the wild type, but clear localization to the cell plate was observed in *club-2* background (Fig. 3.2.6E; n = 16 for wild type, n = 12 for *club-2*). An enrichment factor for plasma membrane at the cell plates was measured as signal intensity at the cell plate compared to the signal intensity at the plasma membrane, normalized against FM4-64 (Rybak et al., 2014). Enrichment factors at the cell plate were shown to vary from 9.5 to 0.3 in the wild type but only 1.0 in *club-2* (Rybak et al., 2014). Taken together, the TRAPPII complex appeared to be required for protein sorting at the cell plate.

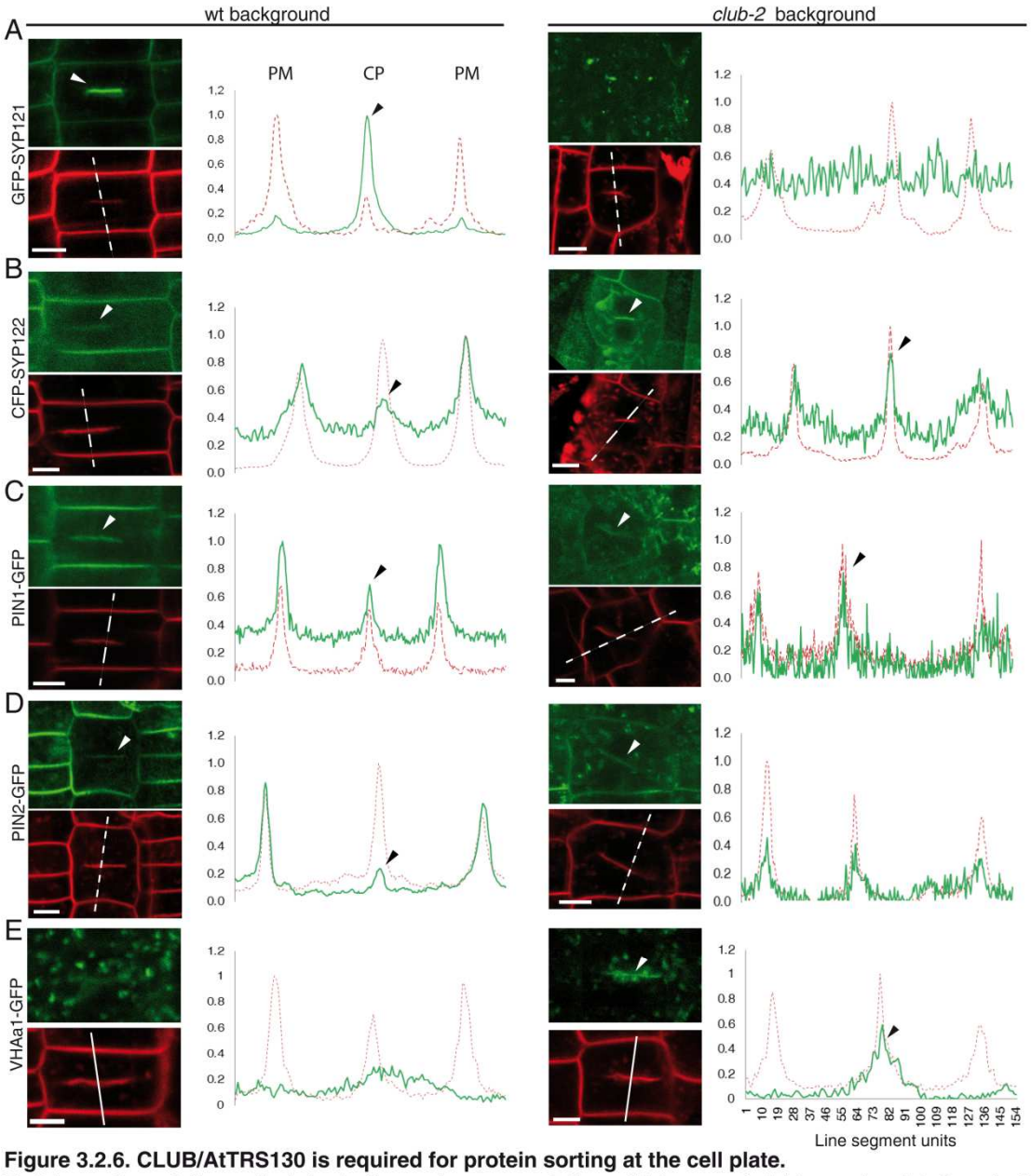

Figure 3.2.6. CLUB/AtTRS130 is required for protein sorting at the cell plate.
Protein sorting at the cell plate. Left panels represent the wild type and right panels *club-2* mutant backgrounds. The line graphs depict scaled relative fluorescence intensity, with FM4-64 (red) used to position on the plasma membranes (PM) and cell plate (arrowhead; CP).
(A) P_{SYP121}::GFP-SYP121.
(B) P_{35S}::CFP-SYP122.
(C) P_{PIN1}::PIN1-GFP.
(D) P_{PIN2}::PIN2-GFP.
(E) P_{VHAa1}::VHAa1-GFP.
Note the punctate appearance of all plasma membrane markers in *club-2* background.
Bars = 5 µm.

3.3. Plant cytokinesis is orchestrated by the sequential action of the TRAPPII and exocyst tethering complexes.

Another tethering complex, the exocyst, widely known to be required for polarized secretion (Heider and Munson, 2012) was found to be implicated in plant cytokinesis. Three exocyst subunits EXO70A1, EXO84b (Fendrych et al., 2010), and SEC6 (Wu et al., 2013) were shown to be involved in cytokinesis. The aim of this study was to understand localization dynamics and role of these two tethering factors in cytokinesis over the time in *Arabidopsis*.

3.3.1. TRAPPII and exocyst mutants exhibit different phenotypes.

If both TRAPPII and exocyst complexes are required for cytokinesis, we would expect to observe typical cytokinesis-defective phenotype in both TRAPPII and exocyst mutants. However, the two tethering complexes show different phenotypes (Fig. 3.3.1). TRAPPII mutants show canonical cytokinesis-defective phenotype, like bloated cells (Fig. 3.3.1C, white arrowhead) and cell wall stubs (Fig. 3.3.1C, white arrow). None of such cytokinesis defects were observed in *exo84b-2* hypocotyl and root tips (Fig, 3.3.1E), but cell wall stubs and aberrations in stomata development (e.g. guard cells with incomplete ventral walls) have been observed in *exo84b-2* leaf epidermis (Fendrych et al., 2010). What's more, *exo84b-2* mutants had cell wall related defects, like broken walls in vacuolated cells (Fendrych et al., 2010) as well as radial swelling and expanded hypocotyl cells.

As confocal microscopy cannot resolve small cell wall gaps, Focused Ion Beam/ Scanning Electron Microscopy (FIB/SEM) was applied. FIB/SEM tomographic dataset also failed to reveal reproducible cell wall defects in *exo84b-2* (Fig. 3.3.1G; n > 200 cells), but detected frequent (33%, n = 33 cells) stubs and incomplete walls in *trs120-4* mutants (Fig. 3.3.1H). In summary, we were not able to show canonical cytokinesis defects in *exo84b-2* mutants.

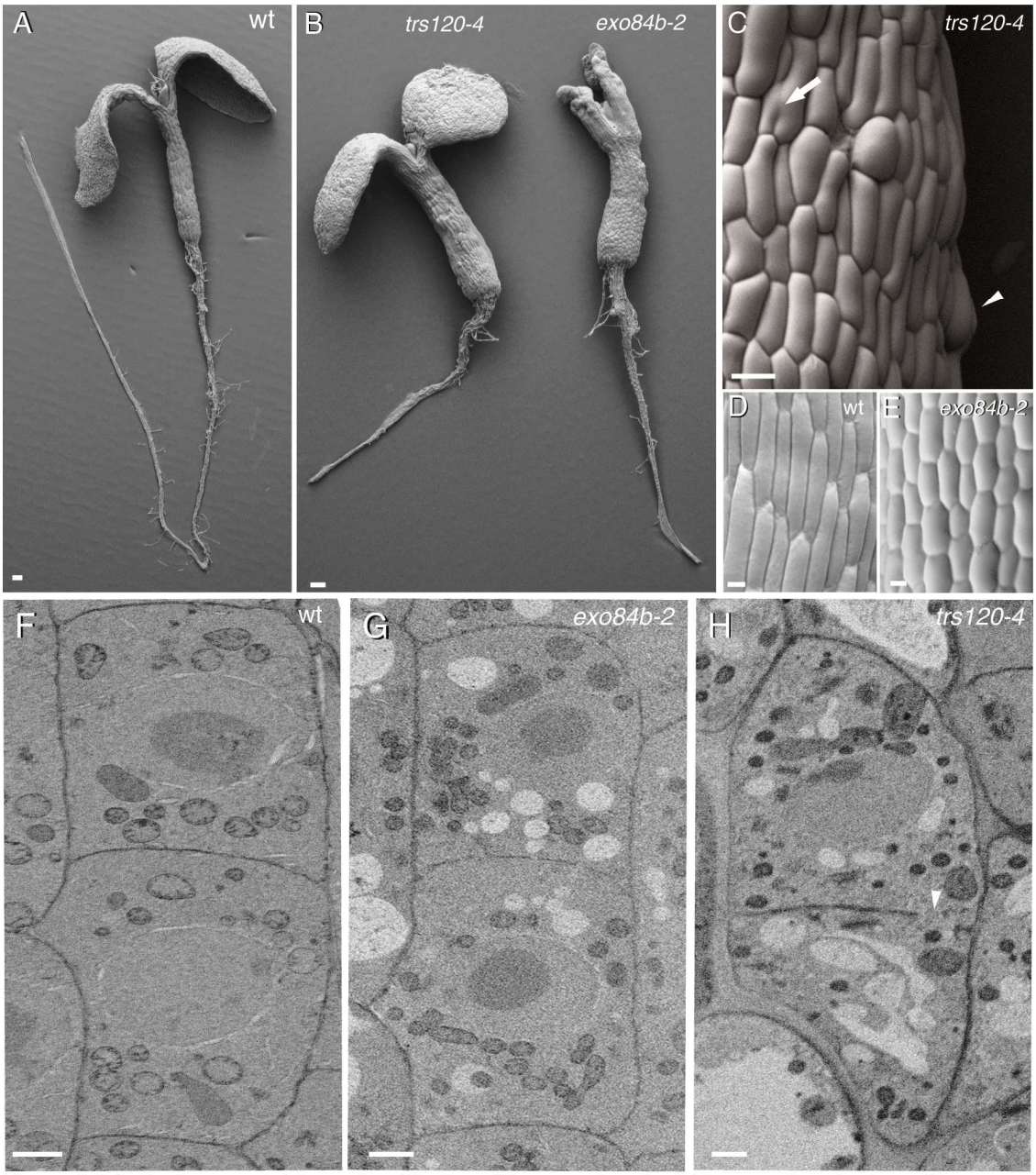

Figure 3.3.1. Environmental Scanning Electron Micrographs of wild type and mutant seedlings.
(A-E) Scanning Electron Micrographs of seedlings.
(A, B) Overviews. (C-E) Close-ups.
(A, D) Wild type.
(B, left; C) *trs120-4.* In (C) the arrow points to a cell wall stub and the arrowhead to a bloated cell.
(B, right; E) *exo84b-2*.
(F-H) Electron Micrographs of high pressure frozen, freeze substituted five-day-old root tips.
(F) Wild type.
(G) *exo84b-2*. Note the regular shape of the cell and the complete cross wall, as in the wild type.
(H) *trs120-4*. Arrowhead points to the cell wall gap in the micrograph.
Bars = 100 µm in (A, B), 20 µm in (C-E) and 2 µm in (F-H).

3.3.2. The appearance of the TRAPPII and exocyst complexes at the cell plate is predominantly sequential, with brief overlap at the onset and end of cytokinesis.

To better understand the role of TRAPPII and exocyst complexes in cytokinesis we compared the localization dynamics over time in dividing cells of TRAPPII specific subunit AtTRS120 and exocyst subunit EXO84b. TRS120-GFP labeled the cell plate throughout the cytokinesis and disappeared after insertion of the cell plate to the lateral cell walls (Fig. 3.3.2A; Fig. 3.2.4B and Fig. 3.2.5B). Different localization dynamics showed that EXO84b-GFP appeared at the cell equator labeling cell plate at the beginning and at the end of cytokinesis as well as newly formed cross walls (Fig. 3.3.2B and Fig. 3.3.5C; Fendrych et al., 2010). Line graphs through expanding cell plates showed that the EXO84b-GFP signal was no longer at the cell plate, but appeared as a diffuse cloud around the plate (Fig. 3.3.2B, 6 minutes).

Next, to better monitor localization of TRS120-GFP and EXO84b-GFP at distinct stages of cytokinesis, Tua5-mCherry was used as a microtubule marker (Gutierrez et al., 2009). At the onset of cytokinesis phragmoplast, a transient array of polar microtubules is assembled. A solid phragmoplast expands during cell plate formation. In telophase, microtubules are translocated to the leading edges by depolimerization of the microtubules at the centre and repolimerization at the outside edges, giving rise to a ring-shaped phragmoplast (McMichael and Bednarek, 2013; Rasmussen et al., 2013). Both TRS120-GFP and EXO84b-GFP appeared at the cell equator at the phragmoplast assembly stage (Fig. 3.3.3A and 3.3.3B). But later, at the solid phragmoplast stage, while TRS120 remained, EXO84b-GFP signal became weaker and diffuse. At the ring-shaped phragmoplast stage TRS120-GFP relocated to the leading edges of the cell plate and subsequently disappeared. By contrast, EXO84b-GFP signal increased and reached peak fluorescence throughout the cross wall as the phragmoplast disappeared (Fig. 3.3.3C and 3.3.3D).

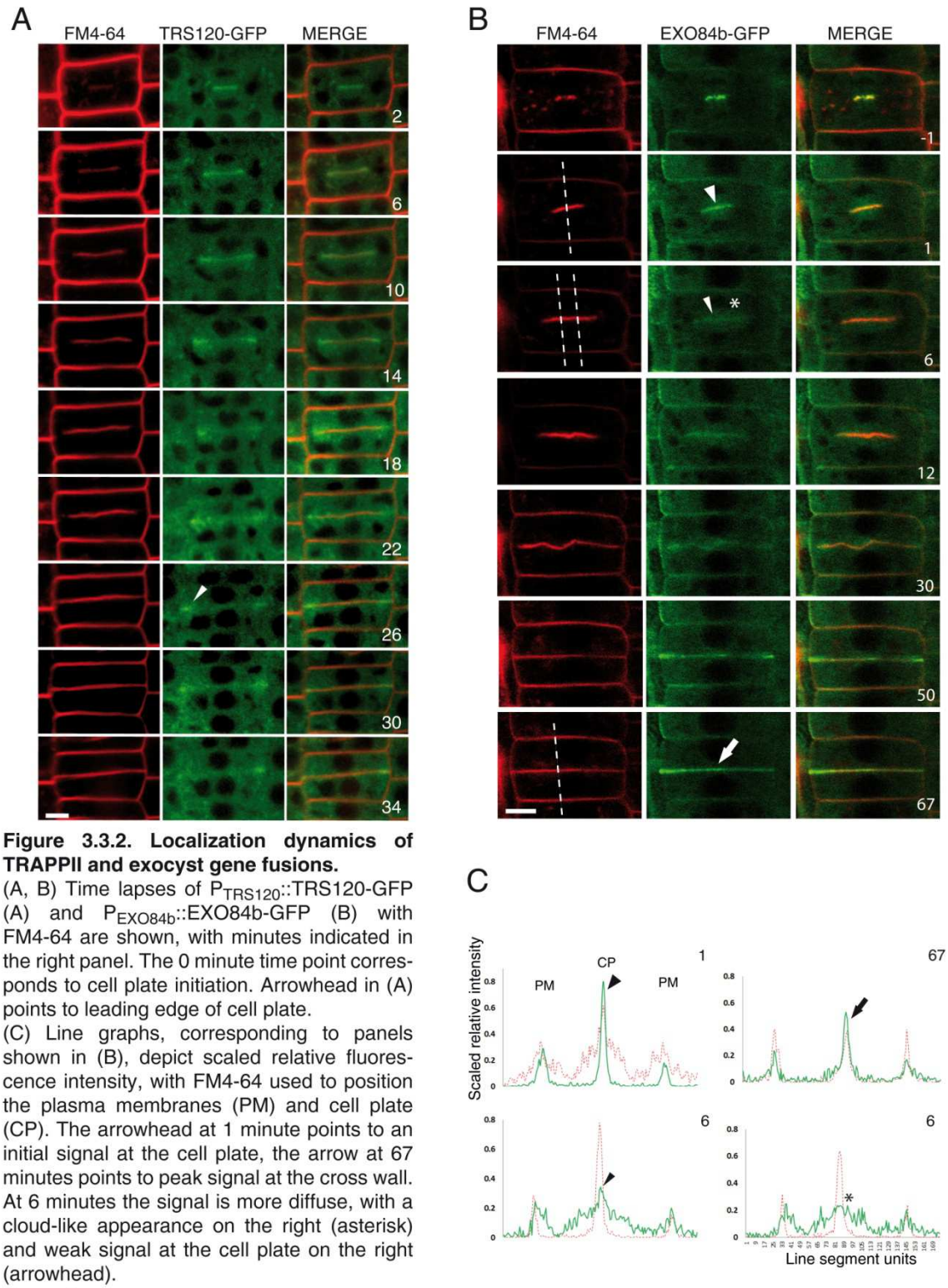

Figure 3.3.2. Localization dynamics of TRAPPII and exocyst gene fusions.
(A, B) Time lapses of P_{TRS120}::TRS120-GFP (A) and P_{EXO84b}::EXO84b-GFP (B) with FM4-64 are shown, with minutes indicated in the right panel. The 0 minute time point corresponds to cell plate initiation. Arrowhead in (A) points to leading edge of cell plate.
(C) Line graphs, corresponding to panels shown in (B), depict scaled relative fluorescence intensity, with FM4-64 used to position the plasma membranes (PM) and cell plate (CP). The arrowhead at 1 minute points to an initial signal at the cell plate, the arrow at 67 minutes points to peak signal at the cross wall. At 6 minutes the signal is more diffuse, with a cloud-like appearance on the right (asterisk) and weak signal at the cell plate on the right (arrowhead).
Bars = 5 µm.

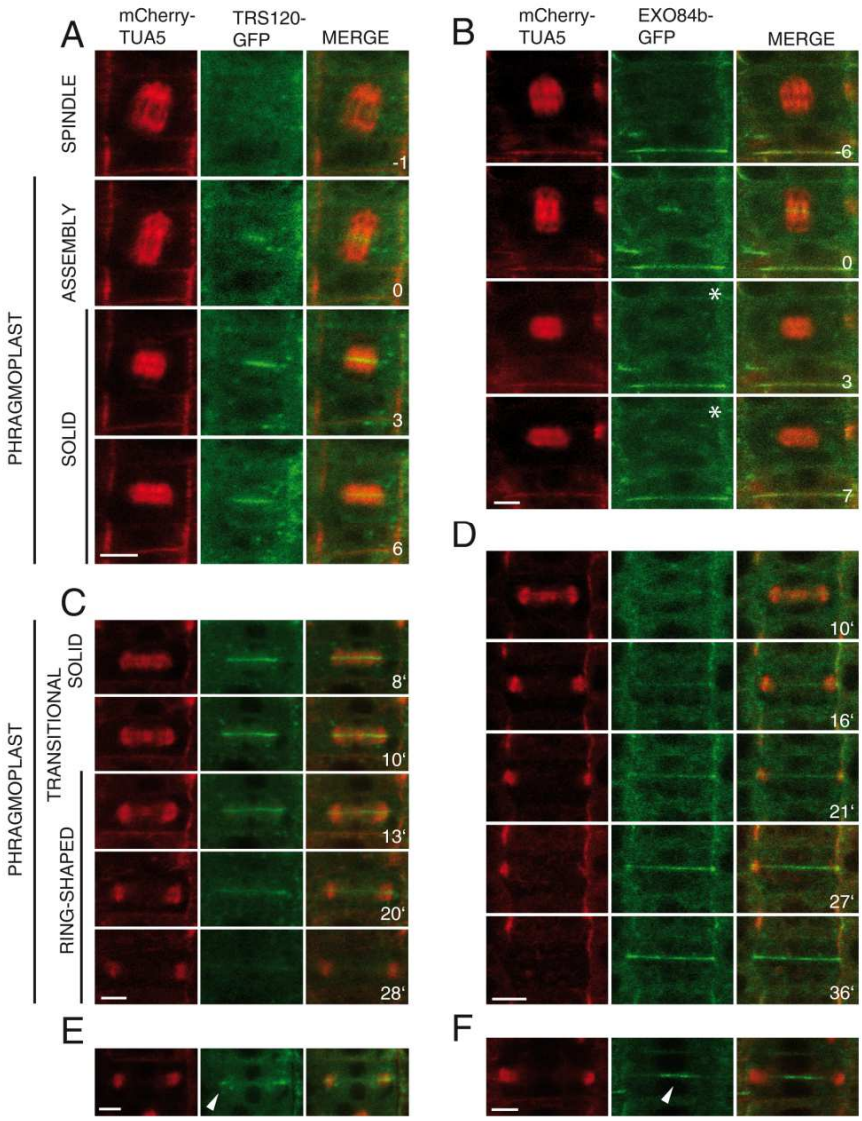

Figure 3.3.3. Localization of TRAPPII and exocyst gene fusions and phragmoplast microtubule dynamics.

(A-F) Time lapses of P_{TRS120}::TRS120-GFP (A, C) and P_{EXO84b}::EXO84b-GFP (B, D) with mCherry-TUA5 are shown, with minutes indicated in the right panel. The 0 minute time point corresponds to cell plate initiation.

(A, B) Anaphase-telophase transition. Star in (B) at 3 and 7 minutes designates barely detectable, diffuse EXO84b-GFP cytosolic signal.

(C, D) Telophase. The time lapse segments start at the solid phragmoplast stage, which occurs on average 8 minutes after cell plate initiation, whence the labeling 8' etc.

(E, F) Ring-shaped phragmoplast stage. Arrowhead in (E) points to leading edge of cell plate. Arrowhead in (F) points to first appearance of the exocyst subunit. The brief window in time shown in (E) and (F) was missed in the time lapses shown in (C) and (D). This is because the fluorescence was low and photobleaching extensive, such that time lapses were carried out with 4 minute intervals.

Bars = 5 µm.

3.3.3. Co-localization of the TRAPPII and the exocyst subunits confirms a sequential localization at the cell plate.

Subsequently, co-localization of TRS120 and three exocyst subunits (SEC6, EXO70A1 and EXO84b) was carried out. All combinations showed the same result. While peak fluorescence of the TRS120 was observed during cell plate formation, peak fluorescence of the exocyst subunit reached the point at the cross wall, where TRS120 was absent (Fig. 3.3.4). An overlap between complexes was observed at the onset of the cytokinesis and at the time of TRS120 recycling away from the cell plate (Rybak et al., 2014). The two tethering factors do not co-localize in non-dividing cells, except for cytosolic pools (Fig. 3.3.4D).

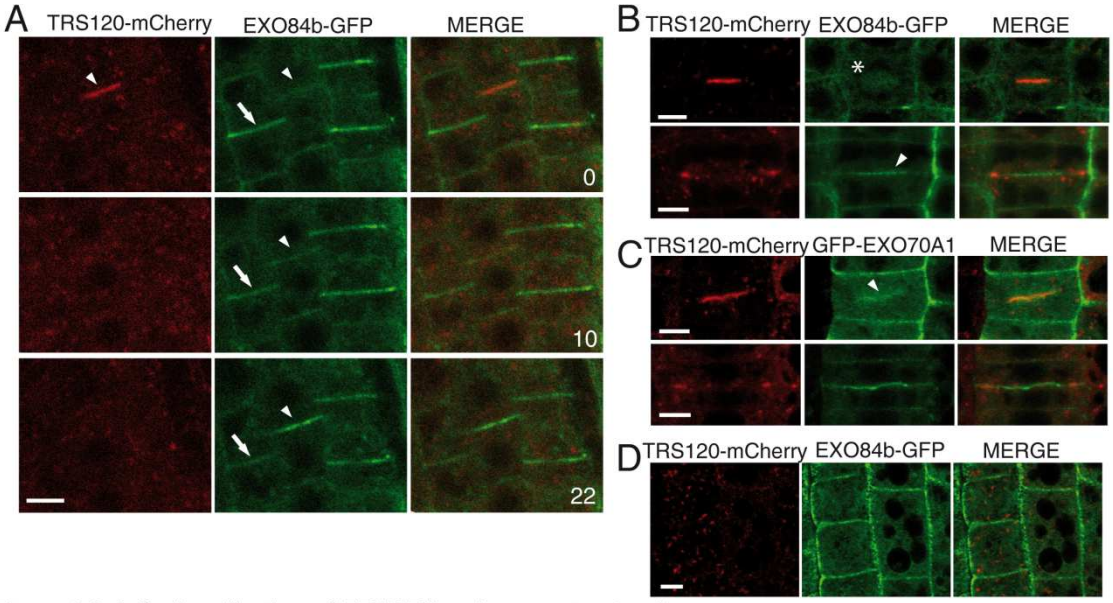

Figure 3.3.4. Co-localization of TRAPPII and exocyst subunits.
(A) Time lapse (minutes indicated in the right panel) shows the sequential appearance of P_{UBQ}::TRS120-mCherry and P_{EXO84b}::EXO84b-GFP (arrowhead) as well as the gradual disappearance of P_{EXO84b}::EXO84b-GFP at the cross wall (arrow).
(B) Upper panel: P_{UBQ}::TRS120-mCherry labels a sharp band at the cell equator, whereas the P_{EXO84b}::EXO84b-GFP signal is diffuse (asterisk). Lower panel: P_{EXO84b}::EXO84b-GFP first appears at the cell plate (arrowhead) after P_{UBQ}::TRS120-mCherry has relocated to the leading edges of the cell plate (arrowhead).
(C) P_{35S}::GFP-EXO70A1 persists at the cell plate (arrowhead) throughout cytokinesis. This discrepancy with P_{EXO84b}::EXO84b-GFP may be related to the overexpression of EXO70A1 under the control of the P35S promotor.
(E) P_{UBQ}::TRS120-mCherry and P_{EXO84b}::EXO84b-GFP do not co-localize in non-dividing cells.
Bars = 5 µm.

We conclude that the appearance of the TRAPPII and the exocyst complexes in dividing cells was mainly sequential with brief overlap at the phragmoplast assembly stage at the onset of cytokinesis, and at the late ring-shaped phragmoplast stage at the end of cytokinesis. No co-localization was observed between these two thethering complexes in non-dividing cells.

3.3.4. Expression levels of the exocyst subunits do not influence localization dynamics throughout cytokinesis.

In order to exclude the possibility of altered localization dynamics due to the different expression level of fusion proteins, quantitative analyses of EXO84b under endogenous and strong P35 promoters, as well as weak and strong EXO70A lines under strong P35S promoter were carried out. An assessment of mean GFP fluorescence intensity via image analysis of confocal scans showed that EXO84b expression was roughly two-fold higher with the P35S than with the endogenous promoter (Fig. 3.3.5A). This difference in fusion protein expression level had no reproducible effect on localization dynamics throughout cytokinesis (Fig. 3.3.5C and Fig. 3.3.2B). Additionally, we ran western blots with antibodies against the EXO84b subunits. The GFP fusion protein expression levels were weaker than the endogenous protein (Fig. 3.3.5B), which is consistent with their low fluorescence level. An alpha tubulin was used as a control. EXO84b-GFP fusion protein (red arrowhead) was detected with the GFP antibody but not with the anti-EXO84b antibody at the exposure levels that detect the endogenous protein (black arrowhead) in the same sample. Confocal and western blot analyses showed that expression level of EXO70A1-GFP also does not alter its localization dynamics (Fig. 3.3.6). Western blots with antibodies against the EXO70A1 subunit were run. EXO70A1-GFP fusion protein (red arrowhead) was detected with GFP antibody but not with the anti-EXO70A1 antibody at the exposure levels that detect the endogenous protein (black arrowhead) in the same sample (Fig. 3.3.6B). Time lapses of two different EXO70A1-GFP expressing lines showed the same localization dynamics in dividing cells (Fig. 3.3.6C and Fig. 3.3.6D). Taken together, expression level of EXO84b and EXO70A1 protein fusion had no influence on localization dynamics in dividing cells.

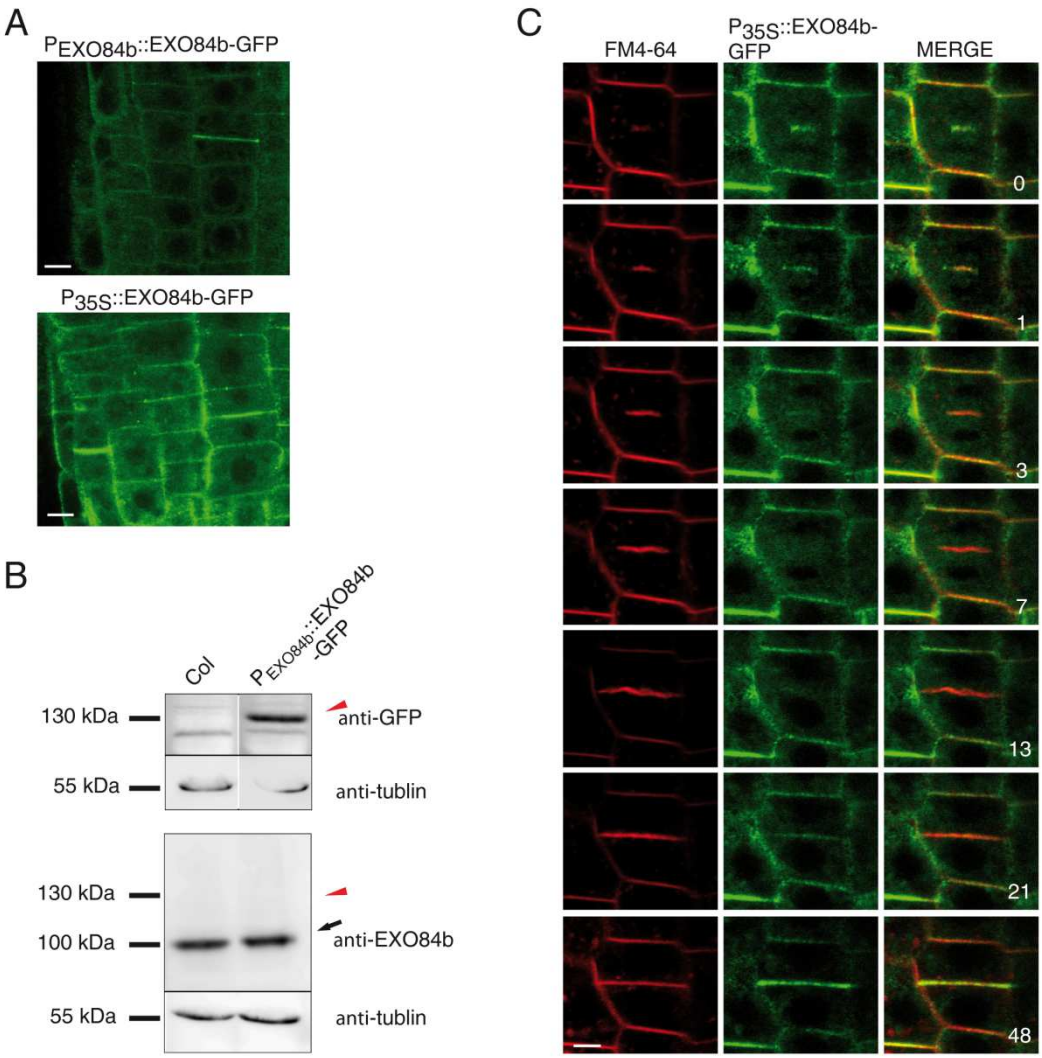

Figure 3.3.5. The effect of EXO84b fusion protein expression levels on localization dynamics.
(A) EXO84b-GFP fusions. P_{EXO84b}::EXO84b-GFP (top panel) and P_{35S}:: EXO84b -GFP (Fendrych et al., 2010; lower panel). Confocal settings and image processing were the same for for both panels, such that the fluorescence intensity can be compared between the lines. The mean signal intensity through the scans show two-fold higher expression level of EXO84b fusion protein under P35S than under endogenous promoter.
(B) Western blots with antibodies against GFP, EXO84B and alpha tubulin as a loading control. 15 µl of S8K fractions were loaded on 8% polyacrylamide gel. The P_{EXO84b}::EXO84b-GFP fusion protein (red arrowhead) is clearly visible with the GFP antibody but not detected with the anti-EXO84b antibody at exposure levels that readily detect the endogenous protein (black arrow) in the same sample. Thus, the GFP fusion protein expression levels were considerably weaker than the endogenous protein, which is consistent with its low fluorescence levels.
(C) Localization dynamics of EXO84b-GFP fusions throughout cytokinesis. Time lapse of P_{35S}::EXO84b-GFP with FM4-64 is shown, with minutes indicated in the right panel. Compare to the time lapse of P_{EXO84b}::EXO84b-GFP Fig. 3.3.2B. Note that the two-fold difference in fusion protein expression levels, as assessed by image analysis (see Materials and Methods) had no reproducible effect on localization dynamics.
Bars = 5 µm.

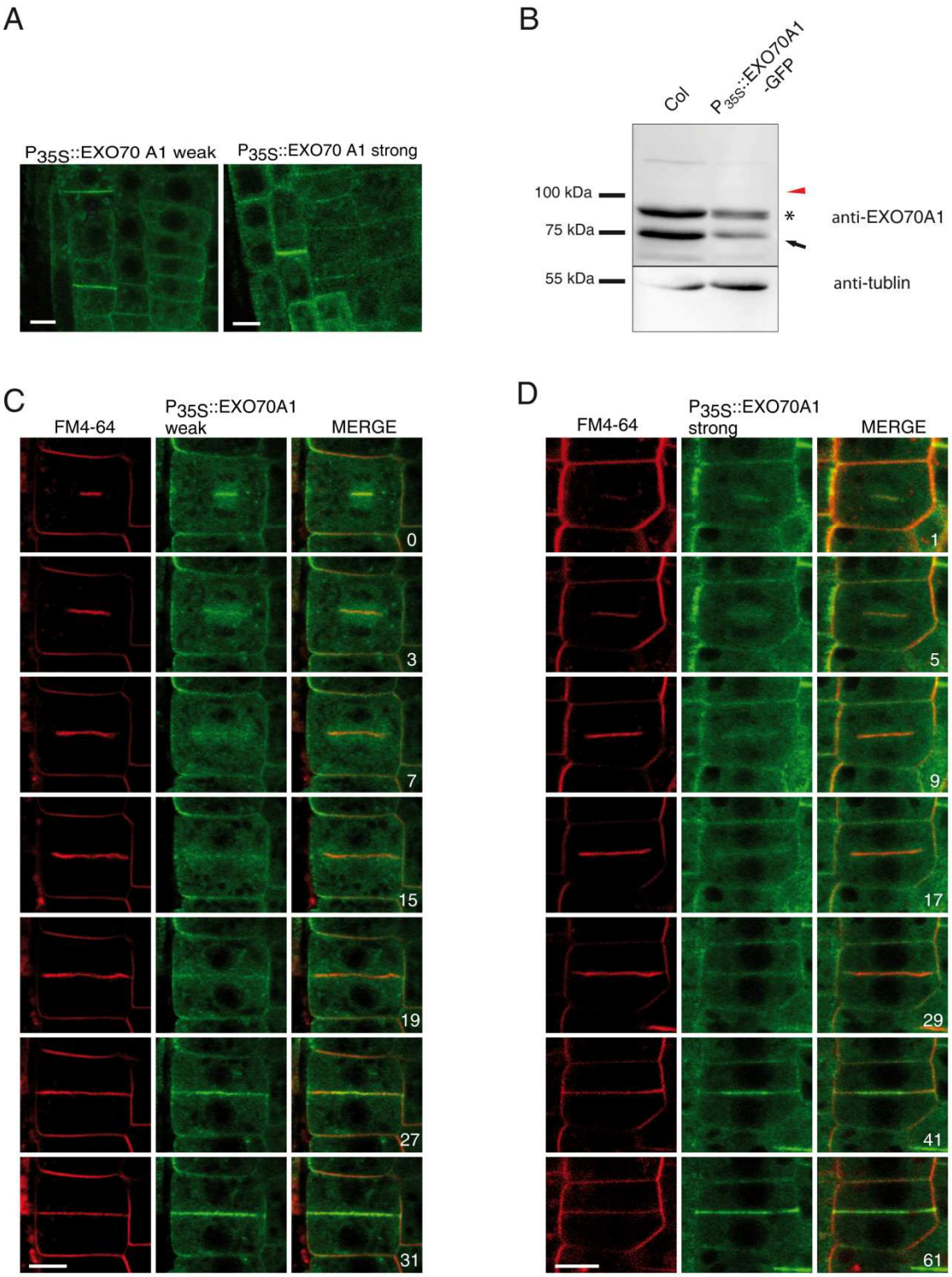

Figure 3.3.6. The effect of EXO70A1 fusion protein expression levels on localization dynamics.
(A) EXO70A1-GFP fusions. P_{35S}::EXO70A1-GFP weakly expressing line (left panel); P_{35S}::EXO70A1-GFP strongly expressing line (right panel). Confocal settings and image processing were the same for both panels, such that the fluorescence intensity can be compared between the lines.
(B) Western blots with antibodies against EXO70A1 and alpha tubulin as a loading control. 15 µl of S8K fractions were loaded on 8% polyacrylamide gel. The P_{35S}::EXO70A1-GFP fusion protein (red arrowhead) is not detected with the anti-EXO70A1 antibody at exposure levels that readily detect the endogenous protein (black arrow) in the same sample. Thus, the GFP fusion protein expression levels were considerably weaker than the endogenous protein, which is consistent with its low fluorescence levels.
(C, D) Localization dynamics of EXO70A1-GFP fusions throughout cytokinesis. Time lapses of P_{35S}::EXO70A1-GFP weakly expressing line (C) and strongly expressing line (D) with FM4-64. Minutes are indicated in the right panel. Note the same localization dynamic for both EXO70A1 expression lines.
Bars = 5 µm.

3.3.5. The TRAPPII complex is required for the proper localization of the exocyst complex.

Our next aim was to check whether TRAPPII complex is required for exocyst localization at the cell plate or plasma membrane and, conversely, if the exocyst regulates TRAPPII complex localization. For this purpose, GFP fusion constructs were crossed into exocyst or TRAPPII mutants. Time lapse of TRS120-GFP with FM4-64 in *exo84b-2* mutant background showed a normal appearance (Fig. 3.3.7A), indicating no infuence of exocyst on TRAPPII complex localization in dividing cells. By contrast, EXO84b-GFP signal in *club-2* mutant background was different to the wild type (Fig. 3.3.7B, top panel). Characteristic punctate appearance and impaired targeting to the newly cross walls and labeling of the cell plate was observed (Fig 3.3.7B). EXO84b-GFP appeared as a faint but sharp line at the cell plate in *club-2* (Fig. 3.3.7B, lower panel), as opposed to a diffuse stain around the cell plate in the wild type (Fig. 3.3.7B, top panel). Enrichment factors at the expanding cell plates (signal intensity at the cell plate compared to the signal at the plasma membrane, normalized against FM4-64 values) were significantly different between the wild type and *club-2* ($p = 0.004$; Rybak et al., 2014). Based on these observations, we conclude that TRAPPII complex acts upstream of the exocyst complex and may be required for sorting the exocyst away from the cell plate during anaphase to telophase and for exocyst targeting to the cell plate initials and to maturing cross wall at the end of cytokinesis.

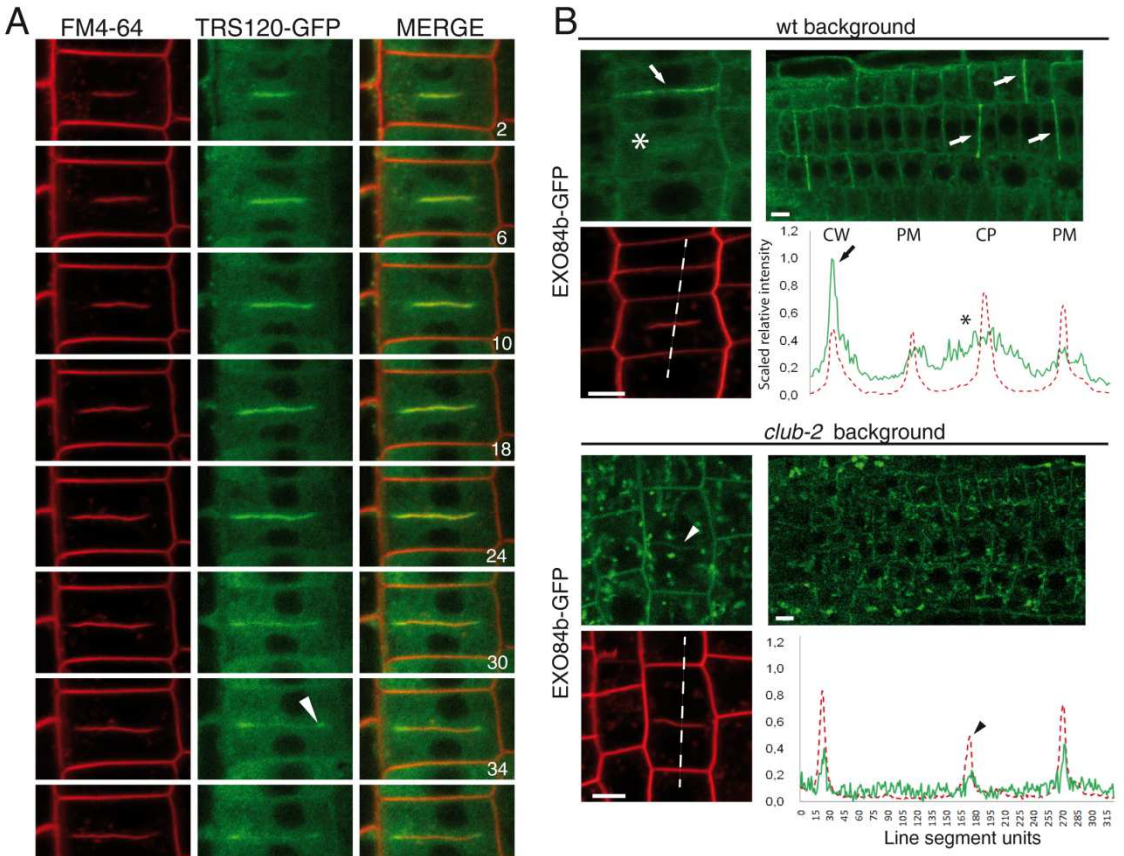

Figure 3.3.7. TRS120-GFP localization dynamics in *exo84b-2* and EXO84b-GFP in *club-2*.
(A) TRS120-GFP localization dynamics in *exo84b-2* mutant background. Time lapse with FM4-64 is shown, with minutes indicated in the right panel. P_{TRS120}::TRS120-GFP localization dynamics in the *exo84b-2* mutant did not differ from the wild type. Note relocalization of the signal to the leading edges of the cell plate (arrowhead at 34 minutes), as in the wild type (Fig. 3.2.5B and Fig. 3.3.2A).
(B) P_{EXO84b}::EXO84b-GFP localization in *club-2* mutant backround. Top panels represent the wild type and lower panels *club-2* mutant backgrounds. The line graphs depict scaled relative fluorescence intensity, with FM4-64 (red) used to position the plasma membranes (PM), cell plate (arrowhead; CP) and the cross wall (arrow; CW). Asterisk indicates a cloud in the wild type (top) and the arrowhead a small peak in *club-2* (lower panel); earlier time points show the same localization pattern.
Bars = 5 µm.

3.3.6. The TRAPPII complex is required for cell plate biogenesis and the exocyst for cell plate maturation.

Next we asked whether TRAPPII or exocyst complexes are required for cell plate biogenesis. *Arabidopsis* TRAPPII mutants are seedling lethal. Exocyst mutants differ from gametophytic lethality to viability. In order to compare TRAPPII and exocyst phenotypes of similar strength, 54 exocyst insertion lines were screened in the Assaad lab in search of strong cytokinesis-defective phenotype (Table S4). An exocyst mutant line, *exo84b-2,* showing a seedling lethal phenotype was identified and used in subsequent study. To compare cell plate formation in TRAPPII and exocyst mutants, immunostain assays were performed. Wild-type and mutant root tips were labeled with DAPI to define the nuclear stage. Anti-microtubule and anti-KNOLLE antibodies were used to stain phragmoplast microtubules and cell plate membranes, respectively. Throughout the early to late solid phragmoplast stages, a defect in cell plate biogenesis was observed in *trs120-4* mutants (Fig. 3.3.8A and 3.3.8B). 84% of *trs120-4* or *club-2* cell plates were absent, patchy or incomplete (n = 183) (Jaber et al., 2010; Thellmann et al., 2010). By contrast, no disruption in cell plate biogenesis was monitored in *exo84b-2* mutants, where 92% of cell plates were complete at this stage (n = 48) similarly to the 84% in wild type (n = 115) (Fig. 3.3.8A and 3.3.8B). While we did not see any difference between the wild type and *exo84b-2* mutants at the beginning of the cytokinesis, a clear aberration was detected at the end of the cytokinesis. At the late ring-shaped phragmoplast stage, when fully expanded cell plates reach the lateral walls, KNOLLE is actively removed from wild type cell plate. We have observed a premature recycling of KNOLLE in *exo84b-2* mutants, where punctate KNOLLE stained cell plate appeared already at the early ring-shaped phragmoplast stages (Fig. 3.3.8C). Taken together, our data show that the TRAPPII complex but not the exocyst complex is required for cell plate biogenesis. Premature removal of KNOLLE in *exo84b-2* mutants might be due to impaired maturation of the cell plate.

It was difficult to obtain a large number of cytokinetic cells in exocyst mutants as the mitotic index in *exo84b-2* was shown to be significantly lower than in TRAPPII mutants ($p = 0{,}004$ for *club-2* and *trs120-4*) than in other canonical cytokinesis-defective mutants such as *massue* (Thiele et al., 2009; Rybak et al., 2014).

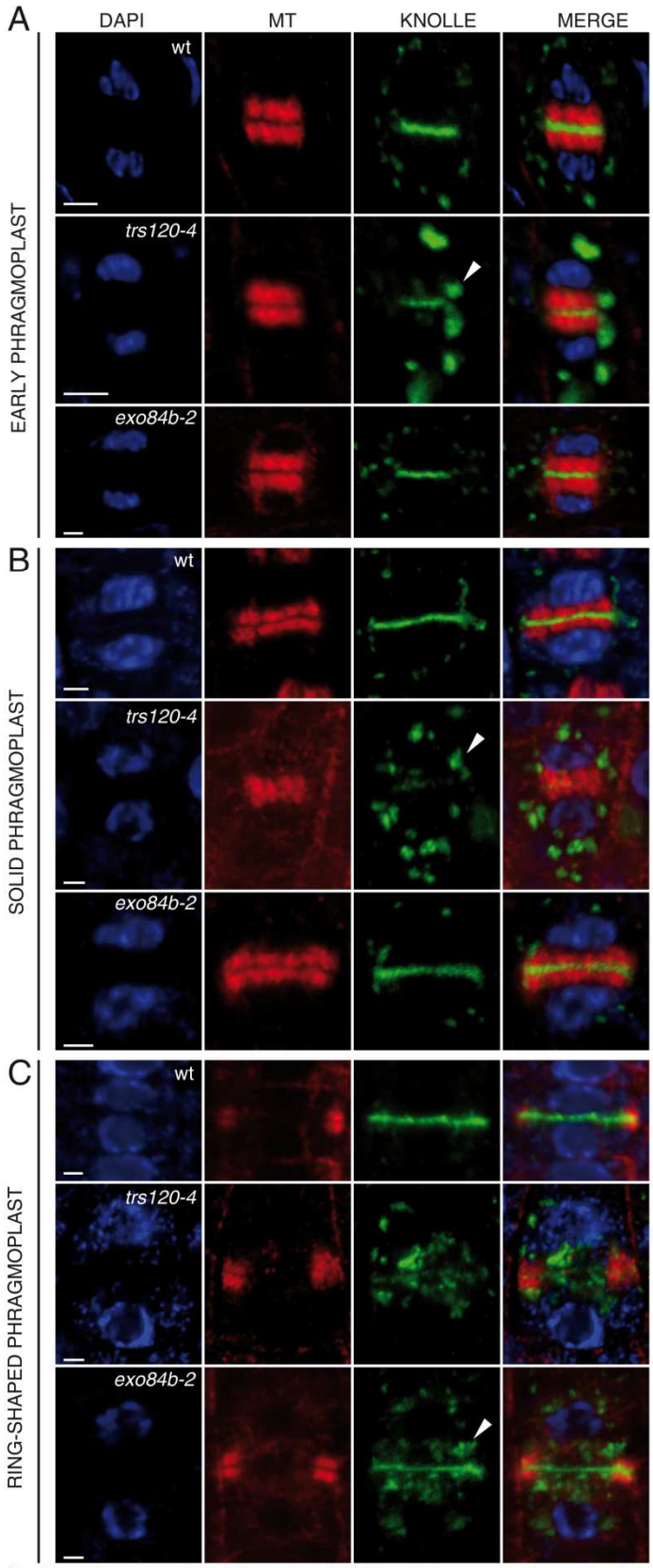

Figure 3.3.8. Cell plate biogenesis and maturation in wild-type and mutant backgrounds.
Antibody stains of root tips. DAPI/nucleus (blue); microtubules (red); KNOLLE protein (green); and merge. The cell cycle stage is indicated on the left and the genotype in the first column. Arrowheads point to large KNOLLE positive compartments surrounding thin or absent cell plates in *trs120-4* (A-C) and surrounding telophase plates in *exo84b-2* (C). See text for a detailed description.
Bars = 2 µm.

In order to determine whether the exocyst is involved in cell plate and cross wall maturation, a survey with thirteen different antibodies against cell wall polysaccharides including callose, cellulose, xyloglucans, pectins and AGP glycans was carried out. We observed fewer callose labeled nascent cross walls in exocyst mutant compared to the wild type (data not shown), but that could be due to the low mitotic index of exocyst mutants. We were not able to detect differences in the appearance of crystalline cellulose (CBM3a; Blake et al., 2006) in TRAPPII and exocyst mutants. We continued with un-esterified pectins (JIM5 antibody, Knox et al., 1990) and methyl-esterified pectins (JIM7 antibody, Claussen et al., 2003), as a good cell plate markers, and with AGP glycans (LM14 antibody, Moller et al, 2008) and xyloglucan (LM25, Pedersen et al., 2012), as the best marker for nascent cross walls and mature cell walls. In the wild type, JIM7 and JIM5 positive compartments were observed at the cell equator as of early anaphase and stained the cell plate throughout cytokinesis. Lateral walls were hardly labeled (Fig. 3.3.9A, left panel and 3.3.9D, left panel). Staining with JIM5 was always punctate. In *club-2* mutants, there was almost no JIM7 signal at the cell plate (Fig. 3.3.9A, middle panel). In *exo84b-2* mutant JIM5 and JIM7 signal at the cell plate was variable (Fig. 3.3.9A, right panel and Fig. 3.3.9D, right panel), and was often ectopically detected on lateral walls and cross walls (Fig. 3.3.9A, right panel and 3.3.9B). In the wild type, LM14 antibody stained mainly lateral walls and cell plate only after insertion (as from late ring-shaped phragmoplast microtubules reach the outer edges of the cell) into lateral walls (Fig. 3.3.9C, left panel). In *club-2* mutants, LM14 signal was ectopically detected in the cytosol and weakly at the cell walls (Fig. 3.3.9C, middle panel). In exocyst mutants, LM14 positive compartments at the cell wall had a punctate appearance and telophase cell plates showed stronger signal compared to the wild type, with little signal on lateral walls (Fig. 3.3.9C, right panel). In the wild type, LM25 antibody labeled cell plate over cytokinesis, cross walls and lateral walls (Fig. 3.3.9E, left panel). In *exo84b-2* mutants, LM25 was mainly absent from the cell plate and often stained in intracellular structures in cytosol (Fig. 3.3.9E, right panel). Immunostaining with JIM7 and LM14 antibodies was carried out three times in the wild type and in *exo84b-2* mutants. Numbers for staining with JIM5 (one replicate) and LM25 (two replicates) antibodies are low and the immunostains need to be repeated.

In summary, the relative content of un-esterified and methyl-esterified pectins, AGP glycans and xyloglucans was altered in the cell plates, cross walls and lateral walls for both TRAPPII and exocyst mutants.

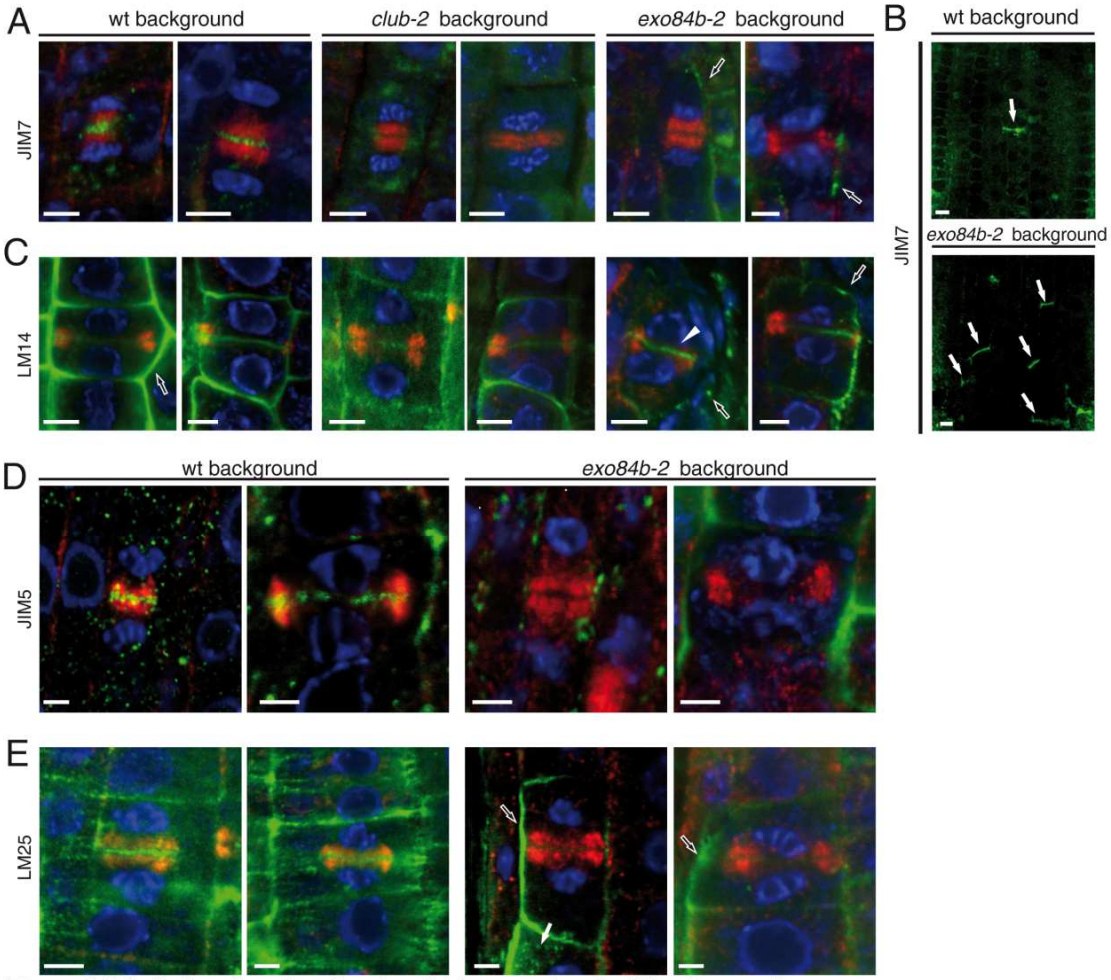

Figure 3.3.9. Cell wall maturation in wild-type and mutant backgrounds.
Cell wall polysaccharide stains of *Arabidopsis* root tips. DAPI/nucleus (blue); microtubules (red); JIM7 or LM14 (green).
(A) JIM7 antibody stain. In the wild type (two left panels), JIM7 positive staining was detected in 97% of cell plates (n = 127). In *club-2* (middle panels), JIM7 staining was absent in 94% of cell plates (n = 68), and in *exo84b-2* (right panels) it was absent from 79% of cell plates (n = 33), but was often detected on lateral walls (white-rimmed black arrow).
(B) Overviews of root tips showing ectopic cross wall stain (arrows) in *exo84b-2* mutants. These were more than ten-fold more frequent in the mutant than in the wild type, in which a rare event is shown.
(C) LM14 antibody stain. In the wild type (two left panels), LM14 positive staining was weak or absent in 83% of expanding cell plates (n = 88). In *club-2* (middle panels), LM14 staining was present as of the ring-shaped phragmoplast in 67% of cell plates (n = 12); the stain was often punctate at the cell wall, and cell plates were labelled with the same intensity as lateral and cross walls. In *exo84b-2* (right panels) the stain was often punctate on lateral walls (white-rimmed black arrows; n = 7) and could be seen on nascent cross walls (arrow; n = 6).
D) JIM5 antibody stain. In the wild type (two left panels), JIM5 stained the cell plate throughout cytokinesis in 78% of cases (n = 32). The stain was mainly punctate. In exo84b-2 (two right panels), JIM5 was absent from the cell plate in 80% of cases (n = 10).
(E) LM25 antibody stain. In the wild type (two left panels), LM25 positive staining was detected in 67% of cell plates throughout cytokinesis (n = 31). In exo84b-2 (two right panels), LM25 staining was absent in 69% of cell plates (n = 13), but was often detected as intracellular pools (arrow; n = 7), as well as on lateral and cross walls (white-rimmed black arrows; n = 8).
Bars = 5 µm.

3.3.7. The TRAPPII and exocyst complexes physically interact.

A brief co-localization of the TRAPPII and exocyst complexes at the beginning and at the end of cytokinesis, as well as the dependence of exocyst localization on TRAPPII function, raised the question as to whether the two tethering complexes physically interact. The TRAPPII complex consists of 9 conserved subunits encoded by 10 genes, and the exocyst complex of 8 subunits encoded by 36 genes in *Arabidopsis*. In order to gauge which subunits might interact, anti-GFP pull-downs of the CLUB-GFP and TRS120-GFP fusions *in planta* were carried out. The purified proteins were identified by mass spectrometry. This approach yielded ten hits including at least one isoform of each of the eight exocyst subunits (Fig. 3.3.10A and 3.3.10B; Table 3.5.2 and 3.5.3). Also, anti-HA immunoisolations of CLUB-HA, TRS120-HA, 3HA-CLUB and 3HA-TRS120 were carried out, but these failed to pull down HA fusion proteins.

Analyses of proteomics data indicate that only a small pool of the TRAPPII bait interacts with exocyst components. All hits for TRAPPII components and the exocyst components were clustered in scatter plots. TRAPPII components have a higher intensity than the exocyst components (Fig. 3.3.10A and 3.3.10B). The p-values for some exocyst components are lower than those for TRAPPII subunits, including the bait itself. It is due to no signal in the soluble GFP empty vector control at all (Fig. 3.3.10C and 3.3.10D). All the co-purified proteins in CLUB-GFP and TRS120-GFP pull-downs shown in scatter plots were represented by at least five unique peptides and were present in all three biological replicates. The ratio was calculated for each protein as the signal intensity in the experiment divided by its intensity in the soluble GFP empty vector control. An artificial line was formed to the right for proteins that had no signal in the control – these were attributed a random value so as not to appear at infinity on the plot. Rubisco is the most abundant protein in plant tissues and was found in the experiment and control at relatively comparable intensities (low log2 ratio; Fig. 3.3.10). A further analysis of proteomics data indicates their high specificity, significance and reproducibility (Fig. 3.3.10; Fig. 3.3.11).

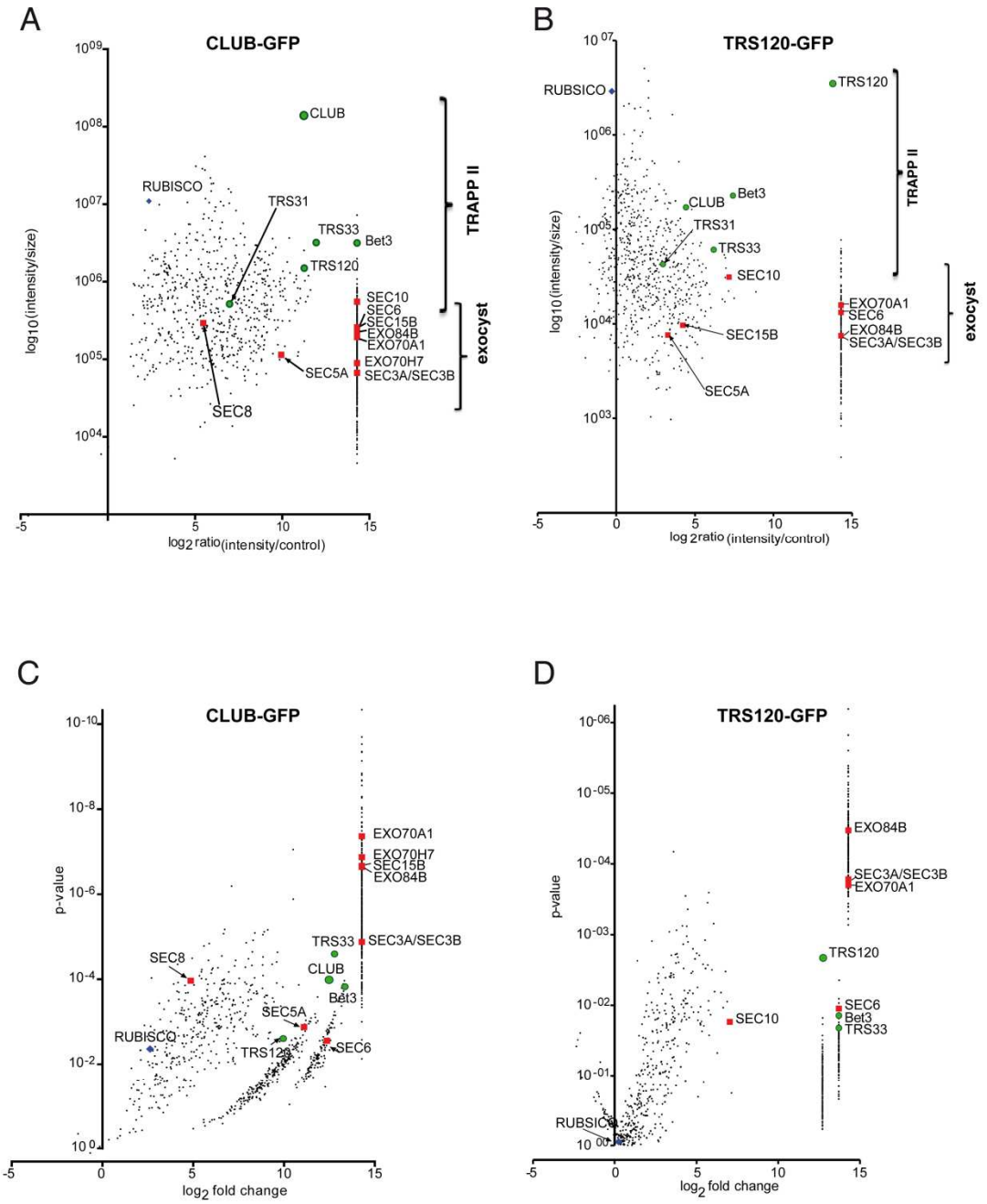

Figure 3.3.10. Physical interactions between the TRAPPII and exocyst complexes.
Scatter plots showing all the co-purified proteins in a CLUB-GFP immunoprecipitate. Each protein is represented by at least five unique peptides and was present in all three biological replicates. The ratio was calculated for each protein as the intensity of the signal in the experiment divided by its intensity in the soluble GFP empty vector control. Green circles: TRAPPII subunits; red squares exocyst subunits; blue diamond: rubisco. (A, B) Signal intensity (normalized against protein size, $\log_{10}$ scale) against the signal ratio ($\log_2$ scale). The CLUB-GFP bait has the highest intensity, as expected. An artificial line is formed to the right for proteins that had no signal in the control – these were attributed a random value so as not to appear at infinity on the plot. Rubisco is the most abundant protein in plant tissues and was found in the experiment and control at relatively comparable intensities (low $\log_2$ ratio). Note that TRAPPII subunits have a higher average signal intensity than exocyst subunits.
(C, D) The p value (Student's t-test; depicted along a negative $\log_{10}$ scale but labeled with actual values) is plotted against the signal ratio. Note that a large number of exocyst components have lower p values than the actual bait, due to the fact that they had no signal in the empty vector control. Shown are hits with $p < 0.02$.

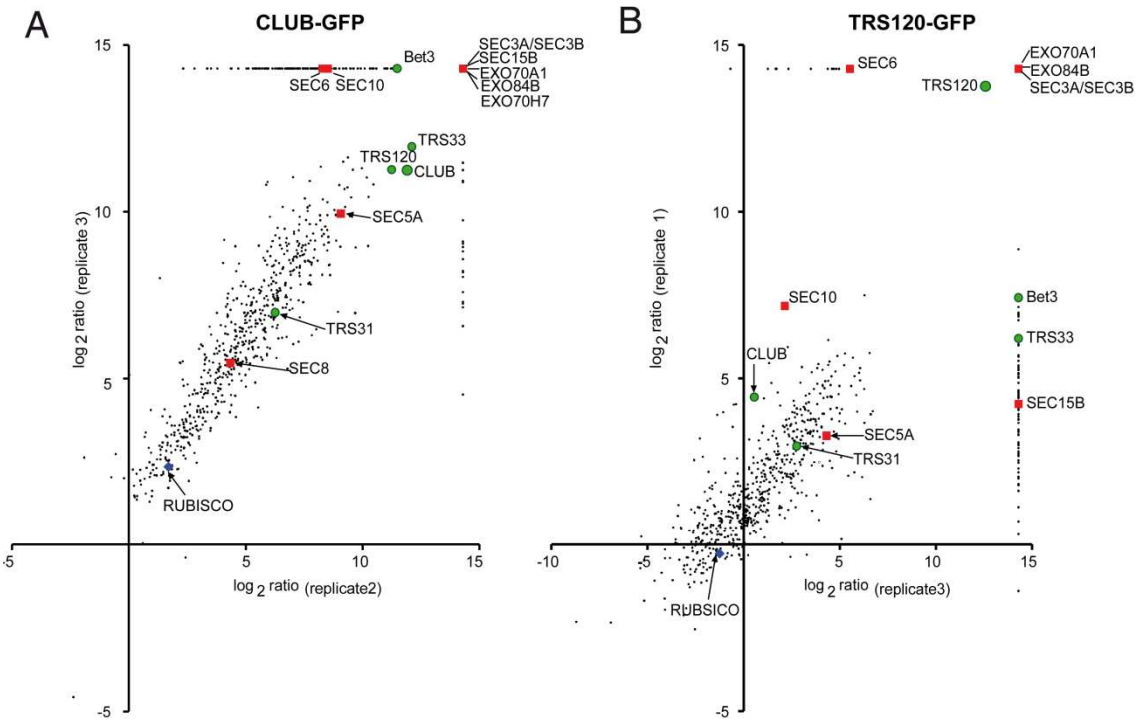

Figure 3.3.11. Reproducibility of proteomic data.
Scatter plots showing all the hits in a pull down experiment with CLUB-GFP (A) or TRS120-GFP (B) as a bait. Each protein is represented by at least five unique peptides and was present in all three biological replicates. The ratio was calculated for each protein as the intensity of the signal in the experiment divided by its intensity in the soluble GFP empty vector control. Green circles: TRAPPII subunits; red squares: exocyst subunits; blue diamond: rubisco.
Reproducibility for CLUB-GFP (A) and TRS120-GFP (B) IPs can be seen as a straight line seen when two replicates are plotted against each other. The horizontal and vertical lines and their intersection represent proteins that had no signal in the control in either replicate or in both.

To confirm this result, western blots of a variety of TRAPPII pull-downs were probed with antibodies against three exocyst subunits. This validated an interaction between CLUB/AtTRS130, AtTRS120 and all the subunits tested, including EXO84b, EXO70A1, and SEC6 (Fig. 3.3.12). Additionally, a yeast two hybrid screen (Y2H) with EXO70H7 as a bait identified AtTRS120, which confirmed a direct physical interaction between those subunits of the two tethering complexes (Rybak et al., 2014). Also, Y2H and bimolecular fluorescence complementation (BiFC) were set up to confirm these results. Based on the co-immunoprecipitation, co-localization and yeast two hybrid assay, we conclude that the TRAPPII and exocyst complexes physically interact.

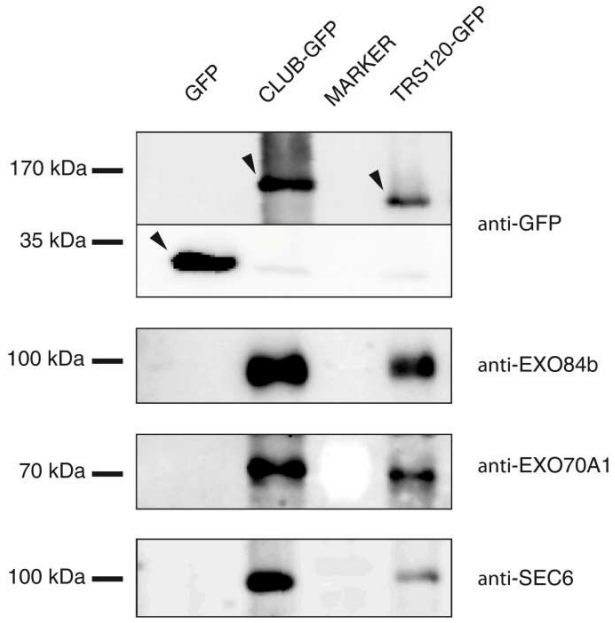

Figure 3.3.12. Physical interactions between the TRAPPII and exocyst complexes.
Western blots of anti-GFP imunoprecipitates. Antibodies used to probe the blots are described at the right of the panels. An anti-GFP antibody detects GFP, CLUB-GFP or TRS120-GFP (arrowheads). Specific bands are seen in the CLUB-GFP and TRS120-GFP IPs but not in the GFP empty cassette control for antibodies against exocyst subunits EXO84b, EXO70A1 and SEC6. Three biological replicates were performed for each transgenic line.

These data were produced with inflorescences. Additionally, pull-downs and mass spectrometry were performed on seedlings and leaves. Similar data to inforescences were obtained for seedlings (Fig. 3.3.13A and 3.3.13B), as both contain dividing and non-dividing cells. In leaves, which consist mainly of non-dividing cells, only few exocyst subunits were found to interact with TRAPPII baits (Fig. 3.3.13C), which is consistent with co-localization data where TRAPPII subunits and exocyst subunits do not co-localize in non-dividing cells, but overlap transiently in dividing cells.

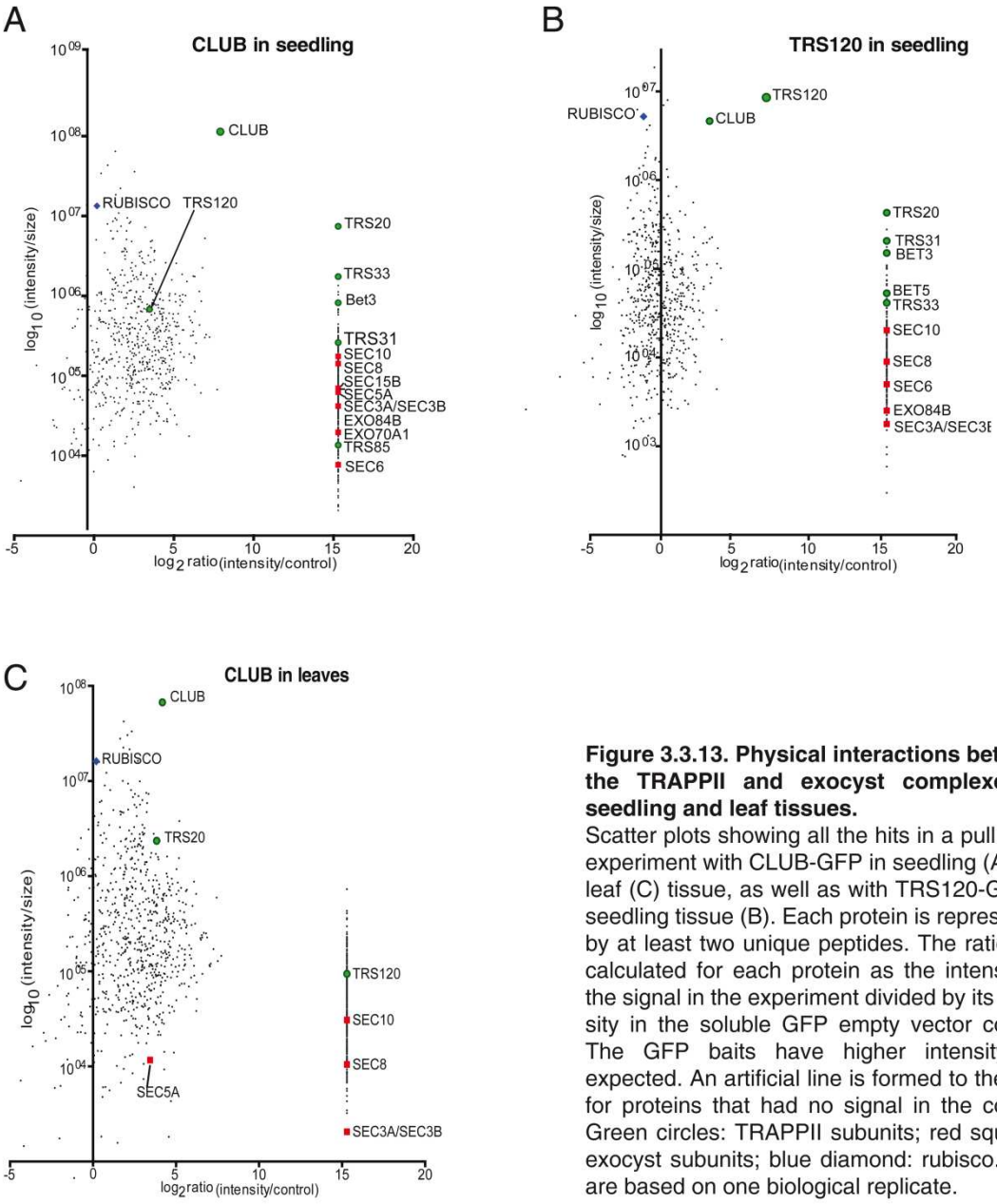

Figure 3.3.13. Physical interactions between the TRAPPII and exocyst complexes in seedling and leaf tissues.
Scatter plots showing all the hits in a pull down experiment with CLUB-GFP in seedling (A) and leaf (C) tissue, as well as with TRS120-GFP in seedling tissue (B). Each protein is represented by at least two unique peptides. The ratio was calculated for each protein as the intensity of the signal in the experiment divided by its intensity in the soluble GFP empty vector control. The GFP baits have higher intensity, as expected. An artificial line is formed to the right for proteins that had no signal in the control. Green circles: TRAPPII subunits; red squares: exocyst subunits; blue diamond: rubisco. Data are based on one biological replicate.

3.4. Localization dynamics of different Rab GTPases throughout cytokinesis.

The *Arabidopsis* Rab GTPase family consists of eight subclasses (Rab-A - Rab-H). Each of them mediates specific transport and fusion events (Segev, 2001). Different Rab GTPases were shown to localize to the cell plate throughout cytokinesis (Chow et al., 2008). The aim of this study was to show the localization dynamics of different Rab GTPases over cytokinesis and their involvement in cell plate formation.

3.4.1. Rab-A2a localizes to the cell plate.

The anti-RAB-A2a was shown to localize to the cell plate during cytokinesis. Rab-A2a appears at the cell plate during anaphase and reorganizes to the leading edges in telophase (Chow et al., 2008). YFP-Rab-A2 proteins co-localized with KNOLLE at the cell plate in the early stages of cytokinesis and at the edges of growing cell plate in later stages (Chow et al., 2008). In order to look at the Rab-A2a localization in *club-2*, *trs120-4* and *exo84b-2* mutants an immunostaining of five-days-old *Arabidopsis* root tips was performed. Wild type and mutant root tips were labeled with DAPI to define the nuclear stage. Anti-microtubule and anti-Rab-A2a antibodies were used to stain cell phragmoplast microtubules and cell plate, respectively. Preliminary stain with anti-Rab-A2a at the concentration of 1:3000 failed in our hands. A signal was diffuse and not clear. The immunostain needs to be optimized for Rab-A2a antibody. A cell plate labeled with Rab-A2a antibody at the anaphase solid phragmoplast stage (anaphase) in comparison to KNOLLE antibody in wild type is shown in Figure 3.4.1.

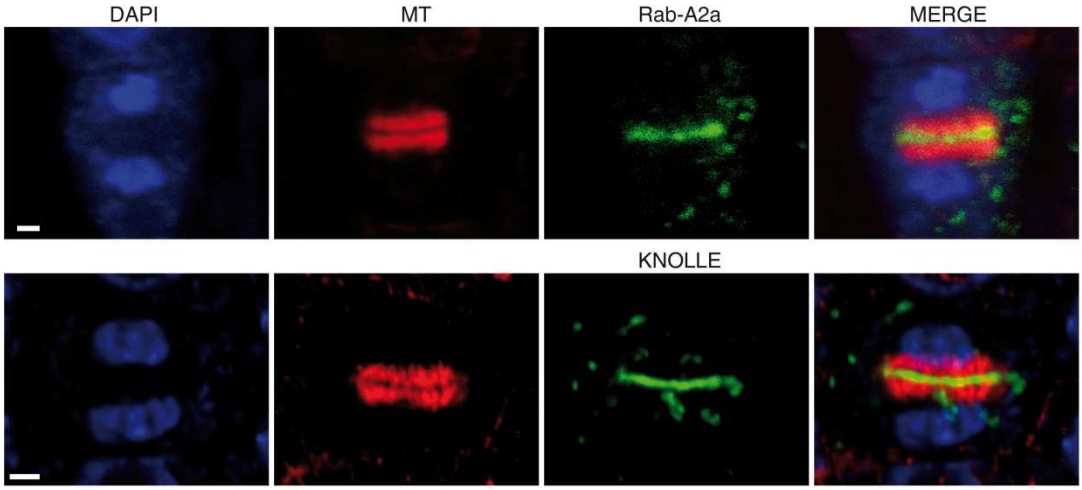

Figure 3.4.1. Rab-A2a localization in dividing cells.
Antibody stains of root tips. DAPI/nucleus (blue); MT/microtubules (red); Rab-A2a (green; top panel) and KNOLLE protein (green; lower panel); and merge. Rab-A2a positive staining was detected at the cell plate in wild type (top panel). Compare to KNOLLE positive staining of the cell plate (lower panel).
Bars = 2 µm.

3.4.2. Rab-E1d localizes to the cell plate throughout cytokinesis and to the maturing cross wall.

Rab-E family was reported to regulate polarized membrane traffic during cytokinesis (Guo et al., 1999b; Segev et al., 2001; Carter et al., 2004; Woollard and Moore, 2008). Yeast homolog Sec4p was shown to be involved in exocyst complex formation and its association with secretory vesicles for targeting them to the plasma membrane (Zerial and McBride, 2001; Ponnambalam and Baldwin, 2003). There are five isoforms of Rab-E GTPases in *Arabidopsis* (a-d; Rutherford and Moore, 2002; Vernoud et al., 2003). Rab-E1d isoform is commonly used for studying Rab-E GTPases function (Zheng et al., 2005; Camacho et al., 2009; Speth et al., 2009) as it was shown to be the most highly expressed Rab-E gene in *Arabidopsis* ecotype Col-0 (Speth et al., 2009).

AtRab-E1d was shown to localize to the Golgi apparatus and cytoplasm in tobacco leaf epidermal cells (Zheng et al., 2005), to the plasma membrane in *Arabidopsis* leaf cells (Speth et al. 2009), as well as to the cell plate in the dividing cells of the root tip (Chow et al., 2008). So far, Rab-E localization dynamics over cytokinesis has not been investigated. In this study, P_{VKHRn6}::YFP-Rab-E1d (Zheng et al., 2005) localization was monitored in *Arabidopsis* root tip over the time in dividing cells. YFP-Rab-E1d appeared at the cell equator at the early stages of cytokinesis and subsequently reorganized to the leading edges of the expanding cell plate. After insertion to the lateral walls, YFP-Rab-E1d signal gradually increased to reach the peak fluorescence throughout the cross wall (Fig. 3.4.2A). Additionally, to better determine the stage of YFP-Rab-E1d appearance at the equator of the cell, a microtubule marker mCherry-TUA5 was used. YFP-Rab-E1d appeared at the cell equator at the phragmoplast assembly stage (Fig. 3.4.2B), similarly to TRS120-GFP and EXO84b-GFP (compare to Fig. 3.3.2A and 3.3.2B). Complete time lapses are not shown because of the weak fluorescence signal and extensive photobleching. Next, it would be interesting to monitor Rab-E1d localization in TRAPPII and exocyst mutants. For this purpose, transgenic plants expressing YFP-Rab-E1d were crossed with *club-2*, *trs120-4* and *exo84b-2* heterozygous plants. Also, co-localization analysis of YFP-Rab-E1d with CLUB-GFP, TRS120-GFP and EXO84b-2 remains to be done.

Our data showed that Rab-E1d appeared at the cell plate at the onset of cytokinesis and subsequently reorganized to the leading edges at the ring-shaped phragmoplast stage, with localization dynamics characteristic of the TRAPPII complex. At the end of cytokinesis, Rab-E1d strongly labeled cross wall, which is a localization dynamics characteristic of the exocyst complex.

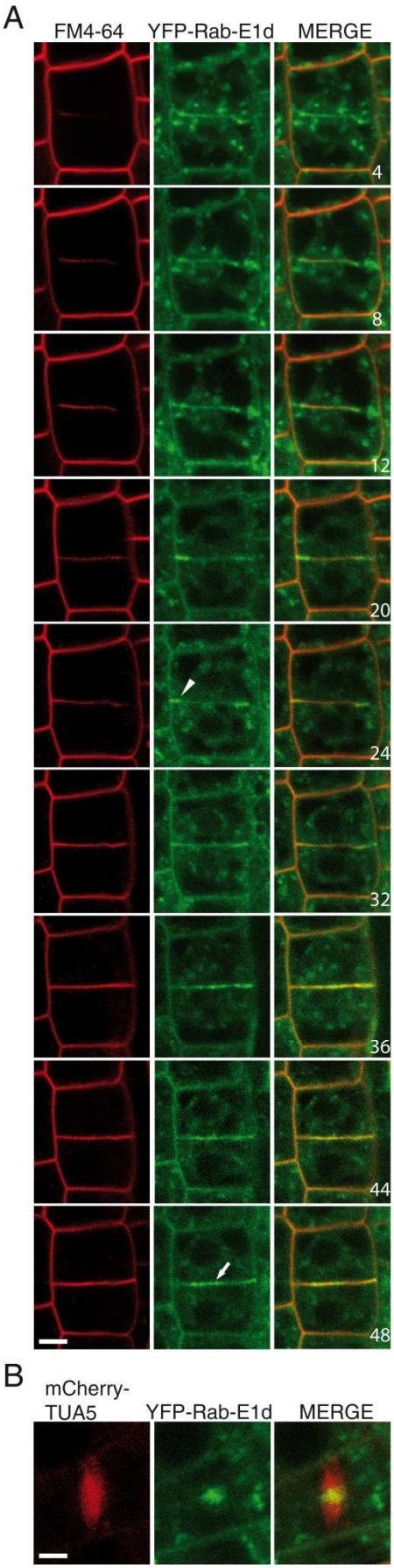

Figure 3.4.2. Rab-E1d dynamics throughout cytokinesis.
(A) Time lapse of P_{VKHRn6}::YFP-Rab-E1d with FM4-64 is shown, with minutes indicated in the right panel. The 0 minute time point corresponds to cell plate initiation. Arrowhead at 24 minutes points to leading edge of cell plate. Arrow at 48 minutes points to cross wall.
(B) P_{VKHRn6}::YFP-Rab-E1d with mCherry-TUA5 at the phragmoplast assemby stage.
Bars = 5 µm.

3.5. CLUB and TRS120 differ with respect to their mutant phenotypes and putative interaction partners.

Despite the fact that CLUB/AtTRS130 and AtTRS120 are members of the same protein complex, some differences between these two subunits in terms of phenotype were observed (Table 3.5.1). Mutants in both subunits were shown to be seedling lethal with a cytokinesis-defective phenotype, reduced T-DNA transmission and impaired cell plate biogenesis (Jaber et al., 2010; Thellmann et al., 2010).

Our observations showed no requirement for either of the TRAPPII specific subunits in exocytosis of the seed mucilage (see Chapter 3.1.2.1), but a clear delay in endocytosis was observed for *club-2* and *trs120-4* mutants. This delay was especially severe in the *trs120-4* mutant (see Chapter 3.1.2.2).

Moreover, co-localization studies of CLUB-GFP and TRS120-GFP with SYP61-CFP, a TGN marker (Robert et al., 2008), showed clear differences (Fig. 3.5.1A). We observed co-localization of TRS120-GFP with SYP61-CFP, but only partial co-localization of CLUB-GFP with a TGN marker was monitored. The data are consistent with the work of Drakakaki et al. (2011), who showed that TRS120 but not CLUB was detected by mass spectrometry when SYP61-CFP was used as a bait. However, our confocal data will need to be further analyzed as this result is based on a preliminary dataset.

	club-2	***trs120-4***
Seedling phenotype	canonical cytokinesis-defective	
Cell plate biogenesis	impaired	
Transmission via pollen	reduced	
Mucilage secretion	normal appearance	
Endocytosis (FM4-64 internalization)	impaired	severely impaired
	CLUB/AtTRS130-GFP	**AtTRS120-GFP**
SYP61-CFP	partially co-localizes	co-localizes
IPs (infuorescences)	398 specific interactors	55 specific interactors
Localisation	cell plate, cytosol, TGN	cell plate, cytosol*, TGN
Localization dynamics throughout cytokinesis	cell plate localization from the onset of cytokinesis and reorganization to the leading edges in telophase	

Table 3.5.1. Similarities and differences between CLUB/AtTRS130 and AtTRS120.
*note that localization of CLUB/AtTRS130-GFP is more cytosolic, than that of AtTRS120-GFP.

Immunoprecipitation and mass spectrometry analyses of CLUB-GFP and TRS120-GFP revealed differences in their potential interactors. Venn diagrams show the number of proteins found in the CLUB and TRS120 immunoprecipitates from inflorescences and their overlap (Fig. 3.5.1B). 398 interactors specific for CLUB were detected compared to just 55 specific for TRS120 (Fig. 3.5.1B). A higher number of interaction partners

(80) specific to the TRS120 subunit were found in seedling tissues compared to 152 CLUB (Fig. 3.5.1C). Overall, in CLUB and TRS120 immunoprecipitates from inflorescences and seedling tissues, 67% of protein interactors were specific for CLUB (Fig. 3.5.1B and 3.5.1C). Inflorescences and seedlings contain both dividing and non-dividing cells. Leaves contain mainly non-dividing cells. Only a small overlap in interaction partners was found between CLUB immunoprecipitates from leaf and inflorescences tissues, as well as, seedling tissues (Fig. 3.5.1F and 3.5.1G). Interestingly, 26% of common interactors were detected for CLUB immunoprecipitates from inflorescences compared to seedlings but only 16% in TRS120 (Fig. 3.5.1D and 3.5.1E).

To the common interactors of CLUB and TRS120 belong known components of membrane traffic. We looked at TRAPPI/II/III, exocyst and vacuolar H^+ ATPase (VHA) subunits, as well as, Rab GTPases in immunoprecipitates from inflorescences, seedlings and leaves (Table 3.5.2, Table 3.5.3 and Tables S5-S10). A comparison between inflorescences as dividing cells versus leaves as non-dividing cells showed a discrepancy in components of the trafficking machinery. Not many of these components were found in immunoprecipitates from leaves. Most of the proteins related to membrane traffic that were found in inflorescences were also detected in CLUB and TRS120 immunoprecipitates from seedlings that contain dividing and non-dividing cells, but due to their low significance they are not listed in the table. All conclusions are based on three biological replicates. TRS120 immuoprecipitates are not shown as the experiment was repeated only two times.

Based on our proteomic data, we conclude that CLUB and TRS120 have a large number of non-overlapping interaction partners, even though they are members of the same protein complex. Additionally, as expected, in non-dividing cells fewer components of the cytokinetic machinery were pull-downed.

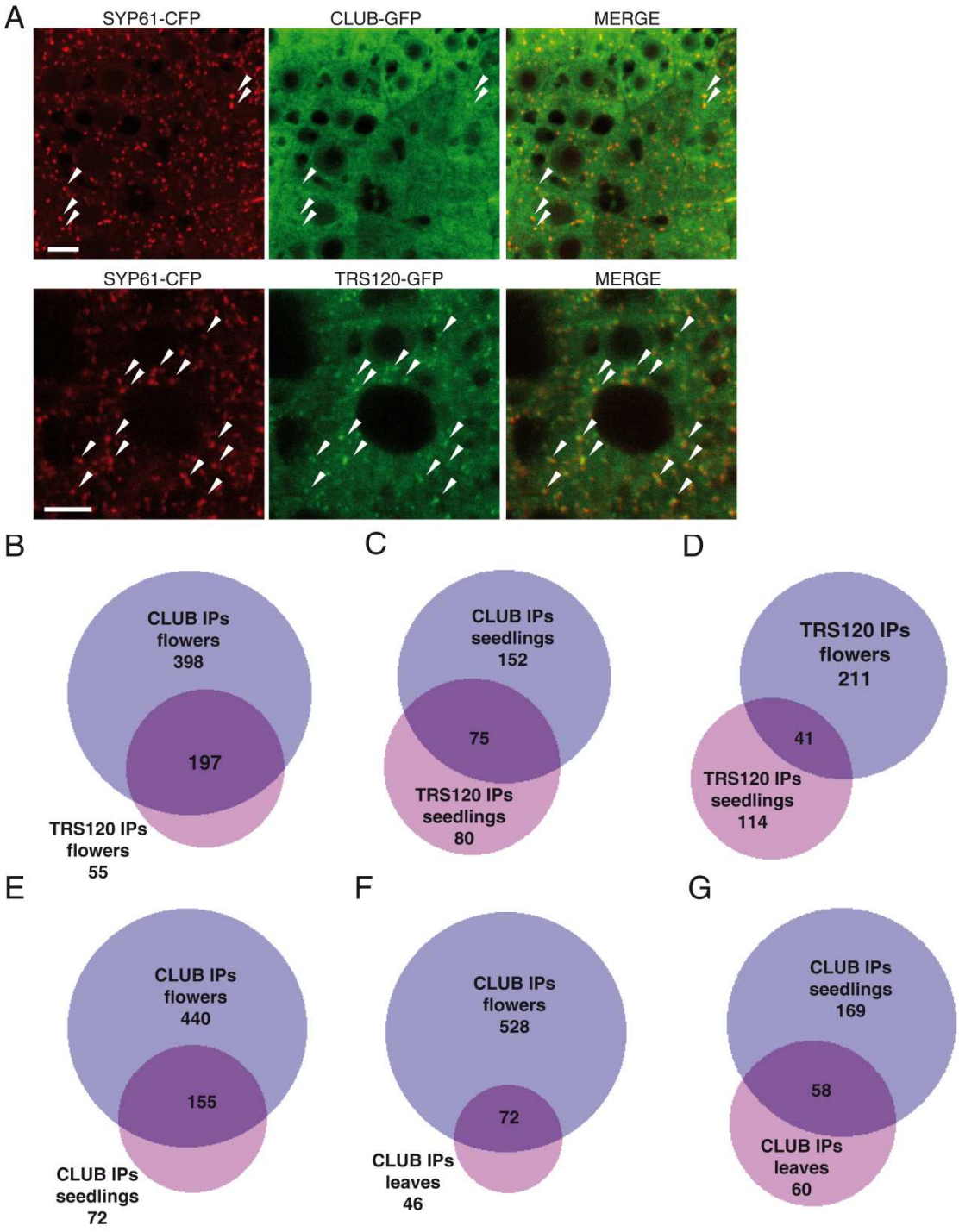

Figure 3.5.1. Differences between CLUB and TRS120.
(A) Co-localization of CLUB-GFP (top panel) and TRS120-GFP (lower panel) with TGN marker SYP61-CFP. TRS120-GFP co-localizes with SYP61-CFP, while CLUB-GFP co-localized only partially. Arrowheads point to the co-localized vesicles. Note the cytosolic phenotype of CLUB-GFP and more punctate appearance of TRS120-GFP.
(B-G) Venn diagrams showing all the hits in a pull down experiment with CLUB-GFP and TRS120-GFP as baits from flowers (B), seedlings (C), with TRS120-GFP as a bait from flowers and seedlings (D), with CLUB-GFP as a bait from flowers and seedlings (E) from flowers and leaves (F) and from seedlings and leaves (G). Each protein is represented by at least five unique peptides and was present in all three biological replicates. The log2 ratio ≤ 5 and was calculated for each protein as the signal intensity in the experiment divided by its intensivity in the soluble GFP empty vector control. As we only had two biological replicates with TRS120-GFP as a bait from leaves, this dataset was not taken into account. See text for a detailed description.
Bars = 5 µm.

Accession number (AGI)	Gene description	CLUB-GFP IP					
		inflorescences		seedlings		leaves	
		Average Log2 (ratio)	p-value	Average Log2 (ratio)	p-value	Average Log2 (ratio)	p-value
TRAPPII subunits							
At5g54440	CLUB/ AtTRS130	12	0,0001	8	0,05	7	0,03
At5g11040	TRS120	11	1,6E-05			5	0,01
At3g05000	TRS33	13	2,5E-05	14/0	0,0002		
At5g54750	Bet3	13	1,5E-04	14/0	0,00001		
At5g16280	Trs20	14	0,01	14/0	0,004		
At5g58030	TRS31	9	0,012	14/0	0,0003		
exocyst subunits							
At5g59730	EXO70H7	14/0	1,4E-07				
At1g21170	SEC5B	10	5,8E-07				
At5g49830	EXO84B	14/0	2,3E-07				
At3g10380	SEC8	5	1,1E-04				
At1g47550, At1g47560	SEC3A, SEC3B	14/0	1,3E-05				
At5g03540	EXO70A1	14/0	4,3E-08	14/0	0,001		
At4g02350	SEC15B	14/0	2,1E-07	14/0	0,01		
At1g71820	SEC6	12	2,8E-04	14/0	0,001		
At5g12370	SEC10	10	0,0078	13	0,02		
At1g76850	SEC5A	11	0,0013				
Rab GTPases							
At5g45750	AtRab-A1c	4	0,02				
At5g47200	AtRab-D2b	4	0,004	14/0	0,01		
At4g17530	AtRab-D2c			14/0	0,01		
VHA subunits							
At1g78900	VHA-A	4	0,002				
At4g11150	, VHA-E1	4	0,002				
At3g58730	VHA-D	6	0,02			8	0,05
At3g42050	VHA-H	7	0,01				
At3g01390	VHA-G1	3	0,01				
At1g20260	VAB3	4	0,003			3	0,03
At4g38510	VAB2	4	0,02	14/0	0,01		
At4g23710	VHA-G2	3	0,02				

Table 3.5.2. Analysis of CLUB-GFP immunoprecipitates from inflorescences, seedlings and leaves via mass spectrometry.

The data are based on three biological replicates. AGI: *Arabidopsis* genome initiative accessions (www.arabidopsis.org). a: The $\log_2$ ratio for each protein was calculated as its signal intensity in the experiment divided by its intensity in the control. Note that the $\log_2$ ratios for exocyst subunits are comparable to those of the TRAPPII subunits, supporting their identification as a complex. b: P values (< 0.02 for inflorescences, < 0.05 for seedlings and leaves) were calculated using the Student's t-test (two-sided). This table lists only TRAPPII and exocyst components, as well as Rab GTPases and VHA subunits detected in the IPs from inflorescences, seedlings and leaves.

Accession number (AGI)	Gene description	TRS120-GFP IP			
		inflorescences		seedlings	
		Average Log2 (ratio)	p-value	Average Log2 (ratio)	p-value
TRAPPII subunits					
At5g11040	TRS120	12	0,002	10	0,05
At3g05000	TRS33	12	0,02	14/0	0,001
At5g54750	Bet3	12	0,014	14/0	0,01
At5g16280	Trs20			14/0	0,0002
At5g58030	TRS31			14/0	0,003
exocyst subunits					
At5g49830	EXO84B	14,29/0	3,4E-05		
At1g47550, At1g47560	SEC3A, SEC3B	14,29/0	1,6E-04		
At5g03540	EXO70A1	14,29/0	0,0002		
At4g02350	SEC15B			14/0	0.001
At1g71820	SEC6	11	0,011		
At5g12370	SEC10	6	0,017	14/0	0,004
Rab GTPases					
At1g09630	AtRab-A2a			14/0	0,001
At2g44610	AtRab-H1b	9	0,004		
At4g17530	AtRab-D2c			11	0,05
At5g47200	AtRab-D2b			11	0,04
VHA subunits					
At1g78900	VHA-A				
At4g11150	, VHA-E1				
At3g58730	VHA-D	8	0,03	11	0,02
At3g42050	VHA-H				
At3g01390	VHA-G1	1	3,2E-01		
At1g20260	VAB3				
At4g38510	VAB2			14/0	0,001
At4g23710	VHA-G2				

Table 3.5.3. Analysis of TRS120-GFP immunoprecipitates from inflorescences and seedlings via mass spectrometry.

The data are based on three biological replicates. AGI: *Arabidopsis* genome initiative accessions (www.arabidopsis.org). a: The $\log_2$ ratio for each protein was calculated as its signal intensity in the experiment divided by its intensity in the control. Note that the $\log_2$ ratios for exocyst subunits are comparable to those of the TRAPPII subunits, supporting their identification as a complex. b: P values (< 0.03 for inflorescences and < 0.05 for seedlings) were calculated using the Student's t-test (two-sided). This table lists only TRAPPII and exocyst components, as well as Rab GTPases and VHA subunits detected in the IPs from inflorescences and seedlings.

Additionally, an etiolation response was carried out for *club-2* and *trs120-4* mutants in order to check whether CLUB/AtTRS130 or AtTRS120 are required for regulation of differential growth. Both alleles were capable of elongating their shoots in the dark, which indicates no impairment of light perception in those mutants ($p = 5,7E-33$ for *club-2* and $p = 1,4E-23$ for *trs120-4*). Also, TRAPPII mutants were capable of modulating their shoot-root ratio in response to light conditions ($p = 2.4E-07$ for *club-2* and $p = 2.1E-10$ for *trs120-4*). All conclusions are based on three biological replicates.

Taken together, despite the fact the two TRAPPII tethering complex specific subunits CLUB/AtTRS130 and AtTRS120 belong to the same protein complex, they show some differences that are listed in the Table 3.5.1.

4. Discussion.

In this study, we used a reverse genetic approach to search for cytokinesis-defective mutants. The strongest canonical cytokinesis-defective phenotypes described to date are seedling lethal (Söllner et al., 2002). We focused on tethering factors that could potentially be involved in cell plate biogenesis. We show that TRAPPII mutants but not exocyst mutants exhibit strong cytokinesis-defective phenotypes. Our data support a model for the sequential but overlapping, coordinated action of the TRAPPII and exocyst complexes in the regulation of plant cytokinesis. Plant cytokinesis can be divided into four stages: initiation, biogenesis, expansion and maturation (Fig. 4.5.1). Based on the localization dynamics of these two complexes throughout cytokinesis, we speculate that both complexes coordinate the spatio-temporal regulation of cell plate initiation. Later, the TRAPPII complex acts at the juvenile phases of cytokinesis and is required for the biogenesis and growth of the cell plate, while the exocyst acts at the late stages of cytokinesis and is implicated in cross wall maturation. The switch in action of these two complexes at the cell plate leads to the transition in cell plate membrane identity from TGN to plasma membrane (Fig. 4.5.1). These two complexes interact physically in dividing cells. Moreover, mis-localization of cell plate markers (including exocyst) in TRAPPII mutant background suggests its role in protein sorting at the cell plate. We propose a “relay race” model in which two protein complexes play a different role, and interact transiently to coordinate transitions (as in passing the buck to each other between laps). Additionally, we present preliminary data suggesting distinct roles for two TRAPPII specific subunits.

4.1. Tethering factors in cytokinesis.

4.1.1. TRAPPII mutants exhibit a strong cytokinesis-defective phenotype.

In yeast, the TRAPPII complex was shown to reside on the TGN, where it mediates both exocytosis and endocytosis (Cai et al., 2005). Little is known about the TRAPPII complex in plants. All TRAPPII subunits found in yeast except for Trs65 are conserved in the *Arabidopsis* genome (Table 1.3.1; Cox et al., 2007; Koumandou et al., 2007; Klinger et al., 2013). The *Arabidopsis* TRAPPII complex was reported to be implicated in cytokinesis (Jaber et al., 2010; Thellmann et al., 2010; Qi et al., 2011). Two TRAPPII specific subunits CLUB/AtTRS130 and AtTRS120 are encoded by single genes in the *Arabidopsis* genome. *club-2/trs130-2* was identified in a forward genetic screen and described by Jaber et al. (2010). Electron microscopy on *Arabidopsis* TRAPPII mutant root tips revealed characteristic cytokinesis-defective phenotypes such as cell wall stubs, vesicles at the equator of the cell that failed to assemble into a cell plate, enlarged cells and incomplete cell walls. Furthermore, immunochistochemical analyses showed that the TRAPPII complex is required for the assembly of the cell plate (Jaber et al., 2010; Thellmann et al., 2010; in this study).

4.1.2. Role of the GARP complex in cytokinesis.

In yeast, the GARP complex resides on the TGN and has been implicated in the tethering of endosome-derived vesicles at the TGN (Conibear et al., 2003; Cai et al., 2005; Quenneville et al., 2006). In mammals, the GARP complex was shown to be required for the sorting of lysosomal proteins and the maintenance of lysosome function (Luo et al., 2011). This raises a question as to whether the GARP complex is required for recycling of proteins back to the TGN or protein transport to vacuole for degradation. The GARP complex was localized to the TGN and PVC compartments in *Arabidopsis* (Pahari et al., 2014). It was reported that mutations in a GARP subunit, Vps51, results in defective targeting to the vacuole (Pahari et al., 2014). The localization of the GARP complex to the cell plate has not been reported so far. In all GARP insertion lines that we screened, we found no evidence for cytokinesis-defective phenotypes. However, based on our observations, we also cannot exclude its role in cell plate biogenesis. The possible role for GARP complex throughout cytokinesis could be the recycling of membranes and of cell plate materials from the middle of the cell plate to its leading edges. Moreover, it was reported that endocytosis is required for the spatial restriction of KNOLLE to the cell plate (Boutté et al., 2009); a disruption in endocytosis via drugs or mutation led to the lateral diffusion of KNOLLE after the cell

plate had fused with the parental plasma membrane. Many studies were carried out to determine the origin of the cell plate. According to Dhonukshe et al. (2006) plant cytokinesis requires endocytosis. It is inconsistent with the work of Reichardt et al. (2007), who showed that exocytosis but not endocytosis plays important role in cell plate formation. Proteins that cycle between endosomes and the plasma membrane in interphase are suggested to accumulate at the cell plate (Reichardt et al., 2011). Indeed, we show that the PIN proteins, which are known to cycle between TGN/EE and plasma membrane (Dhonukshe et al., 2007) localize to cell plate.

Moreover, it is interesting that the TRAPPII specific subunit, AtTRS120 and the GARP subunit, Vps51, have recently been reported to be implicated in vein development (Naramoto et al., 2014; Pahari et al., 2014). The involvement of these two tethering factors in the same process would suggest direct interaction between TRAPPII and GARP tethering complexes. Indeed, we found Vps51 subunit in TRS120-GFP immunoprecipitates via mass spectrometry, which is suggestive of an interaction between these two complexes. Auxin signaling and transport were reported to be involved in vascular pattern formation (Berleth et al., 2000; Sachs, 2000). According to the auxin canalization hypothesis, the auxin signal distribution narrows to a subset of cells with high auxin transport to form veins (Sachs, 1981). Plant-specific PIN-formed (PIN) proteins are localized to the plasma membrane in a polar manner and mediate auxin efflux (Petrášek et al., 2006). The polar localization of PIN proteins is maintained via continuous cycling between endosomes and the plasma membrane (Dhonukshe et al., 2007). The TRAPPII complex has been reported to be involved in polar distribution of PIN2 and AUX1 but not PIN1 (Qi et al., 2011; Qi and Zheng et al., 2011). This is inconsistent with the work of Naramoto et al. (2014), who presented that endocytotic recycling of PIN proteins but not their polar localization is affected in *trs120* mutants. Interestingly, another tethering factor, the exocyst, was shown to be involved in recycling of PIN proteins, and thus in polar auxin transport regulation (Drdova et al., 2013). However, the role of the exocyst in vein development has not been reported so far. The GARP complex has been proposed to function in targeting proteins for degradation (Pahari et al., 2014). A vacuolar targeted fluorophore (AVFY-RFP) in GARP mutant fails to target to vacuole, being instead secreted to the apoplast. Therefore, the GARP complex was suggested to be involved in reducing PIN1 expression via targeting to the lytic vacuole (Pahari et al., 2014). This resembles the role of endosomal sorting complex (ESCRT), which is required for targeting proteins to vacuole for degradation (Spitzer et al., 2009). However, as opposed to GARP mutants, ESCRT mutants were shown to have cytokinesis defects, for example multinucleate

cells (Spitzer et al., 2006 and 2009). Moreover, mutations in ESCRT subunits lead to defects in PIN1 protein localization (Spitzer et al., 2009). Naramoto et al. (2014) proposed that TRS120 is involved in vein development via the maintenance or establishment of the PIN1-GFP expression domain (PED) rather than via the establishment of the polar localization of PIN proteins. Pahari et al. (2014) suggested that the expanded marginal PED in GARP mutants leaves might be due to a defect in the targeting of PIN1 to the lytic vacuole. These two tethering factors play an important role in vein patterning and development via the regulation of PIN1 protein localization (Naramoto et al., 2014; Pahari et al., 2014).

4.2. The role of endocytosis and secretion in plant cytokinesis.

The TGN works as a sorting station for proteins destined to the plasma membrane and to the vacuole. Endocytosed material from the plasma membrane was shown to pass through the TGN before targeting its final destinations (Dettmer et al., 2008; Viotti et al., 2010). The TRAPPII complex has been reported to reside on the TGN in yeast and is required for exocytosis and endocytosis (Cai et al., 2005). The *Arabidopsis* TRAPPII complex was shown to be implicated in post-Golgi traffic (Qi et al., 2011). These findings posed a question as to whether *Arabidopsis* TRAPPII is required for both exocytosis and endocytosis. However, based on our results, we have no evidence for the involvement of the TRAPPII complex in secretion. Our observations are inconsistent with work of Qi et al. (2011), who showed some defects in secretion in TRAPPII mutants. This discrepancy may be due to the fact that we used different approaches to test this. Qi et al. (2011) monitored the secGFP marker in TRAPPII mutants. secGFP is a secreted form of GFP, which is synthesized in the ER and subsequently transported to the cell wall through the Golgi and TGN. After secretion, fluorescence is dim due to the low pH of the apoplast (Zheng et al., 2004). Indeed, in TRAPPII mutants, secGFP was retained at the TGN in *Arabidopsis* seedling root tip (Qi et al., 2011). We monitored the secretion of mucilage in *Arabidopsis* seeds. Although we did not observe any differences between the wild type and TRAPPII mutants, in mucilage secretion, a clear defect was monitored in TRAPPI mutants presumably due to impaired traffic between the ER and Golgi. Moreover, further studies excluded TRAPPII involvement in cuticular wax secretion. Wax transport occurs via vesicle secretion from the ER through the Golgi apparatus to the TGN and to the plasma membrane (McFarlane et al., 2014). Wax secretion was monitored in several trafficking mutants including a TRAPPII mutant (McFarlane et al., 2011). As TRAPPII knockout alleles are seedling lethal (Thellman et al., 2010; Qi et al., 2011) and the process of cuticular wax export can be studied only in mature plants, McFarlane et al. (2014) used

a viable hypomorph of *trs120* that has a dwarfed phenotype (Qi et al., 2011). It would be interesting to test wax secretion in TRAPPII homozygous mutants. However, it is surprising that secretion monitored via the secGFP marker is defected but not wax secretion was visible in *trs120* viable hypomorph (McFarlane et al., 2014). Interestingly, wax secretion was perturbed in the *ech* mutant (McFarlane et al., 2014). ECHIDNA is a TGN localized protein required for TGN integrity, protein sorting at the TGN and secretion of cell wall polysaccharides (Gendre et al., 2011 and 2013). This could suggest distinct roles of the TRAPPII complex and ECHIDNA at the TGN. ECHIDNA is required for secretion to the cell wall, but is not implicated in transport to the vacuole or endocytosis (Gendre et al., 2011 and 2013). We could postulate that transport of different cargoes to different destinations could be mediated by distinct factors.

Additionally, here we show that TRAPPII is required for protein targeting at the cell plate and for endocytosis. FM4-64 is a lipophilic styryl fluorescent dye, which is used to study endocytosis in plants (Bolte et al., 2004; Dettmer et al., 2006: Jelinkova et al., 2010). It was shown by Dettmer et al. (2006) that upon FM4-64 dye application to the *Arabidopsis* root tip it takes about six minutes to reach the TGN/EE compartment, one hour to reach a late endosome and two hours to stain the tonoplast. We monitored FM4-64 internalization in *Arabidopsis* wild-type and TRAPPII mutant root tips and, as expected, we found defects in endocytosis in both *club-2* and *trs120-4* mutants. It is surprising that Qi et al. (2011) reported normal appearance of FM4-64 dye transport to the tonoplast. A possible explanation could be that Qi et al. (2011) measured FM4-64 transport to the tonoplast after two hours, while we monitored transport to the early TGN/EE, which was delayed in TRAPPII mutants. Additionally, we observed about two times less TGN compartments labeled by VHA-a1-GFP in *club-2* mutants compared to the wild type. It correlates with TEM data of the Qi et al. (2011) study, where fewer vesicles were observed around the Golgi in TRAPPII mutants. Moreover, Qi et al. (2011) observed lack of typical TGN compartments in TRAPPII mutants.

4.3. The TRAPPII complex is localized to the cell plate.

The cell plate is considered to be a TGN/EE specialized compartment (Thellmann et al., 2010). VHA-a1 labels TGN/EE compartment and it was shown to co-localize with FM4-64 rapidly after the brief uptake (Dettmer et al., 2006). The observation that VHA-a1 resides on the TGN but is excluded from the cell plate indicates the presence of different TGN subcompartments. Rab-A GTPases label TGN and partially overlap with VHA-a1. (Chow et al., 2008; Qi et al., 2011; Qi and Zheng, 2011 and 2013). Rab-A2 and Rab-A3 co-localize with KNOLLE at the cell plate throughout cytokiesis (Chow et

al., 2008). The TRAPPII complex has been shown to reside on TGN in yeasts, whereas it localizes to the early Golgi in animals (Cai et al., 2005; Yamasaki et al., 2009). AtTRS120 was localized to the TGN in the *Arabidopsis* root tip (Naramoto et al., 2014). Tethering factors define the specific membrane compartment in the secretory pathway, as well as specific trafficking steps. Therefore, tethers can be used as a markers of the specific membrane compartment and they have been shown to co-localize with other markers such SNARE and Rab GTPases (Robinson et al., 2008; Richter et al., 2009). Here we show for the first time that the TRAPPII complex localizes to the growing cell plate in dividing cells. This observation supports the model that the cell plate is a specialized TGN/EE compartment. Moreover, we show that CLUB and AtTRS120 localize to the cell plate throughout cytokinesis in a KNOLLE-like manner. However, the co-localization studies between TRAPPII subunits and KNOLLE have not been investigated so far.

4.4. Role of the exocyst in cytokinesis.

One of our goals in this study was to understand the role of the exocyst complex in cytokinesis. The exocyst complex is one of the most studied tethering factors. In plants, the exocyst complex was shown to play an important role in seed coat formation (Kulich et al., 2010), embryo development (Zhang et al., 2013), plant-pathogen interaction (Pecenkova et al., 2011), PIN proteins localization and the recycling of proteins mediating polar auxin transport (Drdova et al., 2012), autophagy-related transport to the vacuole (Kulich et al., 2013; Tzfadia and Galili, 2013), plant development, cell morphogenesis (Synek et al., 2006; Hala et al., 2008), as well as germination and pollen tube growth (Cole et al., 2007). Recently, the exocyst was reported to be involved in cytokinesis (Fendrych et al., 2010). A number of cytokinesis-defective defects were reported in leaf epidermis but not in root tips. These include cell wall stubs and defects in stomatal development (for example incomplete ventral walls in stomata cells; Fendrych et al., 2010). Moreover, the possible requirement of EXO70A1 in early stages of cell plate assembly was reported by Fendrych et al. (2010), who observed aberrant, donut-shaped FM4-64 cell plates membranes at the equator of root tip cells of *exo70a1* mutants at the beginning of cytokinesis. Surprisingly, at later stages of cytokinesis the cell plates exhibit normal appearance in those mutants. Furthermore, another exocyst subunit, the SEC6 subunit was shown to interact in vitro and in vivo with KEULE, an SM protein (Assaad et al., 1996 and 2001; Wu et al., 2013). Additionally, pollen-rescued *sec6* mutants, which are gametophytic lethal, were shown to exhibit cytokinesis-defective phenotype in the embryonic cells such as cell walls stubs, enlarged and multinucleate cells (Wu et al., 2013). In the work

of Zhang et al. (2013) the *sec3a* mutant was shown to have defects in establishment of cell polarity, but not in cytokinesis in the globular to heart stage transition during embryogenesis.

In spite of the observation that *exo84b-2* mutants have cell wall stubs in expanding cells of the leaf epidermis (Fendrych et al., 2010), we failed to detect such defects in meristematic cells in the root via SEM and TEM. We postulate that cell wall stubs described by Fendrych et al. (2010) might be due to the mechanical disruption of cell walls during cell expansion rather than to a defect in cell plate formation. Based on our observations, exocyst mutants have two features in common with canonical cell wall mutants: broken walls in vacuolated cells and isodiametric cells in the elongation zones of the root and in seedling hypocotyls. KORRIGAN encodes a membrane localized endo-1,4-b-D-glucanase (Nicol et al., 1998; Zuo et al., 2000; Lane et al., 2001). PROCUSTE (Fagard et al., 2000) and RSW1/RMS (Zuo et al., 2000, Lane et al., 2001) encode cellulose synthases. In these mutants cell wall stubs and characteristic radial swelling were reported (Fagard et al., 2000; Zuo et al., 2000).

Although, the exocyst complex was reported to be required for cytokinesis (Fendrych et al., 2010), its role remains unclear. In non-dividing cells the exocyst complex is localized to the plasma membrane and cytoplasm. Live imaging of *Arabidopsis* dividing cells in root tips showed that exocyst subunits localize to the cell plate at the beginning and the end of cytokinesis, as well as to postcytokinetic cross walls (Fendrych et al., 2010; Rybak et al., 2014). Recently, it was reported that the assembly of the exocyst complex is disrupted throughout mitosis by the cell cycle-dependent phosphorylation of Exo84p in yeast (Luo et al., 2013). That could be the possible explanation of diffuse, cloudy appearance of the exocyst at the cell plate throughout cytokinesis. Interestingly, SEC6 was shown to localize to KEULE in dividing cells, which is a localization characteristic of TRAPPII subunits (Wu et al., 2013). This is discrepant with the localization of SEC6 as described by Fendrych et al. (2010) and Rybak et al. (2014). The possible explanation for different localization dynamics of exocyst subunits might be the fact that Fendrych et al. (2010) and Rybak et al. (2014) used *Arabidopsis* root tips and Wu et al. (2013) tobacco BY-2 cells. In this study we present the sequential but overlapping localization of the TRAPPII and the exocyst complexes at the cell plate. Both tethering complexes appear at the onset of cytokinesis at the phragmoplast assembly stage. Thereafter, throughout the solid phragmoplast stage the TRAPPII subunits sharply label the cell plate and reorganize to the leading edges at the ring-shape phragmoplast stage. Exocyst subunits persisted at the cell plate as a diffuse cloud around the cell plate throughout cytokinesis, and the signal became sharper at

the ring-shape phragmoplast stage after the TRAPPII subunit had reorganized to the leading edges of the cell plate. After the TRAPPII signal disappeared, the exocyst reached peak fluorescence at the cross wall. Co-localization studies confirmed the sequential but overlapping localization dynamics of these two complexes at the cell plate (in this study; Rybak et al., 2014). The overlap between the complexes occurred at two key transitions: during the phragmoplast assembly stage at the onset of cytokinesis, and at the late ring-shaped phragmoplast stage, which is concomitant with cell plate insertion into the lateral walls at the end of cytokinesis.

4.5. The TRAPPII complex is required for cell plate assembly and the exocyst for cell wall maturation.

In this study, we present that both tethering factors the TRAPPII and the exocyst localize to the cell plate at the phragmoplast assembly stage (Fig. 3.5.1). Moreover, exocyst-like complexes, which tether vesicles that form cell plate before fusion were found in the electron tomographs (Samuels et al., 1995; Segui-Simarro et al., 2004). The localization of these two tethering complexes at the onset of cytokinesis led us to suggest that both tethering complexes could be implicated in cell plate biogenesis. However, our data show clearly that TRAPPII but not exocyst complex is required for cell plate assembly. It is confirmed by immunostain analyses that show patchy, incomplete cell plates in TRAPPII mutants. We were not able to detect any cytokinesis defects in exocyst mutants of *Arabidopsis* root tips using antibody staining analyses, TEM and SEM.

A strong exocyst signal at the cross wall, at the end of cytokinesis raises the question as to the role of the exocyst in cell wall maturation. Additionally, the exocyst complex was localized to the insertion sites at the end of cytokinesis (Fendrych et al., 2010). This would suggest its role in final stages of cytokinesis. Another protein, TPLATE, was shown to localize to the area around the insertion sites at the end of cytokinesis and was proposed to be required for cell plate fusion to the parental membranes (Van Damme et al., 2006; Van Damme et al., 2010). It would be interesting to examine whether the exocyst is involved in the process of cell plate anchoring as well. It was suggested that the exocyst could be required for delivery of cell wall materials to complete cell wall maturation (Fendrych et al., 2010; Kulich et al., 2010). TPLATE localizes to the growing cell plate throughout cytokinesis and was shown to be involved in clathrin-mediated endocytosis (Van Damme et al., 2011; Gadeyne et al., 2014). The postcytokinetic cross wall maturation starts after insetion of the cell plate to the parental cell wall (Mineyuki and Gunning, 1990) and changes in cell wall composition including

callose exchange with cellulose (Samuels et al., 1995). The plant cell wall is composed of cellulose, non-cellulosic polysaccharide polymers (hemicellulose and pectin), and proteins (Bashline et al., 2014). The ratio of cell wall polysaccharides at the cell plate and mature cross walls varies at different steps of cytokinesis. Mature cell walls have high pectin content and low levels of xyloglucans (a major hemicellulose component; His et al., 2001). Indeed, we observed the altered relative content of xyloglucans, AGP glycans, as well as un-esterified pectins and methyl-esterified pectins in the cell plates, cross walls and lateral walls of *exo84b-2* mutant root tips. Callose, a major component of the primary cell wall appears at the cell plate after the initial fusion stage, reaches maximum levels at the fenestrated sheet stage and subsequently disappears after the holes of the fenestrated plate are closed (Samuels et al., 1995). Cellulose is the major component of the mature cross walls and was shown to appear first at the cell plate at the smooth tubular network (TN) stage (Samuels et al., 1995). Later studies have shown cellulose accumulation already at the tubular-vesicular network (TVN) stage (Miart et al., 2013). Callose and cellulose are synthesized by enzyme complexes within the cell plate and at the plasma membrane, respectively (CSCs; Kakimoto and Shiboaka, 1992; Verma and Hong, 2001; Guerriero et al., 2010). Based on our data, we were not able to observe any differences in cellulose (CBM3a; Blake et al., 2006) labeling between wild type and *exo84b-2* mutants. Pectins and hemiceluloses are synthesized in ER and Golgi apparatus and transported to the cell plate in Golgi-derived vesicles (Staehelin and Moore, 1995). That includes highly methyl-esterified pectic polysaccharides (Zhang and Staehelin, 1992), which are later de-esterified by the cell wall localized pectin methylesterases (PMEs; Clausen et al., 2003). The fact that we detected JIM7 at the cell plate is inconsistent with the work of Dhonukshe et al. (2006), but it supports a model presented by Chow et al. (2008) that postulates that the cell plate is a Golgi/TGN derived compartment and does not require endocytosed material. The absence of the ectopic JIM7 staining in lateral and cross wall in *exo84b-2* might be due to a disruption in the delivery of PMEs to the plasma membrane. Another observation that supports the role of exocyst in cross wall maturation is the premature removal of KNOLLE from telophase plates in *exo84b-2*. The loss of KNOLLE as a juvenile trait can be considered as a first step in the maturation of the cell plate into a cross wall. The ESCRT complex is likely involved in the process of KNOLLE removal (Spitzer et al., 2006 and 2009).

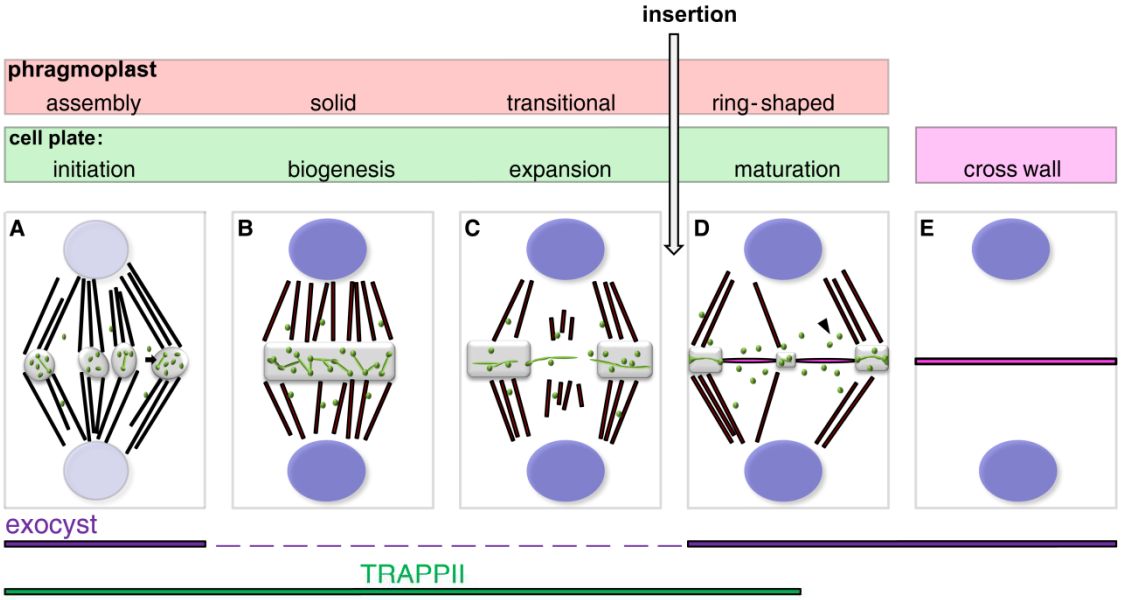

Figure 4.5.1. „Relay race" model for the sequential but overlapping and coordinated action of the TRAPPII and exocyst complexes.
Cytokinesis is broken down into four stages (A-D; adapted from Segui-Simarro et al., 2004).
(A) The phragmoplast is assembled from opposite sets of polar spindle microtubules (red rod-like structures). A first round of vesicle fusion gives rise to dumbell-shaped cell plate initials (arrow).
(B) At the solid phragmoplast stage, cell plate biogenesis occurs within a cell plate assembly matrix (CPAM; grey) via further rounds of membrane fusion.
(C) Cell plate expansion is driven by the reorganization of phragmoplast microtubules and membrane addition at the leading edges of the cell plate.
(D) Insertion occurs once the expanding cell plate has reached the parental walls. This event triggers maturation, which is accompanied by the loss of juvenile traits, including the removal of KNOLLE from cell plate membranes (arrowheads).
(E) At the end of cytokinesis, the cell plate has matured into a cross wall (fuschia) flanked on either side by plasma membranes (black contour lines).
Bottom panel: We postulate that the TRAPPII (dark green bar) and exocyst (purple bars) complexes are both required for the initiation of cytokinesis. Thereafter, the TRAPPII complex drives cell plate biogenesis and expansion, and the exocyst complex is required for cell plate maturation (see text for further details).
Red: phragmoplast microtubules; green: cell plate membranes; pink: mature cell plates and cross wall; blue: nuclei (light blue, dividing nuclei); grey: CPAM.

4.6. Protein sorting at the cell plate.

In this study, we provide an evidence for the role of CLUB/AtTRS130 in protein sorting at the cell plate. We showed that four plasma membrane proteins and cell wall polysaccharides are mis-localized in *club-2/trs130-2* mutant background. Interestingly, TGN localized VHA-a1, which does not label cell plate in the wild type, was localized to cell plate in *club-2* mutants. Based on our results, we show that the cell plate does not work as a sink for plasma membrane proteins as was described by Müller et al. (2003), but as a membrane compartment at which secretory proteins are sorted in a highly differentiated manner. Moreover, differences in the relative signal intensities of plasma membrane proteins and cell wall polysaccharides at the cell plate versus lateral plasma membranes were reported (Rybak et al., 2014). We found interesting the fact that two closely related SYP1 family members, SYP121 and SYP122, had very different

localization patterns at the cell plate, with SYP121 being enriched and SYP122 only very weakly localized at the cell plate. The mis-localization of exocyst subunits in the *club-2/trs130-2* mutant background suggests that the TRAPPII complex might be required for sorting the exocyst complex away from cell plate membranes during the solid phragmoplast stages and, conversely, transports the exocyst to the cell plate at the end of cytokinesis. Indeed, exocyst subunits clearly label the cell plate in the *club-2/trs130-2* background, while their signal at the cell plate in the wild type is diffuse. At the end of cytokinesis, the exocyst subunits label the cross wall strongly but in the mutant background they failed to localize to the maturing cell plate and cross wall membranes. Mis-localization of plasma membrane proteins is not due to the cell plate defect in *club-2/trs130-2* mutants, as we chose mutant cell plates that showed normal appearance on the basis of FM4-64 staining.

Another *Arabidopsis* protein was reported to be implicated in protein sorting at the TGN, the ECHIDNA (Gendre et al., 2011). ECHIDNA was shown to be required for TGN-mediated transport to the plasma membrane and the cell wall (Boutté et al., 2013; Gendre et al., 2013; McFarlane et al., 2013). Cell wall polysaccharides were reported to be mislocalized in *ech* mutants (McFarlane et al., 2013). Additionally, ECHIDNA is thought to be involved in the genesis of secretory vesicles at the TGN and trafficking of auxin influx carrier AUX2 from the TGN to the plasma membrane (Boutté et al., 2013). Interestingly, TRAPPII was reported to be required for polar distribution of AUX1 and PIN2 but, not PIN1 (Qi et al., 2011; Qi and Zheng, 2011). We might expect that these two proteins could interact and work together. However, we did not detect ECHIDNA protein in CLUB-GFP and TRS120-GFP immunoprecipitates. ECHIDNA was not detected on the cell plate so far and it would be interesting to examine its localization and colocalization with TRAPPII subunits in dividing cells.

4.7. Rab GTPases localize to the cell plate in dividing cells.

The Rab GTPases constitute the largest family of the small GTP-binding protein superfamily in *Arabidopsis*. They cycle between inactive, GDP-bound and active GTP-bound form (Sclafani et al., 2010). Phylogenetic analysis of *Arabidopsis* genome identified 57 AtRab GTPases (11 in yeast and 60 in mammals), which, based on sequence similarity, were divided into eight subclasses (Rab-A – Rab-H; Vernoud et al., 2003). Distinct subfamilies cycle between cytosol and membrane-bound form associated to the specific membrane compartment, where they play a role in trafficking (Fig. 1.3.1; Stenmark and Olkkonen, 2001; Zerial and McBride, 2001). Members of almost all subfamilies have been studied so far. These are AtRab-A (Inaba et al., 2002;

Chow et al., 2008; Kang et al., 2011; Feraru et al., 2012; Qi and Zheng, 2013), AtRab-B (Cheung et al., 2002), AtRab-D (Batoko et al., 2000; Pinheiro et al., 2009; Peng et al., 2011), AtRab-E (Camacho et al., 2009; Speth et al., 2009) AtRab-F (Ueda et al., 2001), AtRab-G (Kwon et al., 2013), AtRabH (Bednarek et al., 1994). Rab GTPases are essential for SNARE complex formation (Søgaard et al., 1994).

The *Arabidopsis* subfamily AtRab-A is represented by 26 genes divided into six groups (Rab-A1 – Rab-A6; Woollard and Moore, 2008). However, their functional diversity has not been elucidated. For comparison, there are just three Rab-A homologues in mammals (Rab11A, Rab11B and Rab25) and two in yeast (Ypt31 and Ypt32; Sclafani et al., 2010). The Rab-A GTPase subfamily is involved in post-Golgi trafficking to the cell plate in dividing cells (Chow et al., 2008; Boutte et al., 2009) and to the cell wall in polarized plant cells (Preuss et al., 2004 and 2006; Szumalski and Nielsen, 2009). Rab-A GTPases reside on a TGN/EE compartment (Rab-A2, Rab-A3, Chow et al., 2008; Rab-A4b, Kang et al., 2011; Rab-A1b, Feraru et al., 2012; Rab-A1c, Qi and Zheng, 2012). Rab-A2 and Rab-A3 were detected at the cell plate throughout cytokinesis and co-localize with the cell plate specific t-SNARE, the KNOLLE (Chow et al., 2008). Rab-A4b was shown to be involved in the polar secretion of cell wall components in the tips of growing root hairs (Kang et al., 2004; Preuss et al., 2006) and Rab-A4d in regulation of pollen tube tip growth (Szumalski and Nielsen, 2009). The Rab-A1b was reported to regulate trafficking between the TGN and the plasma membrane (Feraru et al., 2012). Rab-A1b, -A1c, -A2a and -A4b were shown to localize to the same population of the TGN compartment. TRAPPII works as a positive regulator of Rab-A GTPases in plants, likely as a guanine exchange factor (GEF; Qi et al., 2011). In yeast, TRAPPII was shown to work as GEF for Ypt1 and Ypt31/32, which are homologues of plant Rab-D and Rab-A, respectively (Cai et al., 2008; Morozova et al., 2006; Yip et al., 2010). In mammalian cells, TRAPPII serves as a GFP for Rab1, which is a homologue of plant Rab-D GTPase (Yamasaki et al., 2009). The *Arabidopsis* Rab-D subfamily is represented by two isoforms, Rab-D1 and Rab-D2 (Vernoud et al., 2003). Rab-D GTPases are involved in early secretory traffic from the ER to Golgi (Batoko et al., 2000; Pinheiro et al., 2009). Interestingly, Rab-D was localized not only to the Golgi but also to a population of TGN/EE in *Arabidopsis* and tobacco cells (Pinheiro et al., 2009). In *Arabidopsis*, the TRAPPII complex was shown to be functionally linked to Rab-A but not Rab-D GTPases; constant expression of an active form Rab-A1c (Q72L) was shown to partially rescue the *club-2/trs130-2* mutant phenotype (Qi and Zheng, 2011).

Not only Rab-A GTPases but also other subfamilies of Rab GTPases were localized to the cell plate in dividing cells, for example Rab-E GTPases (Chow et al., 2008). The *Arabidopsis* Rab-E GTPase subfamily is represented by five isoforms (Rab-E1a – Rab-E1e). In mammals there are two Rab-E homologues (Rab8 and Rab10) and one (Sec4p) in S. cerevisiae (Segev et al., 2001; Rutherford and Moore, 2002; Vernoud et al., 2003). The Rab-E subfamily was shown to be implicated in polarized secretion (Guo et al., 1999b; Segev et al., 2001, Carter et al., 2004). As cytokinesis in plants is considered to be a form of polarized secretion (Samuels et al., 1995; Assaad, 2001; Lucas and Sack, 2012), we could expect a possible requirement of Rab-E in dividing cells. AtRab-E1d was shown to localize to the Golgi Apparatus and cytoplasm in tobacco leaf epidermal cells (Zheng et al., 2005), to the plasma membrane in *Arabidopsis* leaf cells (Speth et al. 2009), as well as to the cell plate in the dividing cells of the root tip (Chow et al., 2008). Here we show for the first time the localization dynamics of Rab-E-YFP throughout cytokinesis. We show that from the early pharagmoplast assembly stage until the ring-shape phragmoplast stage, the Rab-E1d showed localization dynamics at the cell plate, which is characteristic of TRAPPII complex. At the end of cytokinesis, Rab-E1d strongly labeled the cross wall, which is a localization dynamics characteristic of the exocyst complex. Based on this observation, it would be interesting to examine whether Rab-E is functionally linked to the TRAPPII complex in plants. Does the TRAPPII complex also act as a GEF for Rab-E GTPases? However, we detected one of the five isoforms of the Rab-E GTPases subfamily, the Rab-E1a in immunoprecipitates of the CLUB and TRS120 GFP fusions. No evidence for cytokinesis defects was shown in dominant inhibitory mutants of Rab-E so far.

In plants, AtRab-E was reported to play a role in plant defence responses. AvrPto is a *Pseudomonas syringae* effector, which was shown to interact with GTP bound form of Rab-E but not with other members of the Rab family (Speth et al., 2009). Moreover, a polarized accumulation of Rab-E1d in mesophyll cells upon infection with *P. syringae* was reported (Speth et al., 2009). In plants, the fungal or bacterial attack leads to activation of different defence responses. These include formation of papillae, which are callose-rich cell wall appositions and the activation of the secretory pathway (Assaad et al., 2004). In yeast, Sec4p was reported to be required for exocyst complex formation (Guo et al., 1999b). The exocyst was shown to be involved in the immune response to different pathogens (Pacenkova et al., 2011; Stegmann et al., 2013). In yeast, the exocyst complex serves as an effector for Sec4p (Guo et al., 1999b). We could speculate that the exocyst complex works together with Rab-E GTPases in response to pathogen attack.

4.8. CLUB and TRS120 differ with respect to their putative interaction partners.

Immunoprecipitation and mass spectrometry analyses of CLUB-GFP and TRS120-GFP revealed a variety of membrane trafficking components. These includes VHA-a1 (Dettmer et al., 2006), Rab-GTPases (Pinheiro et al., 2009; Speth et al., 2009; Qi et al., 2011), clathrin coat components, SNARE proteins and the SM protein KEULE (Assaad et al., 2001; Wu et al., 2013). Moreover, we found proteins involved in the synthesis of cell wall components, including callose and cellulose synthases. Callose is synthesized by callose synthase enzyme complex within the cell plate (Kakimoto and Shiboaka, 1992; Verma and Hong, 2001). *Arabidopsis* genome encodes twelve callose synthases (Thiele et al., 2009). We detected three of them in CLUB-GFP and TRS120-GFP immunoprecipitates. We expected to find MASSUE, a callose synthase, which was shown to localize to the cell plate and to be required for cytokinesis (Thiele et al., 2009). Taking into account that MASSUE mutants show phenotype similar to *club-2* mutants, we would suggest that they might play a role in the same process and could potentially interact. However, MASSUE was not detected by mass spectrometry. Cellulose is synthesized by a membrane-bound cellulose synthase complex (CSCs; Guerriero et al., 2010). Five cellulose synthase proteins were found in CLUB-GFP and TRS120-GFP immunoprecipitates.

Interestingly, except for TRAPP subunits, other tethering factors were also found to interact with CLUB and TRS120. These are members of the exocyst complex (Elias et al., 2003), the GARP complex (Lobstein et al., 2004; Guarmonprez et al., 2008) and the COG complex (Ishikawa et al., 2008). This raises the question as to whether different tethering complexes communicate between each other, as we have shown for TRAPPII and exocyst complexes.

Additionally, we found many components involved in plant-pathogen interactions in CLUB and TRS120 immunoisolates, for example an ARF-GTP exchange factor. Other effectors that were found in immunoisolates are involved in response to environmental cues. This suggests a role for TRAPPII complex in pathogen responses.

Interestingly, despite the fact that CLUB and TRS120 proteins are subunits of the same protein complex, we found a number of different interactors in their immunoprecipitates. CLUB-specific hits include components involved in signaling and development, for example, proteins required for proper cytokinesis during seed development, for induction of flowering and involved in pre-prophase band (PPB) formation.

Recently, the successful attempt of the TGN proteome isolation was reported (Drakakaki et al., 2012; Groen et al., 2014). Immunoisolation assays using two TGN markers the SYP61 and the VHA-a1 as baits generated in 147 hits and 105 hits, respectively (Drakakaki et al., 2012; Groen et al., 2014). Considering the fact that SYP61 was detected in VHA-a1 immunoisolates and vice versa, we would postulate that both markers represent the same population of TGN (Drakakaki et al., 2012; Groen et al., 2014). However, the overlap between these two fractions is just 32% (Groen et al., 2014). Interestingly, Groen et al. (2014) identified both TRAPPII specific subunits, CLUB/AtTRS130 and AtTRS120, in the TGN proteome. In the work of Drakakaki et al. (2012) only AtTRS120 was found to be associated with SYP61-TGN compartments. This can be attributed to the fact that Groen et al. (2014) used *Arabidopsis* roots for an isolation TGN membrane proteome, which are mainly dividing cells, while Drakakaki et al. (2012) used leaves, which consist mainly of non-dividing cells. We showed that TRAPPII specific subunits localize to cytosolic and membrane fractions. Our preliminary confocal data showed that both TRAPPII specific subunits co-localize with SYP61-CFP. TRS120-GFP showed more membrane-bound localization. CLUB was predominantly cytosolic and co-localized with SYP61-CFP partially. As we carried out our confocal analyses on *Arabidopsis* root tip, it would be worth to examine the co-localization analysis also in leaves. Moreover, TRS120 was shown to co-localize with the VHA-a1 compartment (Naramoto et al., 2014). Additionally, we demonstrated that VHA-a1 TGN localization is dependent on CLUB. We detected VHA-a1 but not SYP61 in immunoprecipitates where CLUB-GFP and TRS120-GFP were used as baits.

As immunoisolation assay is not sufficient to distinguish TGN residents from transient and trafficking cargo. Localization of organelle protein by isotope tagging (LOPIT) followed by selected reaction monitoring (SRM) analysis was used to identify TGN proteome in *Arabidopsis* roots by Groen et al. (2014). In one out of two LOPIT experiments CLUB and TRS120 were detected. However, as considered only proteins with at least one trans-membrane domain, CLUB and TRS120 were excluded from the final TGN membrane proteome (Groen et al., 2014). Cox et al. (2007) based on bioinformatical analysis showed that yeast Trs130p does not function as a trans-membrane protein. Moreover, TRAPP complex was reported to be only membrane-associated as can be extracted from the membrane by salts but not by detergent (Cox et al., 2007). Additionally, Naramoto et al. (2014) reported that AtTRS120 protein is a peripheral membrane protein, associated with membranes via non-electrostatic interactions. It is consistent with our and Groen et al. (2014) bioinformatical data

analyses using TMHMM Server v.2.0, where we found that neither TRS130 nor TRS120 is a trans-membrane protein. TRS130 and TRS120 are conserved in almost all eukaryotes (Koumandou et al., 2007; Cox et al., 2007). The AtTRS130 gene (At5g54440) spans 6523 bp and encodes a protein of 1259 amino acids. There are three well-conserved domains (33 to 314 amino acids) across the length of TRS130 (Cox et al., 2007); two first domains are highly conserved and they are suggested to be responsible for protein-protein interactions, as well as for catalytic functions; the third domain does not contain highly conserved amino acids. The AtTRS120 gene (At5g11040) spans 5636 bp and encodes a protein of 1186 amino acids. There are five well-conserved domains (20 to 165 amino acids) across the length of TRS120 and they are characterized by high-quality sequence similarities and by the presence of highly conserved amino acids (Cox et al., 2007). Most of the highly conserved amino acids such as aspartic and glutamic acid, are potentially involved in catalytic processes (Cox et al., 2007). The position of the domains in AtTRS120 and AtTRS130 are shown in Figure 4.8.1. Moreover, the fact that the primary and the secondary structure of Trs120 and Trs130 is conserved (Cox et al., 2007) indicates their important function in cellular processes. The secondary structure of both TRAPPII specific subunits is conserved not only in distinct domains but over the entire length of the proteins (Cox et al., 2007).

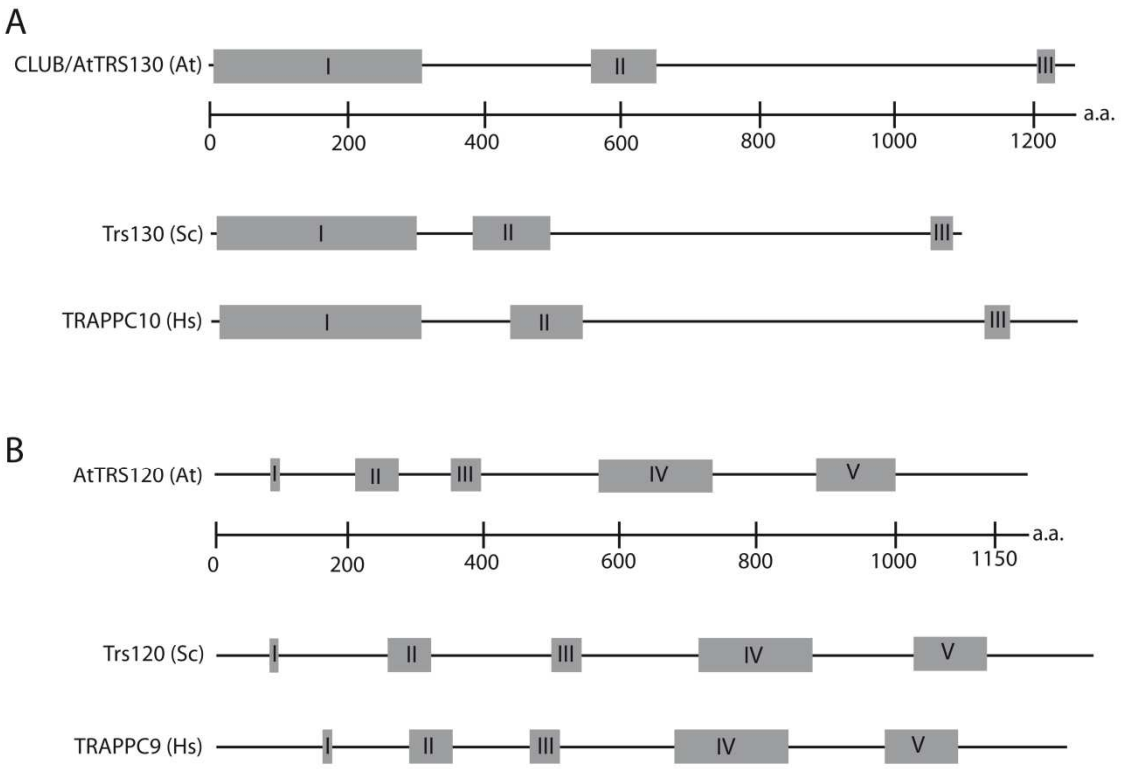

Figure 4.8.1. Position of conserved domains of CLUB/TRS130 and TRS120 proteins in eukaryotes.
At, Sc and Hs correspond to *Arabidopsis thaliana*, *Saccharomyces cerevisiae* and *Homo sapiens*, respectively. The data shown are based on Cox et al. (2007).
(A) The domain structure of CLUB/TRS130 is shown, the protein contains three conserved domains (I-III).
(B) The domain structure of TRS120 is shown, the protein contains five conserved domains (I-V).

The crystal structure of the plant TRAPPI and TRAPPII complexes has not been determined to date. The crystal structure of the mammalian TRAPPI complex was determined by Kim et al. (2006) and was shown to be composed of two TRAPP subcomplexes. The crystal structure of the yeast TRAPPI was described by Cai et al. (2008). Four subunits (Bet3p, Bet5p, Trs23p and Trs31p) that constitute the middle of the TRAPPI complex were shown to be essential for GEF activity in TRAPPI towards Rab GTPases, the yeast Ypt1 (Cai et al., 2008). A successful characterization of the structure and subunit organization of the native yeast TRAPPII complex was carried out by Yip et al., (2010) via single-particle electron microscopy. According to Yip et al. (2010), the TRAPPII subunits dimerize into a diamond-shaped structure; the TRAPPI form the two outer layers of the structure; Trs120 and Trs130 are at the sides of the complex; Trs65/Kre11was shown to be involved in mediating the dimerization and dimer stabilization. Taking into account that mammalian and plant TRAPPII lack Trs65 subunit, we suggest that it is present only as a monomer. The Trs130 subunit was shown to be required for Ypt31/32 activity (Morozova et al., 2006). In future studies, it will be interesting to characterise plant TRAPPII complex at a structural level and to compare their structure and subunit organization with the yeast TRAPPII complex.

5. Conclusion.

Cytokinesis is a final step of the cell cycle, which leads to a precise distribution of cystoplasm between two daughter cells. Plant cytokinesis starts with the formation of the cell plate. The cell plate is a plant specific transient membrane compartment that undergoes biogenesis, expansion and maturation throughout cytokinesis. After its insertion to the parental membrane, the cell plate matures into a cross wall.

To better understand the origin and the identity of cell plate membranes, I searched for cytokinesis-defective phenotypes in tethering factors via a reverse genetic approach. Tethering factors initiate the first physical contact between donor and target membranes. The cell plate is formed via vesicle fusion. As tethering factors are associated to a specific compartment in the secretory pathway, they constitute good markers to monitor specific processes of vesicle fusion. This study shows that the TRAPPII mutants exhibit a strong cytokinesis-defective phenotype. In contrast, mutations in the TRAPPI tethering factor lead to an attenuated cytokinesis-defective phenotype and exocyst mutants exhibit cytokinetic defects in the epidermal layer of leaves but not in *Arabidopsis* root tips. Extensive analyses of the localization dynamics of the TRAPPII and exocyst complexes in dividing cells indicate sequential identity of the cell plate membranes, with overlap at the onset of cytokinesis. The TRAPPII complex localizes to the cell plate throughout cytokinesis whereas the exocyst localizes to cross walls. I propose a model whereby the cell plate membranes switch from the trans-Golgi network to plasma membrane identity. I provide evidence that these two tethering complexes interact physically in vivo. Immunostain analyses revealed that the TRAPPII complex is required for cell plate biogenesis, whereas the exocyst is required for cross wall maturation.

6. References.

Abas, L., Benjamins, R., Malenica, N., Paciorek, T., Wiśniewska, J., Moulinier-Anzola, J.C., Sieberer, T., Friml, J., and Luschnig, C. (2006). Intracellular trafficking and proteolysis of the Arabidopsis auxin-efflux facilitator PIN2 are involved in root gravitropism. Nat. Cell Biol. *8*, 249-256.

Arsovski, A.A., Villota, M.M., Rowland, O., Subramaniam, R., and Western, T.L. (2009). MUM ENHANCERS are important for seed coat mucilage production and mucilage secretory cell differentiation in Arabidopsis thaliana. J Exp Bot. *60*, 2601-2612.

Assaad, F.F., Mayer, U., Wanner, G., and Jürgens, G. (1996). The KEULE gene is involved in cytokinesis in Arabidopsis. Mol. Gen. Genet. *253*, 267-277.

Assaad, H., Huet, Y., Mayer, M. and Jürgens, G. (2001). The Cytokinesis Gene KEULE Encodes a Sec1 Protein That Binds the Syntaxin KNOLLE. J. Cell Biol. *152*, 531-543.

Assaad, F.F., Qiu, J.L., Youngs, H., Ehrhardt, D., Zimmerli, L., Kalde, M., Wanner, G., Peck, S.C., Edwards, H., Ramonell, K., Somerville, C.R., and Thordal-Christensen, H. (2004). The PEN1 Syntaxin Defines a Novel Cellular Compartment upon Fungal Attack and Is Required for the Timely Assembly of Papillae. Mol. Biol. Cell *15*, 5118-5129.

Assaad, F.F. (2008). The membrane Dynamics of Root hair morphogenesis. In: Emons AMC., Ketelaar T (eds) Root hairs: excellent tools for the study for the study of plant molecular biology. (Springer, Berlin Heidelberg New York).

Barrowman, J., Bhandari, D., Reinisch, K., and Ferro-Novick, S. (2010). TRAPP complexes in membrane traffic: convergence through a common Rab. Nat. Rev. Mol. Cell Biol. *11*, 759-763.

Bashline, L., Lei, L., Li, S., and Gu, Y. (2014). Cell wall, cytoskeleton, and cell expansion in higher plants. Mol. Plant. *7*, 586-600.

Batoko, H., Zheng, H.Q., Hawes, C., and Moore, I. (2000). A rab1 GTPase is required for transport between the endoplasmic reticulum and golgi apparatus and for normal Golgi movement in plants. Plant Cell *12*, 2201-2218.

Bednarek, S.Y., Reynolds, T.L., Schroeder, M., Grabowski, R., Hengst, L., Gallwitz, D., and Raikhel, N.V. (1994). A small GTP-binding protein from Arabidopsis thaliana functionally complements the yeast YPT6 null mutant. Plant Physiol. *104*, 591-596.

Benková, E., Michniewicz, M., Sauer, M., Teichmann, T., Seifertová, D., Jürgens, G., and Friml J. (2003). Local, efflux-dependent auxin gradients as a common module for plant organ formation. Cell *115*, 591-602.

Berleth, T., Mattsson, J., and Hardtke, C.S. (2000). Vascular continuity and auxin signals. Trends Plant Sci. *5*, 387-393.

Blake, A.W., McCartney, L., Flint, J.E., Bolam, D.N., Boraston, A.B., Gilbert, H.J., and Knox, J.P. (2006). Understanding the biological rationale for the diversity of cellulose directed carbohydrate-binding modules in prokaryotic enzymes. J. Biol. Chem. *281*, 29321-29329.

Bolte, S., Talbot, C., Boutte, Y., Catrice, O., Read, N.D., and Satiat-Jeunemaitre, B. (2004). FM-dyes as experimental probes for dissecting vesicle trafficking in living plant cells. J. Microsc. *214*, 159-173.

Boutté, Y., Frescatada-Rosa, M., Men, S., Chow, C.M., Ebine, K., Gustavsson, A., Johansson, L., Ueda, T., Moore, I., Jürgens, G., and Grebe, M. (2009). Endocytosis restricts Arabidopsis KNOLLE syntaxin to the cell division plane during late cytokinesis. EMBO J. *29*, 546-558.

Boutté, Y., Jonsson, K., McFarlane, H.E., Johnson, E., Gendre, D., Swarup, R., Friml, J., Samuels, L., Robert, S., and Bhalerao, R.P. (2013). ECHIDNA-mediated post-Golgi trafficking of auxin carriers for differential cell elongation. Proc. Natl. Acad. Sci. USA *110*, 16259-16264.

Boyd, C., Hughes, T., Pypaert, M.,and Novick, P. (2004). Vesicles carry most exocyst subunits to exocytic sites marked by the remaining two subunits, Sec3p and Exo70p. J. Cell Biol. *167*, 889-901.

Cai, H., Zhang, Y., Pypaert, M., Walker, L., and Ferro-Novick, S. (2005). Mutants in trs120 disrupt traffic from the early endosome to the late Golgi. J. Cell Biol. *171*, 823-833.

Cai, Y., Chin, H.F., Lazarova, D., Menon, S., Fu, C., Cai, H., Sclafani, A., Rodgers, D.W., De La Cruz, E.M., Ferro-Novick, S., and Reinisch, K.M. (2008). The structural basis for activation of the Rab Ypt1p by the TRAPP membrane-tethering complexes. Cell *133*, 1202-1213.

Camacho, L., Smertenko, A.P., Pérez-Gómez, J., Hussey, P.J., and Moore, I. (2009). Arabidopsis Rab-E GTPases exhibit a novel interaction with a plasma-membrane phosphatidylinositol-4-phosphate 5-kinase. J. Cell Sci. *122*, 4383-4392.

Cao, X., Ballew, N., and Barlowe, C. (1998). Initial docking of ER-derived vesicles requires Uso1p and Ypt1p but is independent of SNARE proteins. EMBO J. *17*, 2156-2165.

Carter, C.J., Bednarek, S.Y., and Raikhel, N.V. (2004). Membrane trafficking in plants: new discoveries and approaches. Curr. Opin. Plant Biol. *7*, 701-707.

Cheung, A.Y., Chen, C.Y., Glaven, R.H., de Graaf, B.H., Vidali, L., Hepler, P.K., and Wu, H.M. (2002). Rab2 GTPase regulates vesicle trafficking between the endoplasmic reticulum and the Golgi bodies and is important to pollen tube growth. Plant Cell *14*, 945-962.

Choi, C., Davey, M., Schluter, C., Pandher, P., Fang, Y., Foster, L.J., and Conibear, E. (2011). Organization and assembly of the TRAPPII complex. Traffic *12*, 715-725.

Chow, C.-M., Neto, H., Foucart, C., and Moore, I. (2008). Rab-A2 and Rab-A3 GTPases Define a trans-Golgi Endosomal Membrane Domain in Arabidopsis That Contributes Substantially to the Cell Plate. Plant Cell *20*, 101-123.

Clausen, M.H., Willats, W.G., and Knox, J.P. (2003). Synthetic methyl hexagalacturonate hapten inhibitors of anti-homogalacturonan monoclonal antibodies LM7, JIM5 and JIM7. Carbohydr. Res. *338*, 1797-1800.

Clough, S.J., and Bent, A.F. (1998). Floral dip: a simplified method for Agrobacterium mediated transformation of Arabidopsis thaliana. Plant J. *16*, 735-743.

Cole, R.A., Synek, L., Zarsky, V., and Fowler, J.E. (2005). SEC8, a Subunit of the Putative Arabidopsis Exocyst Complex, Facilitates Pollen Germination and Competitive Pollen Tube Growth. Plant Physiol. *138*, 2005-2018.

Collins, N., Thordal-Christensen, H., Lipka, V., Bau, S., Kombrink, E., Qiu, J., Huckelhoven, R., Stein, M., Freialdenhoven, A., and Somerville, S., and Schulze-Lefert, P. (2003). SNARE-protein-mediated disease resistance at the plant cell wall. Nature *425*, 973- 977.

Conibear, E., and Stevens, T.H. (2000). Vps52p, Vps53p, and Vps54p form a novel multisubunit complex required for protein sorting at the yeast late Golgi. Mol. Biol. Cell. *11*, 305-323.

Conibear, E., Cleck, J.N., and Stevens, T.H. (2003). Vps51p mediates the association of the GARP (Vps52/53/54) complex with the late Golgi t-SNARE Tlg1p. Mol. Biol. Cell *14*, 1610-1623.

Cox, R., Chen, S.H., Yoo, E., Segev, N. (2007). Conservation of the TRAPPII-specific subunits of a Ypt/Rab exchanger complex. BMC Evol. Biol. *7*, 12.

Cutler S.R., Ehrhardt D.W., Griffitts J.S., and Somerville C.R. (2000). Random GFP:cDNA fusions enable visualization of subcellular structures in cells of Arabidopsis at a high frequency. Proc. Natl. Acad. Sci. USA *97*, 3718–3723.

Cvrckova, F., Elias, M., Hala, M., Obermeyer, G., and Zarsky, V. (2001). Small GTPases and conserved signalling pathways in plant cell morpho-genesis: from exocytosis to the exocyst. In: Cell biology of plant and fungal tip growth, A. Geitmann, M. Cresti, I.B. Heath, eds. (Amsterdam: IOS Press), pp. 105–122.

Dettmer, J., Hong-Hermesdorf, A., Stierhof, Y.D., and Schumacher, K. (2006). Vacuolar H+-ATPase activity is required for endocytic and secretory trafficking in Arabidopsis. Plant Cell *18*, 715-730.

Dhonukshe, P., Baluska, F., Schlicht, M., Hlavacka, A., Samaj, J., Friml, J., and Gadella, T.W. Jr. (2006). Endocytosis of cell surface material mediates cell plate formation during plant cytokinesis. Dev. Cell *10*, 137-150.

Drakakaki, G., van de Ven, W., Pan, S., Miao, Y., Wang, J., Keinath, N.F., Weatherly, B., Jiang, L., Schumacher, K., Hicks, G., and Raikhel, N. (2012). Isolation and proteomic analysis of the SYP61 compartment reveal its role in exocytic trafficking in Arabidopsis. Cell Res. *22,* 413-424.

Drdová, E,J., Synek, L., Pečenková, T., Hála, M., Kulich, I., Fowler, J.E., Murphy, A.S., and Zárský, V. (2013). The exocyst complex contributes to PIN auxin efflux carrier recycling and polar auxin transport in Arabidopsis. Plant J. *73*, 709-719.

Earley, K.W., Haag, J.R., Pontes, O., Opper, K., Juehne, T., Song, K. and Pikaard, C.S. (2006). Gateway-compatible vectors for plant functional genomics and proteomics. Plant J. *45*, 616-629.

El Kasmi, F., Krause, C., Hiller, U., Stierhof, Y.D., Mayer, U., Conner, L., Kong, L., Reichardt, I., Sanderfoot, A.A. and Jürgens, G. (2013). SNARE complexes of different composition jointly mediate membrane fusion in Arabidopsis cytokinesis. Mol. Biol. Cell *24*, 1593-1601.

Elias, M., Drdova, E., Ziak, D., Bavlnka, B., Hala, M., Cvrckova, F., Soukupova, H., and Zarsky, V. (2003). The exocyst complex in plants. Cell Biol. Int. *27*, 199-201.

Fagard, M., Desnos, T., Desprez, T., Goubet, F., Refregier, G., Mouille, G., McCann, M., Rayon, C., Vernhettes, S., and Hoefte. H. (2000). PROCUSTE1 encodes a cellulose synthase required for normal cell elongation specifically in roots and dark-grown hypocotyls of Arabidopsis. Plant Cell *12*, 2409-2423.

Fendrych, M., Synek, L., Pecenkova, T., Toupalova, H., Cole, R., Drdova, E., Nebesarova, J., Sedinova, M., Hala, M., Fowler, J.E., and Zársky, V. (2010). The Arabidopsis Exocyst Complex Is Involved in Cytokinesis and Cell Plate Maturation. Plant Cell *22*, 3053-3065.

Fendrych, M., Synek, L., Pecenková, T., Drdová, E.J., Sekeres, J., de Rycke, R., Nowack, M.K., and Zársky, V. (2013). Visualization of the exocyst complex dynamics at the plasma membrane of Arabidopsis thaliana. Mol. Biol. Cell *24*, 510-520.

Feraru, E., Feraru, M.I., Asaoka, R., Paciorek, T., De Rycke, R., Tanaka, H., Nakano, A., and Friml, J. (2012). BEX5/RabA1b regulates trans-Golgi network-to-plasma membrane protein trafficking in Arabidopsis. Plant Cell *24*, 3074-3086.

Gadeyne, A., Sánchez-Rodríguez, C., Vanneste, S., Di Rubbo, S., Zauber, H., Vanneste, K., Van Leene, J., De Winne, N., Eeckhout, D., Persiau, G., Van De Slijke, E., Cannoot, B., Vercruysse, L., Mayers, J.R., Adamowski, M., Kania, U., Ehrlich, M., Schweighofer, A., Ketelaar, T., Maere, S., Bednarek, S.Y., Friml, J., Gevaert, K., Witters, E., Russinova, E., Persson, S., De Jaeger, G., and Van Damme, D. (2014). The TPLATE adaptor complex drives clathrin-mediated endocytosis in plants. Cell *156*, 691-704.

Gehl, C., Waadt, R., Kudla,. J, Mendel, R.R., and Hänsch, R. (2009). New GATEWAY vectors for high throughput analyses of protein-protein interactions by bimolecular fluorescence complementation. Mol. Plant *2*, 1051-1058.

Gendre, D., Oh, J., Boutte, Y., Best, J.G., Samuels, L., Nilsson, R., Uemura, T., Marchant, A., Bennett, M.J., and Grebe, M., and Bhalerao, R.P. (2011). Conserved Arabidopsis ECHIDNA protein mediates trans-Golgi-network trafficking and cell elongation. Proc. Natl. Acad. Sci. USA *108*, 8048-8053.

Gendre, D., McFarlane, H.E., Johnson, E., Mouille, G., Sjödin, A., Oh, J., Levesque- Tremblay, G., Watanabe, Y., Samuels, L., and Bhalerao, R.P. (2013). Trans-Golgi Network Localized ECHIDNA/Ypt Interacting Protein Complex Is Required for the Secretion of Cell Wall Polysaccharides in Arabidopsis. Plant Cell *25*, 2633-2646.

Grefen, C., Donald, N., Hashimoto, K., Kudla, J., Schumacher, K., and Blatt, M.R. (2010). A ubiquitin-10 promoter-based vector set for fluorescent protein tagging facilitates temporal stability and native proteindistribution in transient and stable expression studies. Plant J. *64*, 355-365.

Groen, A.J., Sancho-Andrés, G., Breckels, L.M., Gatto, L., Aniento, F., and Lilley, K.S. (2014). Identification of trans-golgi network proteins in Arabidopsis thaliana root tissue. J. Proteome Res. *13*, 763-776.

Guermonprez, H., Smertenko, A., Crosnier, M.T., Durandet, M., Vrielynck, N., Guerche, P., Hussey, P.J., Satiat-Jeunemaitre, B., and Bonhomme, S. (2008). The POK/AtVPS52 protein localizes to several distinct post-Golgi compartments in sporophytic and gametophytic cells. J. Exp. Bot. *59*, 3087-9308.

Guerriero, G., Fugelstad, J., and Bulone, V. (2010). What do we really know about cellulose biosynthesis in higher plants? J. Integr. Plant Biol. *52*, 161-175.

Guo, W., Grant, A., and Novick, P. (1999a). Exo84p is an exocyst protein essential for secretion. J. Biol. Chem. *274*, 23558-23564.

Guo, W., Roth, D., Walch-Solimena, C., and Novick, P. (1999b). The exocyst is an effector for Sec4p, targeting secretory vesicles to sites of exocytosis. EMBO J. *18*, 1071-1080.

Gutierrez, R., Lindeboom, J.J., Paredez, A.R., Emons, A.M.C., and Ehrhardt, D.W. (2009). Arabidopsis cortical microtubules position cellulose synthase delivery to the plasma membrane and interact with cellulose synthase trafficking compartments. Nat. Cell Biol. *11*, 797-806.

Hala, M., Cole, R., Synek, L., Drdova, E., Pecenkova, T., Nordheim, A., Lamkemeyer, T., Madlung, J., Hochholdinger, F., Fowler, J.E., and Zárský, V. (2008). An exocyst complex functions in plant cell growth in Arabidopsis and tobacco. Plant Cell *20*, 1330-1345.

Haughn, G.W., and Western, T.L. (2012). Arabidopsis Seed Coat Mucilage is a Specialized Cell Wall that Can be Used as a Model for Genetic Analysis of Plant Cell Wall Structure and Function. Front Plant Sci. *3*, 64.

He, B., Xi, F., Zhang, J., TerBush, D., Zhang, X., and Guo, W. (2007). Exo70p mediates the secretion of specific exocytic vesicles at early stages of the cell cycle for polarized cell growth. J. Cell Biol. *176*, 771-177.

He, B., and Guo, W. (2009). The exocyst complex in polarized exocytosis. Curr. Opin. Cell Biol. *21*, 537-542.

Heese, M., Gansel, X., Sticher, L., Wick, P., Grebe, M., Granier, F., and Jurgens, G. (2001). Functional characterization of the KNOLLE-interacting t-SNARE AtSNAP33 and its role in plant cytokinesis. J. Cell Biol. *155*, 239-249.

Heider, M.R., and Munson, M. (2012). Exorcising the Exocyst Complex. Traffic *13*, 898-907.

His, I., Driouich, A., Nicol, F., Jauneau, A., and Hoefte, H. (2001). Altered pectin composition in primary cell walls of korrigan, a dwarf mutant of Arabidopsis deficient in a membrane-bound endo-1,4-b-glucanase. Planta *212*, 348-358.

Hung, W.F., Chen, L.J., Boldt, R., Sun, C.W., and Li, H.M. (2004). Characterization of Arabidopsis glutamine phosphoribosyl pyrophosphate amidotransferase-deficient mutants. Plant Physiol. *135*, 1314-1323.

Inaba, T., Nagano, Y., Nagasaki, T., and Sasaki, Y. (2002). Distinct localization of two closely related Ypt3/Rab11 proteins on the trafficking pathway in higher plants. J. Biol. Chem. *277*, 9183-9188.

Ishikawa, T., Machida, C., Yoshioka, Y., Ueda, T., Nakano, A., and Machida, Y. (2008). EMBRYO YELLOW gene, encoding a subunit of the conserved oligomeric Golgi complex, is required for appropriate cell expansion and meristem organization in Arabidopsis thaliana. Genes Cells *13*, 521-535.

Isono, E., Katsiarimpa, A., Müller, I.K., Anzenberger, F., Stierhof, Y.D., Geldner, N., Chory, J., and Schwechheimer, C. (2010). The deubiquitinating enzyme AMSH3 is required for intracellular trafficking and vacuole biogenesis in Arabidopsis thaliana. Plant Cell *22*, 1826-1837.

Isono, E., and Schwechheimer, R. (2010). Co-immunoprecipitation and protein blots. Methods Mol. Biol. *655*, 377-387.

Jaber, E., Thiele, K., Kindzierski, V., Loderer, C., Rybak, K., Jürgens, G., Mayer, U., Söllner, R., Wanner, G., and Assaad, F.F. (2010). A putative TRAPPII tethering factor is required for cell plate assembly during cytokinesis in Arabidopsis. New Phytol. *187*, 751-763.

Jelínková, A., Malínská, K., Simon, S., Kleine-Vehn, J., Parezová, M., Pejchar, P., Kubes, M., Martinec, J., Friml, J., Zazímalová, E., and Petrásek, J. (2010). Probing plant membranes with FM dyes: tracking, dragging or blocking? Plant J. *61*, 883-892.

Jones L., Seymour G.B., and Knox, J.P. (1997). Localization of pectic galactan in tomato cell walls using a monoclonal antibody specific to (1[->]4)-[beta]-D-galactan. Plant Physiol. *113*, 1405-1412.

Jürgens, G. (2005). Plant cytokinesis: fission by fusion. Trends Cell Biol. *15*, 277-283.

Kakimoto, T., and Shiboaka, H. (1992). Synthesis of polysaccharides in phragmo-plasts isolated from tobacco BY-2 cells. Plant Cell Physiol. *33*, 353-361.

Kang, B.H., Nielsen, E., Preuss, M.L., Mastronarde, D., and Staehelin, L.A. (2011). Electron tomography of RabA4b- and PI-4Kβ1-labeled trans Golgi network compartments in Arabidopsis. Traffic *12*, 313-329.

Klinger, C.M., Klute, M.J., and Dacks, J.B. (2013). Comparative genomic analysis of multi-subunit tethering complexes demonstrates an ancient pan-eukaryotic complement and sculpting in apicomplexa. PLoS One *8*, e76278.

Kim, Y.G., Sohn, E.J., Seo, J., Lee, K.J., Lee, H.S., Hwang, I., Whiteway, M., Sacher, M., and Oh, B.H. (2005). Crystal structure of bet3 reveals a novel mechanism for Golgi localization of tethering factor TRAPP. Nat. Struct. Mol. Biol. *12*, 38-45.

Knox, J.P., Linstead, P.J., King, J., Cooper C., and Roberts, K. (1990). Pectin esterification is spatially regulated both within cell walls and between developing tissues of root apices. Planta *181*, 512-521.

Koncz, C., and Schell, J. (1986). The promoter of TL-DNA gene 5 controls the tissue specific expression of chimaeric genes carried by a novel type of Agrobacterium binary vector. Mol. Gen. Genet. *204*, 383-396.

Koumandou, V.L., Dacks, J.B., Coulson, R.M., and Field, M.C. (2007). Control systems for membrane fusion in the ancestral eukaryote; evolution of tethering complexes and SM proteins. BMC Evol. Biol. *7*, 29.

Kulich, I., Cole, R., Drdová, E., Cvrcková, F., Soukup, A., Fowler, J., and Zárský, V. (2010). Arabidopsis exocyst subunits SEC8 and EXO70A1 and exocyst interactor ROH1 are involved in the localized deposition of seed coat pectin. New Phytol. *188*, 615-625.

Kwon, S.I., Cho, H.J., Kim, S.R., and Park, O.K. (2013). The Rab GTPase RabG3b positively regulates autophagy and immunity-associated hypersensitive cell death in Arabidopsis. Plant Physiol. *161*, 1722-1736.

Laemmli, U.K., Molbert, E., Showe, M., and Kelenberger, E. (1970). Form-determining function of genes required for the assembly of the head of bacteriophage T4. J. Mol. Biol. *49*, 99-113.

Lane, D.R., Wiedemeier, A., Peng, L., Höfte, H., Vernhettes, S., Desprez, T., Hocart, C.H., Birch, R.J., Baskin, T.I., Burn, J.E., Arioli, T., Betzner, A.S., and Williamson, R.E. (2001). Temperature-sensitive alleles of RSW2 link the KORRIGAN endo-1,4-beta-glucanase to cellulose synthesis and cytokinesis in Arabidopsis. Plant Physiol. *126*, 278-288.

Lauber, M.H., Waizenegger, I., Steinmann, T., Schwarz, H., Mayer, U., Hwang, I., Lukowitz, W., and Jürgens, G. (1997). The Arabidopsis KNOLLE protein is a cytokinesis-specific syntaxin. J. Cell Biol. *139*, 1485-1493.

Lee, C.F., Pu, H.Y., Wang, L.C., Sayler, R.J., Yeh, C.H., and Wu, S. (2006). Mutation in a homolog of yeast Vps53p accounts for the heat and osmotic hypersensitive phenotypes in Arabidopsis *hit1-1* mutant. Planta *224*, 330-338.

Liu, C., Johnson, S., and Wang, T.L. (1995). *Cyd*, a mutant of pea that alters embryo morphology is defective in cytokinesis. Dev Genet *16*, 321-331.

Lobstein, E., Guyon, A., Férault, M., Twell, D., Pelletier, G., and Bonhomme, S. (2004) The putative Arabidopsis homolog of yeast vps52p is required for pollen tube elongation, localizes to Golgi, and might be involved in vesicle trafficking. Plant Physiol. *135*, 1480-1490.

Lucas, J.R., and Sack, F.D. (2012). Polar development of preprophase bands and cell plates in the Arabidopsis leaf epidermis. Plant J. *69*, 501-509.

Lukowitz, W., Mayer, U., and Jürgens, G. (1996). Cytokinesis in the Arabidopsis embryo involves the syntaxin-related KNOLLE gene product. Cell *84*, 61-71.

Luo, L., Hannemann, M., Koenig, S., Hegermann, J., Ailion, M., Cho, M.K., and Sasidharan, N., Zweckstetter, M., Rensing, S.A., Eimer, S. (2011). The Caenorhabditis elegans GARP complex contains the conserved Vps51 subunit and is required to maintain lysosomal morphology. Mol. Biol. Cell *22*, 2564-2578.

Luo, G., Zhang, J., Luca, F.C., and Guo, W. (2013). Mitotic phosphorylation of Exo84 disrupts exocyst assembly and arrests cell growth. J. Cell Biol. *202*, 97-111.

Lynch-Day, M.A., Bhandari, D., Menon, S., Huang, J., Cai, H., Bartholomew, C.R., Brumell, J.H., Ferro-Novick, S., and Klionsky, D.J. (2010). Trs85 directs a Ypt1 GEF, TRAPPIII, to the phagophore to promote autophagy. Proc. Natl. Acad. Sci. USA *107*, 7811-7816.

Marcus, S.E., Verhertbruggen, Y., Hervé, C., Ordaz-Ortiz, J.J., Farkas, V., Pedersen, H.L., Willats, W.G., and Knox, J.P. (2008). Pectic homogalacturonan masks abundant sets of xyloglucan epitopes in plant cell walls. BMC Plant Biol. *8*, 60.

Mayer, U., Torres Ruiz, R.A., Berleth, T., Misera, S., and Jürgens, G. (1991). Mutations affecting body organization in the *Arabidopsis* embryo. Nature *353*, 402-407.

McFarlane, H.E., Watanabe, Y., Gendre, D., Carruthers, K., Levesque-Tremblay, G., Haughn, G.W., Bhalerao, R.P.,and Samuels, L. (2013). Cell Wall Polysaccharides are Mislocalized to the Vacuole in echidna Mutants. Plant Cell Physiol. *54*, 1867-1880.

McFarlane, H.E., Watanabe, Y., Yang, W., Huang, Y., Ohlrogge, J., and Samuels, A.L. (2014). Golgi- and trans-Golgi network-mediated vesicle trafficking is required for wax secretion from epidermal cells. Plant Physiol. *164*, 1250-1260.

McMichael, C.M., and Bednarek, S.Y. (2013). Cytoskeletal and membrane dynamics during higher plant cytokinesis. New Phytol. *197*, 1039-1057.

Miart, F., Desprez, T., Biot, E., Morin, H., Belcram, K., Höfte, H., Gonneau, M., and Vernhettes, S. (2014). Spatio-temporal analysis of cellulose synthesis during cell plate formation in Arabidopsis. Plant J. *77*, 71-84.

Mineyuki, Y., and Gunning, B.E.S. (1990). A role for preprophase bands of microtubules in maturation of new cell walls, and a general proposal on the function of the preprophase band sites in cell division in higher plants. J. Sci. *97*, 527-537.

Moller, I., Marcus, S.E., Haeger, A., Verhertbruggen, Y., Verhoef, R., Schols, H., Ulvskov, P., Mikkelsen, J.D., Knox, J.P., and Willats, W. (2008). High-throughput screening of monoclonal antibodies against plant cell wall glycans by hierarchical clustering of their carbohydrate microarray binding profiles. Glycoconj. J. *25*, 37-48.

Montpetit, B., and Conibear, E. (2009). Identification of the novel TRAPP associated protein Tca17. Traffic *10*, 713-723.

Morozova, N., Liang, Y., Tokarev, A.A., Chen, S.H., Cox, R., Andrejic, J., Lipatova, Z., Sciorra, V.A., Emr, S.D., and Segev, N. (2006). TRAPPII subunits are required for the specificity switch of a Ypt-Rab GEF. Nat. Cell Biol. *8*, 1263-1269.

Murashige, T., and Skoog, F. (1962). A revised medium for rapid growth and bioassays with tobacco tissue cultures. Physiol. Plant *15*, 473-497.

Murray, M.G., and Thompson, W.F. (1980). Rapid isolation of high molecular weight plant DNA. Nucleic Acids Res. *8*, 4321-4325.

Müller, I., Wagner, W., Völker, A., Schellmann, S., Nacry, P., Küttner, F., Schwarz-Sommer, Z., Mayer, U., and Jürgens, G. (2003). Syntaxin specificity of cytokinesis in Arabidopsis. Nat. Cell Biol. *5*, 531-534.

Müller, S., Smertenko, A., Wagner, V., Heinrich, M., Hussey, P., and Hauser, M. (2004). The plant microtubule-associated protein AtMAP65-3/PLE is essential for cytokinetic phragmoplast function. Curr. Biol. *14*, 412-417.

Naramoto, S., Nodzyłski, T., Dainobu, T., Takatsuka, H., Okada, T., Friml, J., and Fukuda, H. (2014). VAN4 encodes a putative TRS120 that is required for normal cell growth and vein development in *Arabidopsis*. Plant Cell Physiol. *55*, 750-763.

Neto, H., and Gould, G.W. (2011). The regulation of abscission by multi-protein complexes.J. Cell Sci. *124*, 3199-3207.

Nicol, F., His, I., Jauneau, A., Vernhettes, S., Canut, H., and Hofte, H. (1998). A plasma membrane–bound putative endo-1,4-β-d-glucanase is required for normal wall assembly and cell elongation in *Arabidopsis*. EMBO J. *17*, 5563-5576.

Novick, P., Field, C., and Schekman, R. (1980). Identification of 23 complementation groups required for post-translational events in the yeast secretory pathway. Cell. *21*, 205-215.

Otegui, M.S., and Staehelin, L.A. (2004). Electron tomographic analysis of post-meiotic cytokinesis during pollen development in Arabidopsis thaliana. Planta. *218*, 501-515.

Park, M., Touihri, S., Müller, I., Mayer, U., and Jürgens, G. (2012). Sec1/Munc18 Protein Stabilizes Fusion-Competent Syntaxin for Membrane Fusion in Arabidopsis Cytokinesis. Dev. Cell *22*, 989-1000.

Pahari, S., Cormark, R.D., Blackshaw, M.T., Liu, C., Erickson, J.L., and Schultz, E.A. (2014). Arabidopsis UNHINGED encodes a VPS51 homolog and reveals a role for the GARP complex in leaf shape and vein patterning. Development *141*, 1894-1905.

Palade, G. (1975). Intracellular aspects of the process of protein synthesis. Science *189*, 347-358.

Pattathil, S., Avci, U., Baldwin, D., Swennes, A.G., McGill, J.A., Popper, Z., Bootten, T., Albert, A., Davis, R.H., Chennareddy, C., Dong, R., O'Shea, B., Rossi, R., Leoff, C., Freshour, G., Narra, R., O'Neil, M., York, W.S., and Hahn, M.G. (2010). A Comprehensive Toolkit of Plant Cell Wall Glycan-Directed Monoclonal Antibodies. Plant Physiol. *153***,** 514-525.

Pecenková, T., Hála, M., Kulich, I., Kocourková, D., Drdová, E., Fendrych, M., Toupalová, H., and Zársky, V. (2011). The role for the exocyst complex subunits Exo70B2 and Exo70H1 in the plant-pathogen interaction. J. Exp. Bot. *62*, 2107-2116.

Pedersen, H.L., Fangel, J.U., McCleary, B., Ruzanski, C., Rydahl, M.G., Ralet, M.C., Farkas, V., von Schantz, L., Marcus, S.E., Andersen, M.C. Field, R., Ohlin, M., Knox, J.P., Clausen, M.H., and Willats, W.G. (2012). Versatile high resolution oligosaccharide microarrays for plant glycobiology and cell wall research. J. Biol. Chem. *47,* 39429-39438.

Peng, J., Ilarslan, H., Wurtele, E.S., and Bassham, D.C. (2011). AtRabD2b and AtRabD2c have overlapping functions in pollen development and pollen tube growth. BMC Plant Biol. *11*, 25.

Petrásek, J., Mravec, J., Bouchard, R., Blakeslee, J.J., Abas, M., Seifertová, D., Wisniewska, J., Tadele, Z., Kubes, M., Covanová, M., Dhonukshe, P., Skupa, P., Benková, E., Perry, L., Krecek, P., Lee, O.R., Fink, G.R., Geisler, M., Murphy, A.S., Luschnig, C., Zazímalová, E., and Friml, J. (2006). PIN proteins perform a rate-limiting function in cellular auxin efflux. Science *312*, 914-891.

Pinheiro, H., Samalova, M., Geldner, N., Chory, J., Martinez, A., and Moore, I. (2009). Genetic evidence that the higher plant Rab-D1 and Rab-D2 GTPases exhibit distinct but overlapping interactions in the early secretory pathway. J. Cell Sci. *122*, 3749-3758.

Ponnambalam, S., and Baldwin, S.A. (2003). Constitutive protein secretion from the trans-Golgi network to the plasma membrane. Mol. Membr. Biol. *20*, 129-139.

Preuss, M.L., Serna, J., Falbel, T.G., Bednarek, S.Y., and Nielsen, E. (2004). The Arabidopsis Rab GTPase RabA4b localizes to the tips of growing root hair cells. Plant Cell *16*, 1589-1603.

Preuss, M.L., Schmitz, A.J., Thole, J.M., Bonner, H.K., Otegui, M.S., and Nielsen, E. (2006). A role for the RabA4b effector protein PI-4Kbeta1 in polarized expansion of root hair cells in Arabidopsis thaliana. J. Cell Biol. *172*, 991-998.

Puhlmann, J., Bucheli, E., Swain, M. J., Dunning, N., Albersheim, P., Darvill, A. G., and Hahn M.G. (1994). Generation of monoclonal antibodies against plant cell wall polysaccharides. I. Characterization of a monoclonal antibody to a terminal alpha-(1,2)-linked fucosyl-containing epitope. Plant Physiol. *104*, 699-710.

Qi, X., Kaneda, M., Chen, J., Geitmann, A., and Zheng, H. (2011). A specific role for Arabidopsis TRAPPII in post-Golgi trafficking that is crucial for cytokinesis and cell polarity. Plant J. *68*, 234-248.

Qi, X., and Zheng, H. (2011). Arabidopsis TRAPPII is functionally linked to Rab-A, but not Rab-D in polar protein trafficking in trans-Golgi network. Plant Signal Behav. *6*, 1679-1683.

Qi, X., and Zheng, H. (2013). Rab-A1c GTPase defines a population of the trans-Golgi network that is sensitive to endosidin1 during cytokinesis in Arabidopsis. Mol. Plant *6*, 847-859.

Quenneville, N.R., Chao, T.Y., McCaffery, J.M., and Conibear, E. (2006). Domains within the GARP subunit Vps54 confer separate functions in complex assembly and early endosome recognition. Mol. Biol. Cell *17*, 1859-18570.

Rasmussen, C.G., Wright, A.J., and Müller, S. (2013). The role of the cytoskeleton and associated proteins in determination of the plant cell division plane. Plant J. *75*, 258-269.

Reichardt, I., Stierhofm Y.D., Mayer, U., Richter, S., Schwarz, H., Schumacher, K., Jürgens, G. (2007). Plant cytokinesis requires de novo secretory trafficking but not endocytosis. Curr. Biol. 17, 2047-2053.

Reichardt, I., Slane, D., El Kasmi, F., Knöll, C., Fuchs, R., Mayer, U., Lipka, V., and Jürgens, G. (2011). Mechanisms of functional specificity among plasma-membrane syntaxins in Arabidopsis. Traffic *12*, 1269-1280.

Richter, S., Voss, U., and Jürgens, G. (2009). Post-Golgi traffic in plants. Traffic *10*, 819-828.

Robert, S., Chary, S.N., Drakakaki, G., Li, S., Yang, Z., Raikhel, N.V., and Hicks, G.R. (2008). Endosidin1 defines a compartment involved in endocytosis of the brassinosteroid receptor BRI1 and the auxin transporters PIN2 and AUX1. Proc. Natl. Acad. Sci. USA *105*, 8464-8469.

Robinson, D.G., Jiang, L., and Schumacher, K. (2008). The endosomal system of plants: charting new and familiar territories. Plant Physiol. *147*, 1482-1492.

Rosso, M.G., Li, Y., Strizhov, N., Reiss, B., Dekker, K., and Weisshaar, B. (2003). An Arabidopsis thaliana T-DNA mutagenized population (GABI-Kat) for flanking sequence tag-based reverse genetics. Plant Mol. Biol. *53*, 247-259.

Rutherford, S., and Moore, I. (2002). The Arabidopsis Rab GTPase family: another enigma variation. Curr. Opin. Plant Biol. *5*, 518-528.

Rybak, K., Steiner, A., Synek, L., Klaeger, S., Kulich, I., Facher, E., Wanner, G., Kuster, B., Zarsky, V., Persson, S., and Assaad, F.F. (2014). Plant Cytokinesis Is Orchestrated by the Sequential Action of the TRAPPII and Exocyst Tethering Complexes. Dev. Cell *29*, 607-620.

Sacher, M., Jiang, Y., Barrowman, J., Scarpa, A., Burston, J., Zhang, L., Schieltz, D., Yates, J.R. 3rd, Abeliovich, H., and Ferro-Novick, S. (1998). TRAPP, a highly conserved novel complex on the cis-Golgi that mediates vesicle docking and fusion. EMBO J. *17*, 2494-2503.

Sacher, M., Barrowman, J., Wang, W., Horecka, J., Zhang, Y., Pypaert, M., and Ferro-Novick, S. (2001). TRAPP I implicated in the specificity of tethering in ER-to-Golgi transport. Mol. Cell *7*, 433-442.

Sachs, T. (1981). The control of patterned differentiation in vascular tissues. Adv. Bot. Res. *9*, 151-162.

Sachs, T. (2000). Integrating cellular and organismic aspects of vascular differentiation. Plant Cell Physiol. *41*, 649-656.

Sambrook, J., Fritsch, E.F., and Maniatis, T. (1989). Molecular cloning: A laboratory Manual. II edn. (New York: Cold Spring Harbourn Laboratory Press).

Samson, F., Brunaud, V., Balzergue, S., Dubreucq, B., Lepiniec, L., Pelletier, G., Caboche, M., and Lecharny, A. (2002). FLAGdb/FST: a database for mapped flanking insertion sites (FSTs) of Arabidopsis thaliana T-DNA transformants. Nucleic Acids Res. *30*, 94-97.

Samuels, A.L., Giddings, T.H., and Staehelin, L.A. (1995). Cytokinesis in Tobacco BY-2 and Root Tip Cells: A New Model of Cell Plate Formation in Higher Plants. J. Cell Biol. *130*, 1345-1357.

Sasabe, M., Boudolf, V., De Veylder, L., Inzé, D., Genschik, P., and Machida, Y. (2011). Phosphorylation of a mitotic kinesin-like protein and a MAPKKK by cyclin-dependent kinases (CDKs) is involved in the transition to cytokinesis in plants. Proc. Natl. Acad. Sci. USA *108*, 17844-17849.

Scheuring, D., Viotti, C., Krüger, F., Künzl, F., Sturm, S., Bubeck, J., Hillmer, S., Frigerio, L., Robinson, D.G., Pimpl, P., and Schumacher, K. (2011). Multivesicular bodies mature from the trans-Golgi network/early endosome in Arabidopsis. Plant Cell *23*, 3463-3481.

Scholl, R.L., May, S.T., and Ware, D.H. (2000). Seed and molecular resources for Arabidopsis. Plant Physiol. *124*, 1477-1480.

Schopfer, C.R., and P.K. Hepler. (1991). Distribution of membranes and the cytoskeleton during cell plate formation in pollen mother cells of Tradescantia. J. Cell Sci. *100*, 717-728.

Sclafani, A., Chen, S., Rivera-Molina, F., Reinisch, K., Novick, P., and Ferro-Novick, S. (2010). Establishing a role for the GTPase Ypt1p at the late Golgi. Traffic *11*, 520-532.

Scrivens, P.J., Shahrzad, N., Moores, A., Morin, A., Brunet, S., and Sacher, M. (2009). TRAPPC2L is a novel, highly conserved TRAPP-interacting protein. Traffic *10*, 724-736.

Segev, N. (2001). Ypt and Rab GTPases: insight into functions through novel interactions. Curr. Opin. Cell Biol. *13*, 500-511.

Segui-Simarro, J.M., Austin, J.R. 2nd, White, E.A., and Staehelin, L.A. (2004). Electron Tomographic Analysis of Somatic Cell Plate Formation in Meristematic Cells of Arabidopsis Preserved by High-Pressure Freezing. Plant Cell *16*, 836-856.

Shu, X., Lev-Ram, V., Deerinck, T.J., Qi, Y., Ramko, E.B., Davidson, M.W., Jin, Y., Ellisman, M.H., Tsien, R.Y., and McIntosh, J.R. (2011). A Genetically Encoded Tag for Correlated Light and Electron Microscopy of Intact Cells, Tissues, and Organisms. PLoS Biol. *9*, e1001041.

Søgaard, M., Tani, K., Ye, R.R., Geromanos, S., Tempst, P., Kirchhausen, T., Rothman, J.E., and Söllner, T. (1994). A rab protein is required for the assembly of SNARE complexes in the docking of transport vesicles. Cell *78*, 937-948.

Söllner, R., Glässer, G., Wanner, G., Somerville, C.R., Jürgens, G., and Assaad, F.F. (2002). Cytokinesis-Defective Mutants of Arabidopsis. Plant Physiol. *129*, 678-690.

Speth, E.B., Imboden, L., Hauck, P., and He, S.Y. (2009). Subcellular localization and functional analysis of the Arabidopsis GTPase RabE. Plant Physiol. *149*, 1824-1837.

Spitzer, C., Schellmann. S., Sabovljevic, A., Shahriari, M., Keshavaiah, C., Bechtold, N., Herzog, M., Müller, S., Hanisch, F. G., and Hülskamp, M. (2006).The Arabidopsis elch mutant reveals functions of an ESCRT component in cytokinesis. Development *133*, 4679-4689.

Spitzer, C., Reyes, F.C., Buono, R., Sliwinski, M.K., Haas, T.J., and Otegui, M.S. (2009). The ESCRT-related CHMP1A and B proteins mediate multivesicular body sorting of auxin carriers in Arabidopsis and are required for plant development. Plant Cell *21*, 749-766.

Staehelin, L.A., and Hepler, P.K. (1996). Cytokinesis in higher plants. Cell. *84*, 821-824.

Staehelin, L.A., and Moore, I. (1995). The plant Golgi apparatus: Structure, functional organization and trafficking mechanisms. Annu. Rev. Plant Physiol. Plant Mol. Biol. *46*, 261-288.

Stegmann, M., Anderson, R.G., Westphal, L., Rosahl, S., McDowell, J.M., and Trujillo, M. (2013). The exocyst subunit Exo70B1 is involved in the immune response of Arabidopsis thaliana to different pathogens and cell death. Plant Signal Behav. *8*, e27421.

Stenmark, H., and Olkkonen, V.M. (2001). The Rab GTPase family. Genome Biol. *2*, REVIEWS3007.

Strompen, G., El Kasmi, F., Richter, S., Lukowitz, W., Assaad, F.F., Jürgens, G., and Mayer, U. (2002). The Arabidopsis HINKEL gene encodes a kinesin-related protein involved in cytokinesis and is expressed in a cell cycle-dependent manner. Curr. Biol. *12*, 153-158.

Südhof, T.C., and Rothman, J.E. (2009). Membrane fusion: grappling with SNARE and SM proteins. Science *23*, 474-477.

Swarbreck, D., Wilks, C., Lamesch, P., Berardini, T.Z., Garcia-Hernandez, M., Foerster, H., Li, D., Meyer, T., Muller, R., and Ploetz, L., Radenbaugh, A., Singh, S., Swing, V., Tissier, C., Zhang, P., and Huala, E. (2007). The Arabidopsis Information Resource (TAIR): gene structure and function annotation. Nucleic Acids Res. *36*, 1009-1014.

Synek, L., Schlager, N.,Eliáš, M., Quentin, M., Hauser, M.-T., and Žárský, V. (2006). AtEXO70A1, a member of a family of putative exocyst subunits specifically expanded in land plants, is important for polar growth and plant development. Plant J. *48*, 54-72.

Sztul, E., and Lupashin, V. (2006). Role of tethering factors in secretory membrane traffic. Am. J. Physiol. Cell Physiol. *290*, 11-26.

Takahashi, Y., Soyano, T., Kosetsu, K., Sasabe, M., and Machida, Y. (2010). HINKEL kinesin, ANP MAPKKKs and MKK6/ANQ MAPKK, which phosphorylates and activates MPK4 MAPK, constitute a pathway that is required for cytokinesis in Arabidopsis thaliana. Plant Cell Physiol. *51*, 1766-1776.

Tang, B.L. (2012). Membrane trafficking components in cytokinesis. Cell Physiol. Biochem. *30*, 1097-1108.

TerBush, D.R., Maurice, T., Roth, D., and Novick, P. (1996). The Exocyst is a multiprotein complex required for exocytosis in Saccharomyces cerevisiae. EMBO J. *15*, 6483-6494.

Thellmann, M., Rybak, K., Thiele, K., Wanner, G., and Assaad, F.F. (2010). Tethering Factors Required for Cytokinesis in Arabidopsis. Plant Physiol. *154*, 720-732.

Thiele, K., Wanner, G., Kindzierski, V., Jürgens, G., Mayer, U., Pachl, F., and Assaad, F.F. (2009). The timely deposition of callose is essential for cytokinesis in Arabidopsis. Plant J. *58*, 13-26.

Tzfadia, O., and Galili, G. (2013). The Arabidopsis exocyst subcomplex subunits involved in a golgi-independent transport into the vacuole possess consensus autophagy-associated atg8 interacting motifs. Plant Signal Behav. *8*, e26732.

Ueda, T., Yamaguchi, M., Uchimiya, H., and Nakano, A. (2001). Ara6, a plant-unique novel type Rab GTPase, functions in the endocytic pathway of Arabidopsis thaliana. EMBO J. *20***,** 4730-4741.

Uemura, T., Ueda, T., Ohniwa, R.L., Nakano, A., Takeyasu, K., and Sato, M.H. (2004). Systematic analysis of SNARE molecules in Arabidopsis: dissection of the post-Golgi network in plant cells. Cell Struct. Funct. *29*, 49-65.

Uemura, T., Suda, Y., Ueda, T., and Nakano, A. (2014). Dynamic behavior of the trans-golgi network in root tissues of Arabidopsis revealed by super-resolution live imaging. Plant Cell Physiol. *55*, 694-703.

Van Damme, D., Coutuer, S., De Rycke, R., Bouget, F.Y., Inzé, D., and Geelen, D. (2006). Somatic cytokinesis and pollen maturation in Arabidopsis depend on TPLATE, which has domains similar to coat proteins. Plant Cell *18*, 3502-3518.

Van Damme, D., Gadeyne, A., Vanstraelen, M., Inzé, D., Van Montagu, M.C., De Jaeger, G., Russinova, E., and Geelen, D. (2011). Adaptin-like protein TPLATE and clathrin recruitment during plant somatic cytokinesis occurs via two distinct pathways. Proc. Natl. Acad. Sci. USA *108*, 615-620.

Verma, D.P., and Hong, Z. (2001). Plant callose synthase complexes. Plant Mol. Biol. *47*, 693-701.

Vernoud, V., Horton, A.C., Yang, Z., and Nielsen, E. (2003). Analysis of the small GTPase gene superfamily of Arabidopsis. Plant Physiol. *131*, 1191-1208.

Viotti, C., Bubeck, J., Stierhof, Y.D., Krebs, M., Langhans, M., van den Berg, W., van Dongen, W., Richter, S., Geldner, N., Takano, J., Jürgens, G., de Vries, S.C., Robinson, D.G., and Schumacher, K. (2010). Endocytic and secretory traffic in Arabidopsis merge in the trans-Golgi network/early endosome, an independent and highly dynamic organelle. Plant Cell *22*, 1344-1357.

Völker, A., Stierhof, Y.D., and Jürgens. G. (2001). Cell cycle-independent expression of the Arabidopsis cytokinesis-specific syntaxin KNOLLE results in mistargeting to the plasma membrane and is not sufficient for cytokinesis. Journal of Cell Science *114*, 3001-3012.

Waizenegger, I., Lukowitz, W., Assaad, F.F., Schwarz, H., Jürgens, G., and Mayer, U. (2000). The *Arabidopsis KNOLLE* and *KEULE* genes interact to promote fusion of cytokinetic vesicles during cell plate formation. Curr. Biol. *10*, 1371-1374.

Wang, L.C., Tsai, M.C., Chang, K.Y., Fan, Y.S., Yeh, C.H., and Wu, S.J. (2011). Involvement of the Arabidopsis HIT1/AtVPS53 tethering protein homologue in the acclimation of the plasma membrane to heat stress. J. Exp. Bot. *62*, 3609-3620.

Wang, W., Sacher, M., and Ferro-Novick, S. (2000). TRAPP stimulates guanine nucleotide exchange on Ypt1p. J. Cell Biol. *151*, 289-296.

Whyte, J.R., and Munro, S. (2002). Vesicle tethering complexes in membrane traffic. J. Cell Sci. *115*, 2627-2637.

Willats, W.G., Marcus, S.E., and Knox, J.P. (1998). Generation of monoclonal antibody specific to (1-->5)-alpha-L-arabinan. Carbohydr. Res. *308*, 149-152.

Wilson, S.M., and Bacic, A. (2012). Preparation of plant cells for transmission electron microscopy to optimize immunogold labeling of carbohydrate and protein epitopes. Nat. Protoc. *7*, 1716-1727.

Wong, C., Sridhara, S., Bardwell, J.C., and Jakob, U. (2000). Heating greatly speeds Coomassie blue staining and destaining. Biotechniques. *28*, 426-432.

Woollard, A.A., and Moore, I. (2008). The functions of Rab GTPases in plant membrane traffic. Curr. Opin. Plant Biol. *11*, 610-619.

Wu, J., Tan, X., Wu, C., Cao, K., Li, Y., and Bao, Y. (2013). Regulation of cytokinesis by exocyst subunit SEC6 and KEULE in Arabidopsis thaliana. Mol. Plant *6*, 1863-1876.

Yang, M., Nadeau, JA., Zhao, L., and Sack, F.D. (1999). Characterization of a cytokinesis defective (cyd1) mutant of *Arabidopsis*. J. Exp. Bot. *50*, 1437-1446.

Yamasaki, A., Menon, S., Yu, S., Barrowman, J., Meerloo, T., Oorschot, V., Klumperman, J., Satoh, A., and Ferro-Novick, S. (2009). mTrs130 is a component of a mammalian TRAPPII complex, a Rab1 GEF that binds to COPI-coated vesicles. Mol. Biol. Cell *20*, 4205-4215.

Yip, C.K., Berscheminski, J., and Walz, T. (2010). Molecular architecture of the TRAPPII complex and implications for vesicle tethering. Nat. Struct. Mol. Biol. *17*, 1298-1304.

Young, R.E., McFarlane, H.E., Hahn, M.G., Western, T.L., Haughn, G.W., and Samuels, A.L. (2008). Analysis of the Golgi apparatus in Arabidopsis seed coat cells during polarized secretion of pectin-rich mucilage. Plant Cell *20*, 1623-1638.

Yu, I.M., and Hughson, F.M. (2010). Tethering factors as organizers of intracellular vesicular traffic. Annu. Rev. Cell Dev. Biol. *26*, 137-156.

Yu, H., Tardivo, L., Tam, S., Weiner, E., Gebreab, F., Fan, C., Svrzikapa, N., Hirozane-Kishikawa, T., Rietman, E., Yang, X., Sahalie, J., Salehi-Ashtiani, K., Hao, T.,Cusick, M.E., Hill, D.E., Roth, F.P., Braun, P., and Vidal, M. (2011). Next-generation sequencing to generate interactome datasets. Nat. Methods *8*, 478-480.

Yu, S., and Liang, Y. (2012). A trapper keeper for TRAPP, its structures and functions. Cell Mol. Life Sci. *69*, 3933-3944.

Zerial, M., and McBride, H. (2001). Rab proteins as membrane organizers. Nat. Rev. Mol. Cell Biol. *2*, 107-117.

Zhang, G.F., and Staehelin, L.A. (1992). Functional compartmentation of the Golgi apparatus of plant cells: immunocytochemical analysis of high-pressure frozen-andfreeze-substituted sycamore maple suspension culture cells. Plant Physiol. *99*, 1070-1083.

Zhang, L., Zhang, H., Liu, P., Hao, H., Jin, J.B., and Lin, J. (2011). Arabidopsis R-SNARE proteins VAMP721 and VAMP722 are required for cell plate formation. PLoS One *6*, e26129.

Zhang, Y., Immink, R., Liu, C.-M., Emons, A.M., and Ketelaar, T. (2013). The Arabidopsis exocyst subunit SEC3A is essential for embryo development and accumulates in transient puncta at the plasma membrane. New Phytol. *199*, 74-88.

Zheng, H., Bednarek, S.Y., Sanderfoot, A.A., Alonso, J., Ecker, J.R., and Raikhel, N.V. (2002). NPSN11 is a cell plate-associated SNARE protein that interacts with the syntaxin KNOLLE. Plant Physiol. *129*, 530-539.

Zheng, H., Kunst, L., Hawes, C., and Moore, I. (2004). A GFP-based assay reveals a role for RHD3 in transport between the endoplasmic reticulum and Golgi apparatus. Plant J. *37*, 398-414.

Zheng, H., Camacho, L., Wee, E., Batoko, H., Legen, J., Leaver, C.J., Malhó, R., Hussey, P.J., and Moore, I. (2005). A Rab-E GTPase mutant acts downstream of the Rab-D subclass in biosynthetic membrane traffic to the plasma membrane in tobacco leaf epidermis. Plant Cell. *17*, 2020-2036.

Zuo, J., Niu, Q.W., Nishizawa, N., Wu, Y., Kost, B., and Chua, N.H. (2000). KORRIGAN, an Arabidopsis endo-1,4-beta-glucanase, localizes to the cell plate by polarized targeting and is essential for cytokinesis. Plant Cell *12*, 1137-1152.

Appendix

Allele	AGI	Polymorphism	Position in gene	Accession number	Reference
bet3-1	At5g5450	GABI_318C08	4th intron	N430464	Thellmann et al., 2010
bet5-1	At1g51160	SALK_099482	2nd intron	N599482	This study
bet5-2	At1g51160	SAIL_634_G07	2nd intron	N827313	This study
trs31-1	At5g58030	FLAG_488E06	3rd intron	EWSTV26T3	Thellmann et al., 2010
trs33-1	At3g05000	SALK_109244	3rd exon	N609244	This study
trs33-2	At3g05000	SALK_109724	3rd intron	N609724	This study
club-2/trs130-2	At5g54440	SALK_039353	14th Intron	N539353	Jaber et al., 2010
trs120-1	At5g11040	SALK_125246	1st intron	N625246	This study
trs120-2	At5g11040	SALK_021904	1st intron	N609924	This study
trs120-3	At5g11040	SALK_111574	7th exon	N611574	Thellmann et al., 2010
trs120-4	At5g11040	SAIL_1285_D07	7th intron	N879232	Thellmann et al., 2010
vps52-2	At1g71270	SAlK_055433	16th exon	N555433	This study; Guermonprez et al., 2008
vps53-2	At1g50500	SAIL_87_D06	5th intron	N870946	This study
vps53-3	At1g50500	GABI_400C01	7th exon	N344145	This study
vps53-4	At1g50500	SAIL_117_D11	13th intron	N871277	This study
vps53-5	At1g50500	GABI_463D10	23rd exon	N344181	This study
vps54-1	At4g19490	SALK_036485	1st exon	N536485	This study; Guermonprez et al., 2008
vps54-2	At4g19490	SALK_062261	8th exon	N562261	This study; Guermonprez et al., 2008
exo84b-2	At5g49830	SAIL_736_A04	5th intron	N832876	Fendrych et al., 2010
mas-5	At2g36850	SALK_015454	17th intron	N515454	Thiele et al., 2009

Table S1. Insertion lines used in this study.

AGI: Arabidopsis genome initiative accessions (www.arabidopsis.org); note that the *trs120-4* allele we used (Thellmann et al., 2010) is distinct from the hypomorphic allele later named *trs120-4* by Qi et al. (2011).

Genotype	Primer sequence		LB primer	Tm [℃]
genotype (T-DNA insertion)				
bet3	Forward	5'-TCTCCGGGAGTAAAAACAAC-3'*	Lo8409	55.0
	Reverse	5'-CACGATTTGAGACATTGTGATAC-3'		
bet5-1	Forward	5'-AAGATAATCTGGAACCTGGCTGATTG-3'*	LBa1	60.3
	Reverse	5'-TCGCGTAAATCTCCGGTCTTTG-3'		
bet5-2	Forward	5'-AGAAGAAAATGAGAACCAGGGAGATG-3'*	LB3	60.6
	Reverse	5'-TGGTCAAGATGCAACAGTGGAAG-3'*		
trs31	Forward	5'-TCGATTTCGAGCATCTGCTGATTGG-3'	LB4	62.0
	Reverse	5'-CAACAAACGCTCCGCAGTTGAATG-3'*		
trs33-1	Forward	5'-GCAAACAGAAGCCTGCAATGG-3'*	LBb1.3	55.8
	Reverse	5'-TGAGGCATGTTTTGTTGCTTCTG-3'		
trs33-2	Forward	5'-GCAAACAGAAGCCTGCAATGG-3'*	LBb1.3	55.8
	Reverse	5'-TGAGGCATGTTTTGTTGCTTCTG-3'		
trs120-1	Forward	5'-CTTTGCCACTGTCCCTCGTC-3'*	LBb1.3	55.8
	Reverse	5'-TGAGCATTGGCATCAACAGG-3'*		
trs120-2	Forward	5'-CTTTGCCACTGTCCCTCGTC-3'*	LBb1.3	55.8
	Reverse	5'-TGAGCATTGGCATCAACAGG-3'*		
trs120-3	Forward	5'-GGGCATCCATGTCAAAAGTGTC-3'*	LBa1	60.3
	Reverse	5'-TTTTGCCAGAGTCAGCTAAGAACC-3'		
club-2	Forward	5'-CTCGTCCAAGGAGCGGCAAG-3'	LBa1	59,5
	Reverse	5'-GGCACGAACAGGGACCCAAA-3'*		
trs120-4	Forward	5'-TGATTGAGCATGGTTTTCTGGAG-3'	LB3	58,9
	Reverse	5'-TGTCCACTTGGGAGGAATGG-3'*		
vps53-1	Forward	5'-TCCAATGTACCAGCTCCTTC-3'	LBb1.3	55.8
	Reverse	5'-ACCCAAACCAGCTCATTGTC-3'		
vps52-2	Forward	5'-TCATGATCCAGCCTTTTG-3'*	LBb1.3	51.4
	Reverse	5'-TCAACTCACCTTCAGTACAGC-3'		
vps53-2	Forward	5'-GTGCAAAATTCATCACATGACACAC-3'	LB3	59.3
	Reverse	5'-AGAACATAACCACGACAATCACTGC-3'		
vps53-3	Forward	5'-CGCGTATCAAAATATTTCTTC-3'*	Lo8409	52.0
	Reverse	5'-TGTTGCTTGGTTTACGTAGG-3'		
vps53-4	Forward	5'-CAACCACCTTATCTAAGACCGTGAAG-3'	LB3	59.0
	Reverse	5'-CGCTTCACGAGATTATTTTGTTCC-3'		
vps53-5	Forward	5'-GGAAACAAAGGTGGGAATTG-3'	LO8409	55.3
	Reverse	5'-CCTGATGCCTAAACCCTTTG-3'*		
vps54-1	Forward	5'-GATCCGACTTCCATGGCTAC-3'*	LBb1.3	55.8
	Reverse	5'-TGGCGGAAGCAGTATAGACC-3'*		
vps54-2	Forward	5'-TTCCCGGTCTTTATTGTTGG-3'	LBb1.3	55.3
	Reverse	5'-TTTGCTCGCGAGAGATAAGC-3'*		
exo84b-2	Forward	5'-TGTAGATGTGCTGGTAAGAGC-3'	LB3	57,9
	Reverse	5'-TGGTTCACGTAGTGGGCCATCG-3'*		
GFP fusion			Reverse	
CLUB	Forward	5'-GATGAGGTGTTATATGAAGTCA-3'	GFP	58,8
TRS120	Forward	5'-GCGTAGGCTGGGACGTG-3'		

Table S2. Primers used in this study for genotyping.

*The primers marked by asterisks were used together with the T-DNA left border LB primer to amplify the DNA insertion and flanking genomic sequences, as described at http: //signal.salk.edu. Annealing times were 30 sec for all primer pairs. T-DNA primers were: LBa1: TGGTTCACGTAGTGGGCCATCG; Lb3: TAGCAT CTGAATTTCATAACCAATCTCGA; LbB1.3: ATTTTGCCGATTTCGGAAC; LBo8409: ATATTGACCATCATACTCATTGC; LB4: CGTGTGCC AGGTGCCCACGGAATAGT.

Primer name	Primer sequence
AtTRS120	
574_fwd	5'-GGGCATCCATGTCAAAAGTGTC-3'
904_rev	5'-TGAGCATTGGCATCAACAGG-3'
Trs120_rev	5'-GCTCAATCAAAACACAAGAGAGG-3'
Trs120fwd2	5'-GGTTCTTAGCTGACTCTGGC-3'
Trs120fwd4	5'-GGAGCATTTTAAGCTACCGG-3'
Trs120fwd5	5'-CCCATCTTCTGTCGTGGACC-3'
Trs120fwd6	5'-GCGTAGGCTGGGACGTG-3'
Trs120seq1	5'-TCTTCTGTAGGCAGGTCGCC-3'
Trs120seq2	5'-CGGGTAACACAGGAAGACC-3'
pCambiacolF	5'-GACCTAGTCGTCCTCGTC-3'
pCamR	5'-TTACGTCGCCGTCCAGCT-3'
Trs120Jan1	5'-ATCCAGAGGAGGTTTATGTC-3'
Trs120Jan2	5'-TGTTCCTAACATATCAGTTGCTCC-3'
KV-rev1	5'-TATAGACGTTGTGGCTGTTG-3'
CLUB/AtTRS130	
440_1fwd	5'-AAGGATTACGCAATTAGTGAGGA-3'
440_1rev	5'-TAGTTTTCGGCAGCACCTTT-3'
440_2fwd	5'-TCTTAACCTAACCAAAGGTGCTG-3'
440_2rev	5'-TCAGCTTTTGATGCACCAGT-3'
440_3fwd	5'-CGTATGGAATTGAGATGGAGAG-3'
440_3rev	5'-AGTTCACAGAAACTAAGATTTGAGC-3'
440_Arev	5'-TCTAGCAAAAATATGAGTGATTGC-3'
440_Bfwd	5'-TTAAACAGTTTGCACGATTGC-3'
440_Brev	5'-AAGAGAAAGAAAAATCGACATGC-3'
pCamR	5'-TTACGTCGCCGTCCAGCT-3'
pCAMBIA F	5'-GACCTAGTCGTCCTCGTC-3'
440-1addrev	5'-CTTCATTTCACTGTGTGCAAGA-3'
440-2_add_rev	5'-TTCAAGTTTCAAAGCTACAGTTCTC-3'
440-3_add_rev	5'-CACTCTTGAACACCAAATCTCTC-3'
139seq1	5'-CGCCTATCCAAGGTATTCCTG-3'
130seq2	5'-CCTTTTCTTTTTCAAGCACCTCC-3'
130seq3	5'-CTAGATGCAACTTCAAATGGACG-3'
KV-rev2	5'-TATAGACGTTGTGGCTGTTG-3'
AtTRS120 endogenous promoter	
trs120prom_seq	5'-TGAGCGGATAACAATTTCAC-3'
trs120col-rev	5'-TAGATCCATCGGCATCGAG-3'
mCherry	
Fwd1col	5'-GCTCTTAGTGGAATCTCAATGGAA-3'
mCherry+rev	5'-GTGGCGCTCTATCATAGATG-3'
Rev3col	5'-AGTTGATAAACACGACTCGTGT-3'

Table S3. Primers used for sequencing in this study.

The following primers were used to sequence genomic AtTRS120, genomic CLUB/AtTRS130, 1kB upstream of AtTRS120 and mCherry.

Exocyst insertion lines screened in Farhah Assaad lab						
Allele	**AGI gene identification**	**Polymorphism**	**Intron/exon**	**Accession number**	**Comment**	**Reference**
sec3a	At1g47550	SALK_145185	Intron	N645185	embryo lethal	Zhang et al., 2013
sec5a-1	At1g76850	SALK_010127.56	Intron	N510127	viable	Hala et al., 2008
sec5a-2		GABI_731C01	Exon	N329010		
sec5b-1	At1g21170	SALK_001525	Intron	N501525	viable	Hala et al., 2008
sec6-1	At1g71820	SALK_078235.54	Exon	N578235	male gametophyticlet hal	Hala et al., 2008; Wu et al., 2013
sec6-2		SALK_072337	Exon	N572337		
sec8-1	At3g10380	SALK_057409.49	Intron	N557409	male gametophyticlet hal	Cole et al., 2005
sec8-3		SALK_026204	Intron	N526204		
sec8-4		SALK_118129	Intron	N618129	viable	
sec8-6		SALK_091118	Exon	N591118	viable	
sec8		SAIL_553_A07	Exon	N823395		
		SALK_027307.36	Exon	N527307		
		SALK_039659.53	Exon	N539659		
sec10	At5g12370	SALK_101637.54	Exon	N601637		
		SALK_146417.17	Intron	N646417		
		SALK_120710.53	Exon	N620710		
		SALK_146418.55	Exon	N646418		
sec15a-1	At3g56640	SALK_006302.46	Exon	N506302	male gametophytic lethal	Hala et al., 2008
sec15a-2		SALK_067498	Exon	N567498		
sec15b	At4g02350	SALK_042723.35	Exon	N542723		
exo70A1-1	At5g03540	SALK_014826	Intron	N514826	sterile dwarf	Synek et al, 2006
exo70A1-2		SALK_135462.38	Exon	N635462		Synek et al, 2006 Hala
exo70A1-3		SALK_026036.52	Intron	N526036		
		SALK_026036C	Intron	N665607*		
exo70A2	At5g52340	GABI_824D06	Exon	N329594		
exo70A3	At5g52350	SAIL_860_A02	Exon	N838557		
		SALK_046855.44	Intron	N546855		
		SALK_046855C	Intron	N668196		
		SALK_046993.44	Intron	N546993		
exo70B1	At5g58430	GABI_114C03	Exon	N328817		
		GABI_156G02	Exon	N414954		
exo70B2	At1g07000	SAIL_621_F02	Exon	N859934		
exo70B2-2		SAIL_339_D07	Exon	N873298	viable	Pečenková et al., 2011
exo70C1	At5g13150	GABI_100A02	Exon	N328778		
exo70D1	At1g72470	SALK_067007.28	Exon	N567007		
exo70D2	At1g54090	SALK_003651.25	Exon	N503651		

Allele	AGI gene identification	Polymorphism	Intron/exon	Accession number	Comment	Reference
exo70D3	At3g14090	SAIL_175_D08	Exon	N871831		
		GABI_747E03	Exon	N329494		
exo70E1	At3g29400	GABI_576F04	Exon	N304920		
		SALK_084145.48	Exon	N584145		
exo70F1	At5g50380	SALK_068101.40	Exon	N568101		
		SALK_109094.18	Exon	N609094		
exo70G1	At4g31540	SALK_074915.54	Exon	N574915		
		SALK_074915C	Exon	N672731		
		SALK_124115.54	Exon	N624115		
exo70G2	At1g51640	SALK_097393.49	Exon	N859942		
		SALK_066920.27	Exon	N566920		
exo70H1	At3g55150	SALK_042456.34	Exon	N542456	viable	Pečenková et al., 2011
		SAIL_189_D12	Exon	N808914		
exo70H3	At3g09530	GABI_651C10	Exon	N328929		
exo70H4	At3g09520	SALK_023593.51	Exon	N523593		
		SALK_080458.46	Exon	N580458		
exo70H5	At2g28640	SALK_132040.26	Exon	N859587		
exo70H6	At1g07725	GABI_768C01	Exon	N329559		
		SAIL_673_A11	Exon	N829423		
exo70H7	At5g59730	GABI_058G08	Exon	N328529		
		SALK_072673.42	Exon	N860008		
exo70H8	At2g28650	SALK_014867.55	Exon	N514867		
		SALK_106117.30	Exon	N606117		
		SALK_125606.35	Exon	N860026		
***exo84b*-1**	At5g49830	GABI_459C01	Intron	N443993	seedling lethal	Fendrych et al., 2010
exo84b-2		SAIL_736_A04	Intron	N832876	seedling lethal	Fendrych et al., 2010

Table S4: Insertion lines in exocyst mutants surveyed in Assaad lab for seedling lethal cytokinesis-defective phenotypes.

We indicate the overall segregation or phenotype for published lines only. For unpublished lines, our survey focused only on the identification of canonical cytokinesis-defective phenotypes and segregation analysis was preliminary. a: exo70A1 mutants are very stunted in their growth and produce seeds only very rarely. b: SALK_026036C in EXO70A1 segregated the desired phenotype but was discarded because its phenotype, stronger than that of null alleles, appeared to be synthetically enhanced by a background mutation.

Accession number (AGI)	Gene description	CLUB-GFP IP inflorescences					TRS120-GFP IP inflorescences			
		Average number of unique peptides	Average Log2 (ratio)	Standard deviation	p-value		Average number of unique peptides	Average Log2 (ratio)	Standard deviation	p-value
TRAPPII subunits										
At5g54440	CLUB/ AtTRS130	121	12	1,6	0,0001					
At5g11040	TRS120	40	11	0,4	1,6E-05		72	12	2,4	0,002
At3g05000	TRS33	9	13	1,3	2,5E-05		5	12	4,7	0,02
At5g54750	Bet3	10	13	1,6	1,5E-04		9	12	4,0	0,014
At5g16280	Trs20	8	14	4,5	0,01					
At5g58030	TRS31	6	9	4,4	0,012					
exocyst subunits										
At5g59730	EXO70H7	7	14/0	0,0	1,4E-07					
At1g21170	SEC5B	1	10	0,3	5,8E-07					
At5g49830	EXO84B	10	14/0	0,0	2,3E-07		9	14,29/0	0,0	3,4E-05
At3g10380	SEC8	23	5	0,6	1,1E-04					
At1g47550, At1g47560	SEC3A, SEC3B	10	14/0	0,0	1,3E-05		7	14,29/0	0,0	1,6E-04
At5g03540	EXO70A1	11	14/0	0,0	4,3E-08		6	14,29/0	0,0	0,0002
At4g02350	SEC15B	14	14/0	0,0	2,1E-07					
At1g71820	SEC6	11	12	3,3	2,8E-04		8	11	5,1	0,011
At5g12370	SEC10	21	10	3,7	0,0078		19	6	3,2	0,017
At1g76850	SEC5A	9	11	2,8	0,0013					

Table S5. Analysis of CLUB-GFP and TRS120-GFP immunoprecipitates from inflorescences via mass spectrometry.

Shown proteins correspond to subunits of the TRAPPII and exocyst complexes. The data are based on three biological replicates. AGI: *Arabidopsis* genome initiative accessions (www.arabidopsis.org). a: The $\log_2$ ratio for each protein was calculated as its signal intensity in the experiment divided by its intensity in the control. Note that the $\log_2$ ratios for exocyst subunits are comparable to those of the TRAPPII subunits, supporting their identification as a complex. b: P values (< 0.02) were calculated using the Student's t-test (two-sided). This table lists only TRAPPII and exocyst components detected in the IPs from inflorescences.

Accession number (AGI)	Gene description	CLUB-GFP IP leaves			
		Average number of unique peptides	Average Log2 (ratio)	Standard deviation	p-value
TRAPPII subunits					
At5g54440	CLUB/ AtTRS130	92	7	2,6	0,03
At5g11040	TRS120	11	5	2,7	0,01

Table S6. Analysis of CLUB-GFP immunoprecipitate from leaves via mass spectrometry. Shown proteins correspond to subunits of the TRAPPII complex. The data are based on three biological replicates. AGI: *Arabidopsis* genome initiative accessions (www.arabidopsis.org). a: The $\log_2$ ratio for each protein was calculated as its signal intensity in the experiment divided by its intensity in the control. b: P values (< 0.03) were calculated using the Student's t-test (two-sided). This table lists only TRAPPII and exocyst components detected in the IPs from leaves. Note that exocyst subunits are not listed in the table as CLUB intearaction partners in leaves because they were not detected with high significance.

Accession number (AGI)	Gene descrip-tion	CLUB-GFP IP seedlings					TRS120-GFP IP seedlings			
		Average number of unique peptides	Average Log2 (ratio)	Standard deviation	p-value		Average number of unique peptides	Average Log2 (ratio)	Standard deviation	p-value
TRAPPII subunits										
At5g54440	CLUB/ AtTRS130	95	8	2,5	0,05					
At5g11040	TRS120	21	5	7,9	0,3		63	10	4,8	0,05
At3g05000	TRS33	9	14/0	0.0	0,0002		4	14/0	0,0	0,001
At5g16280	Trs20	6	14/0	0.0	0,004		3	14/0	0,0	0,01
At5g54750	Bet3	9	14/0	0.0	0,0000 1		7	14/0	0,0	0,000 2
At5g58030	TRS31	4	14/0	0.0	0,0003		5	14/0	0,0	0,003
exocyst subunits										
At5g12370	SEC10	11	13	3,0	0,02		5	14/0	0.0	0,004
At1g71820	SEC6	5	14/0	0,0	0,001					
At4g02350	SEC15B	5	14/0	0,0	0,01		2	14/0	0.0	0,001
At5g03540	EXO70A1	2	14/0	0,0	0,001					

Table S7. Analysis of CLUB-GFP and TRS120-GFP immunoprecipitates from seedlings via mass spectrometry.

Shown proteins correspond to subunits of the TRAPPII and exocyst complexes. The data are based on three biological replicates. AGI: *Arabidopsis* genome initiative accessions (www.arabidopsis.org). a: The $\log_2$ ratio for each protein was calculated as its signal intensity in the experiment divided by its intensity in the control. b: P values (< 0.05 except for TRS120 in CLUB-GFP IP) were calculated using the Student's t-test (two-sided). This table lists only TRAPPII and exocyst components detected in the IPs from seedlings.

Accession number (AGI)	Gene description	CLUB-GFP IP inflorescences				TRS120-GFP IP inflorescences			
		Average number of unique peptides	Average Log2 (ratio)	Standard deviation	p-value	Average number of unique peptides	Average Log2 (ratio)	Standard deviation	p-value
Rab GTPases									
At5g45750	AtRab-A1c	3	4	2,2	0,02				
At5g47200	AtRab-D2b	2	4	1,3	0,004				
At2g44610	AtRab-H1b					2	9	0,4	0,004
VHA subunits									
At1g78900	VHA-A	31	4	1,1	0,002				
At4g11150	, VHA-E1	14	4	0,9	0,002				
At3g58730	VHA-D	11	6	2,8	0,02	10	8	3,1	0,03
At3g42050	VHA-H	9	7	2,2	0,01				
At3g01390	VHA-G1	8	3	0,9	0,01	6	1	0,5	3,2E-01
At1g20260	VAB3	3	4	1,1	0,003				
At4g38510	VAB2	3	4	1,4	0,02				
At4g23710	VHA-G2	2	3	1,0	0,02				

Table S8. Analysis of CLUB-GFP and TRS120-GFP immunoprecipitates from inflorescences via mass spectrometry.

The data are based on three biological replicates. AGI: *Arabidopsis* genome initiative accessions (www.arabidopsis.org). a: The $\log_2$ ratio for each protein was calculated as its signal intensity in the experiment divided by its intensity in the control. b: P values (< 0.05) were calculated using the Student's t-test (two-sided). This table lists only Rab GTPases and VHA components detected in the IPs from inforescences.

Accession number (AGI)	Gene description	CLUB-GFP IP seedlings				TRS120-GFP IP seedlings			
		Average number of unique peptides	Average Log2 (ratio)	Standard deviation	p-value	Average number of unique peptides	Average Log2 (ratio)	Standard deviation	p-value
Rab GTPases									
At1g09630	AtRab-A2a					1	14/0	0	0,001
At4g17530	AtRab-D2c	1	14/0	0	0,01	1	11	6,0	0,05
At5g47200	AtRab-D2b	2	14/0	0	0,01	1	11	6,0	0,04
VHA subunits									
At3g58730	VHA-D					7	11	5,1	0,02
At4g38510	VAB2	2	14/0	0	0,0004	2	14/0	0	0,001

Table S9. Analysis of CLUB-GFP and TRS120-GFP immunoprecipitates from seedlings via mass spectrometry.

The data are based on three biological replicates. AGI: *Arabidopsis* genome initiative accessions (www.arabidopsis.org). a: The $\log_2$ ratio for each protein was calculated as its signal intensity in the experiment divided by its intensity in the control. b: P values (< 0.05) were calculated using the Student's t-test (two-sided). This table lists only Rab GTPases and VHA components detected in the IPs from seedlings.

Accession number (AGI)	Gene description	CLUB-GFP IP leaves			
		Average number of unique peptides	Average Log2 (ratio)	Standard deviation	p-value
At3g58730	VHA-D	5	8	5,8	0,05
At1g20260	VAB3	3	3	1,3	0,03

Table S10. Analysis of CLUB-GFP and TRS120-GFP immunoprecipitates from leaves via mass spectrometry.

The data are based on three biological replicates. AGI: *Arabidopsis* genome initiative accessions (www.arabidopsis.org). a: The $\log_2$ ratio for each protein was calculated as its signal intensity in the experiment divided by its intensity in the control. b: P values (< 0.05) were calculated using the Student's t-test (two-sided). This table lists only Rab GTPases and VHA components detected in the IPs from leaves.

Acknowledgments

I would like thank Dr. Farhah Assaad for providing me the opportunity to work in her lab. I am especially thankful for the excellent supervision, stimulating advice during the years of research, as well as for the critical reading of this manuscript.

I would like also thank Prof. Dr. Ralph Hückelhoven and Prof. Dr. Jörg Durner for participation in my committee.

I am deeply appreciative to Alex Steiner for his help and cooperation.

I would like to thank former members of the Assaad research group (Ngoc Nguyen and Knut Thiele) for their help.

I would like to thank Eva-Maria Herold for helping me with the German language related issues.

I am very grateful to Prof. Dr. Bernhardt Küster and Susan Kläger from Chair of Proteomics and Bioanalytics at the Techische Universität München, for providing a LC-MS/MS analysis.

I would like to thank Prof. Gerhardt Wanner, Silvia Dobler from the Ultrastructural Research group of the Ludwig-Maximilians-Universität (München), for performing fast ion beam and electron microscopy.

I would like to thank Eva Facher from Department Biologie I at the Ludwig-Maximilians-Universität (München), for performing scanning electron microscopy.

Special thanks go to Beate Seeliger for help in daily life and bureaucracy.

I would like to thanks to members of Chair of Botany and the Plant Developmental Biology group for the friendly atmosphere.

I would like to thank Deutsche Forschungsgemeinschaft for funding.

Finally, I want to express my gratitude to my mother, brother and sister for their help, support and encouragement during all my life.